The Thesis Committee for Umut Aybar
Certifies that this is the approved version of the following thesis:

Investigation of Analytical Models Incorporating Geomechanical Effects on Production Performance of Hydraulically and Naturally Fractured Unconventional Reservoirs

APPROVED BY
SUPERVISING COMMITTEE:

Kamy Sepehrnoori, Supervisor

Tad Patzek, Co-Supervisor

Investigation of Analytical Models Incorporating Geomechanical Effects on Production Performance of Hydraulically and Naturally Fractured Unconventional Reservoirs

by

Umut Aybar, B.E.

Thesis

Presented to the Faculty of the Graduate School of

The University of Texas at Austin

in Partial Fulfillment

of the Requirements

for the Degree of

Master of Science in Engineering

The University of Texas at Austin

August 2014

Dedication

This thesis is dedicated to Mustafa Kemal Ataturk, the founder of the Turkish Republic. It is also dedicated to Akdem Aybar and Kadri Demir, my lovely grandfathers who passed away during my master studies and my father, Feyzullah Aybar, my mother, Aysun Aybar, my sister Isil Aybar, my aunts, Gonca Aybar and Aysel Degerli, my grandmothers Leman Aybar and Mediha Demir and my fiancé, Gulsah Yavas, who have been a great source of motivation and inspiration.

Acknowledgements

First and foremost, I would like to express my utmost gratitude to my supervisor, Kamy Sepehrnoori for his continuous support and guidance both on academic and personal level. I am also very much grateful to my co-supervisor, Tad Patzek for his guidance and patience during my master studies. It was my pleasure to study under their supervision, and it was very valuable experience for my future career.

I also would like to thank my colleagues in our research group, Mohammad Omidvar Eshkalak and Wei Yu for their technical contributions and friendship.

I always feel myself very lucky to have such a lovely family, and I would like to express my appreciation to their continued love and support not only for this master study, but also for all the success in my life. I also like to thank Gulsah Yavas for her endless love.

Finally, I am thankful to the Turkish Petroleum Corporation for providing the scholarship for my graduate studies.

Abstract

Investigation of Analytical Models Incorporating Geomechanics Effect on Production Performance of Hydraulically and Naturally Fractured Unconventional Reservoirs

Umut Aybar, M.S.E.

The University of Texas at Austin, 2014

Supervisors: Kamy Sepehrnoori and Tad Patzek

Production from unconventional reservoirs became popular in the last decade in the U.S. Promising production results and predictions, as well as improvements in hydraulic fracturing and horizontal drilling technology made unconventional reservoirs economically feasible. Therefore, an effective and efficient reservoir model for unconventional resources became a must. In order to model production from such resources, analytical, semi-analytical, and numerical models have been developed, but analytical models are frequently used due to their practicality, relative simplicity, and also due to limited availability of field data.

This research project has been accomplished in two main parts. In the first part, two analytical models for unconventional reservoirs, one with infinite hydraulic fracture conductivity assumption proposed by Patzek et al. (2013), while the other one with finite hydraulic fracture conductivity assumption developed by Ozkan et al. (2011) are compared. Additionally, a commercial reservoir simulator (CMG, IMEX, 2012) is

employed to compare the results with the analytical models. Sensitivity study is then performed to identify the critical parameters controlling the production performance of unconventional reservoirs.

In the second part, naturally and hydraulically fractured unconventional reservoir is considered. In addition, geomechanical effects on natural and hydraulic fractures are examined. A simple analytical dual porosity model, which represents the natural fractures in unconventional reservoirs, is improved to handle the constant bottom-hole pressure production scenario to identify the production performance differences between the cases with and without geomechanical effects. Finally, geomechanical effects are considered for combined natural and hydraulic fractures, and an evaluation of the circumstances in which the geomechanical effects cause a significant production loss is carried out.

Table of Contents

List of Tables

List of Figures

Chapter 1: Introduction

Technical advances in hydraulic fracturing and horizontal drilling have enabled companies to reach the economically viable recovery from unconventional resources such as shale gas reservoirs. Projections indicate that unconventional resources will be a significant supplier of the world energy demand in the near future. For operating companies, it is crucial to estimate production performance of unconventional reservoirs. A robust reservoir model, which is valid for unconventional reservoirs, is necessary for production forecasts. There are several analytical reservoir models available in the literature incorporating different assumptions and characteristics. These analytical models enhance operator's capability to investigate an accurate and optimum fracturing treatment strategy with minimum effort. Moreover, running these models and having the luxury of high quality output can prove to be a sound reservoir management tool for better and efficient performance analysis of unconventional assets. In addition to these models, numerical reservoir simulators are also available for unconventional reservoir modeling. However, commercial simulators are computationally expensive and require a lot of input data. The aim of this thesis is to show the accuracy of the analytical models by comparing them with a commercial reservoir simulator.

This study is divided into two main parts. The first part investigates the reservoir modeling in homogeneous unconventional reservoirs. For this purpose two analytical models from the existing literature are employed, and also a commercial reservoir simulator is used in order to compare the results obtained from the analytical models. In the first part of this thesis, a sensitivity analysis is also performed to identify important completion design parameters controlling the production performance of unconventional reservoirs. Aim of the first part is to demonstrate whether or not the selected analytical

models can accurately simulate the production performance of unconventional reservoirs. Analytical models are important because operating companies have hundreds of horizontal wells in unconventional assets, and simulating these wells with commercial reservoir simulators is computationally expensive and quite time consuming. As shown in this study, with the analytical models, operators can decide their completion strategies quickly with minimum input data requirements and minimum computational effort.

In the second part of this thesis, naturally and hydraulically fractured unconventional reservoirs and their production behavior are studied both analytically and numerically. In addition, geomechanical effects (fracture closures) on natural and hydraulic fractures are taken into account. Also, a sensitivity analysis is performed to understand under which circumstances geomechanical effects must be considered in the process of modeling and simulation of unconventional reservoirs. Moreover, the second part quantifies the effect of geomechanics on long term production performances of unconventional resources.

This thesis consists of five chapters:

Chapter 1 introduces the content of this study and provides an overview about each chapter.

Chapter 2 presents the literature review on analytical models for unconventional reservoirs, analytical dual porosity models, experimental studies investigating the pressure dependent permeability, and the reservoir models coupled fluid flow with geomechanics.

Chapter 3 gives the details of two analytical models used in this study. Mathematics of the analytical models and assumptions related to these models are stated. Results obtained from the analytical models are compared with the commercial reservoir simulator. In addition, a sensitivity analysis is performed for certain reservoir and design

parameters to identify the most influential parameters controlling the production performance.

Chapter 4 investigates a dual porosity model which is developed to represent natural fractures in unconventional reservoirs. Production performance differences between the conventional homogeneous and naturally fractured unconventional reservoir models are discussed. The original dual porosity model developed by Apaydin (2012) and Cho (2012) cannot simulate the constant bottom hole pressure production scenario. In this study, modifications are proposed to simulate constant bottom hole pressure control, and the results obtained with the new method are verified with the commercial reservoir simulator (CMG, IMEX, 2012). Geomechanical effects on hydraulic and natural fractures are also examined with the commercial reservoir simulator.

Chapter 5 describes the summary and the conclusions of this thesis, and provides recommendations for future studies.

Chapter 2: Literature Review

This chapter presents a literature review on the available analytical models for the hydraulically fractured reservoirs. Also, fractured reservoirs using dual porosity concepts, experimental studies investigating the pressure dependence of rock permeability as well as the reservoir models that have coupled the pressure dependency of permeability with fluid flow in porous medium are presented.

2.1. Analytical Models For Hydraulically Fractured Reservoirs

Unconventional reservoirs, unlike conventional reservoirs, are hydraulically fractured prior to production. Hydraulic fracturing is defined as a special treatment for unconventional shale and tight-sand reservoirs. Highly pressurized fluid, such as water, is pumped into the formation in-order to exceed the rock mechanical strength. Hydraulic fracturing creates highly conductive channels and paths for reservoir fluid to flow from the reservoir pay zones to the wellbore. Fluid flow simulation and modeling in unconventional resources with hydraulically fractured wells is discussed by the researchers mainly in the following categories; analytical, semi-analytical, and numerical models.

Analytical models are widely employed because of their relative simplicity compared to the numerical approaches. The aim of analytical models is to provide a simple solution which covers the fundamental physics of the phenomena. In order to accomplish this goal the models must have simplifying assumptions. Having constant and/or homogeneous rock and fluid properties (density, compressibility, permeability, and viscosity) are the common assumptions for analytical solutions. The purpose of these assumptions is to linearize the governing partial differential equations modeling the transport phenomena, in our case, the diffusion equation.

Analytical solutions for fluid flow in porous medium originate in the methods proposed by Carslaw and Jaeger (1959). However, there are some conditions which cannot be solved using the techniques presented by Carslaw and Jaeger (1959) because of the different boundary conditions. Laplace transformation domain is preferred for these circumstances. Van Everdingen and Hurst (1949) applied the Laplace transformation theory to the fluid flow problems in porous media; due to its simplicity in handling partial differential equations, with various boundary and initial conditions, this technique is customarily the preferred method in analytical solutions. Furthermore, the dual porosity concepts take advantage of the Laplace domain method, since it transforms a partial differential equation into an ordinary differential equation that is easier to solve. Stehfest's (1970) numerical method is commonly used to convert $\underline{s}$ domain (Laplace) back to $\underline{t}$ (time) domain which represents the applicable solutions.

As stated earlier to solve the diffusivity equations analytically there are several assumptions to be made such as constant fluid properties (fluid viscosity and compressibility). Constant viscosity and compressibility assumptions are generally true for oil reservoirs, but because gas properties are strongly pressure dependent, these assumptions need to be modified to address the shortcomings for gas reservoirs. In 1966, Al-Hussainy and Ramey proposed the pseudo pressure concept for gas reservoirs to overcome the problem caused by the pressure dependent gas properties. The pseudo pressure concept introduces an integral transformation that combines the compressibility and viscosity of gas with respect to the pressure.

Earlier analytical models for hydraulically fractured reservoirs were developed to show the hydraulic fracturing treatment effects on production. They were also capable of making practical sensitivity analysis for reservoir and hydraulic fracture parameters. Productivity index comparison is the basis of these analytical models.

McGuire and Sikora (1960) presented a fundamental type curve based on the comparison of the productivity index (PI) of a reservoir. This comparison is made according to the change of PI right before and after the hydraulic fracturing treatment (Figure 2.1 shows McGuire and Sikora's chart). One can simply input the hydraulic fracture, wellbore, and reservoir parameters into their type curve to see the productivity index changing after the hydraulic fracturing treatment. Additionally, general conclusions can be driven by their type curve analysis such as, optimum fracture conductivity, and the theoretical maximum productivity index increment for a particular case.

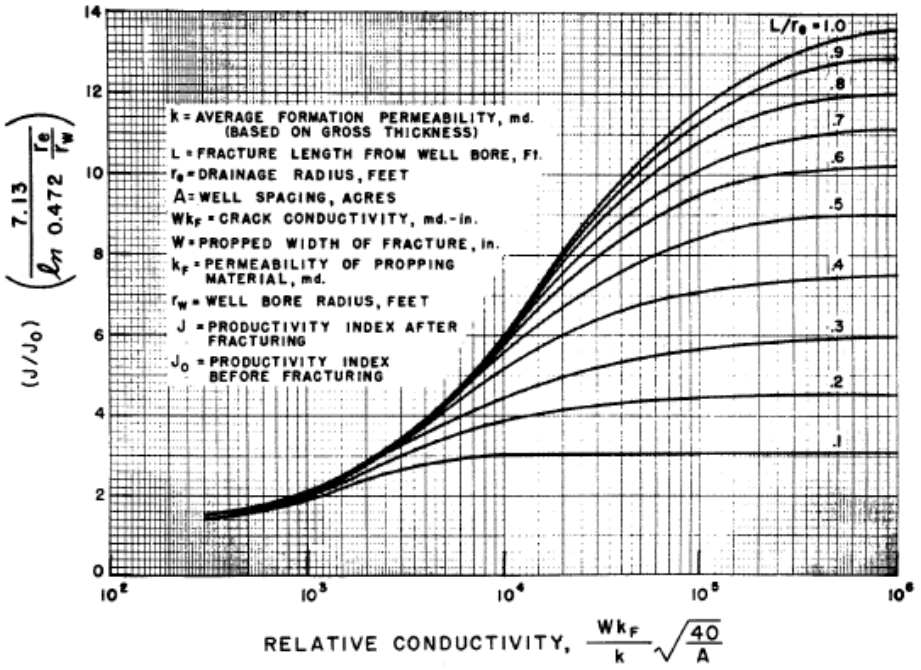

Figure 2.1: McGuire and Sikora's chart, (McGuire and Sikora, 1960)

Prats et al. (1961) studied the flow behavior of compressible fluid flow in reservoirs with hydraulically fractured vertical wells. They assumed a cylindrical reservoir with a vertical fracture at the center and considered the equal height for both hydraulic fracture and formation. They further assumed that there is no pressure drop in

the hydraulic fracture. The main contribution of their work is that the fracture length can be calculated from the production decline rate.

Tinsley et al. (1969) discussed the impact of the hydraulic fracture height on the production rate. In contrast to the other models, which assumed the hydraulic fracture and the formation height are equal, this model is applicable when the formation and hydraulic fracture height are not equal.

In 1974, Gringarten et al. documented the unsteady-state pressure distribution of a well with an infinite conductivity fracture. They reported three main flow regimes: early time linear flow (one-half slope in log-log plots), a pseudo radial flow regime which gives a semi log straight line response, and pseudo steady state flow with a unit slope line. Gringarten et al. (1975) presented the fractured well behavior type curves with the dimensionless variables. In their work, they also proposed an equation for the fracture length calculation based on dimensionless wellbore pressure and formation permeability.

Cinco-ley et al. (1978) studied the transient behavior of wells with single finite conductivity fractures. They presented type curves, which are valid after a specific dimensionless time, and showed the differences between the finite fracture conductivity model and Gringarten et al. (1974) infinite fracture conductivity model. They also identified four different flow regimes: linear, bilinear, formation linear, and pseudo radial flow. Figure 2.2 represents these four different flow regimes. They also compared the results of McGuire and Sikora's, Prats's and their own model for an example case, the results showed a good agreement.

Cinco-ley and Samaniego (1981) proposed a new method for pressure transient analysis for fractured wells with bilinear flow regime (Figure 2.2). Their new model detects the time at which wellbore storage effects disappear. The model considered finite fracture conductivity, and they also proposed a correlation to calculate the effective

wellbore radius. This effective wellbore radius calculation is the basis of their new type curves. Also, the reservoir parameters can be estimated by using the new type curves which are provided for bilinear flow regime.

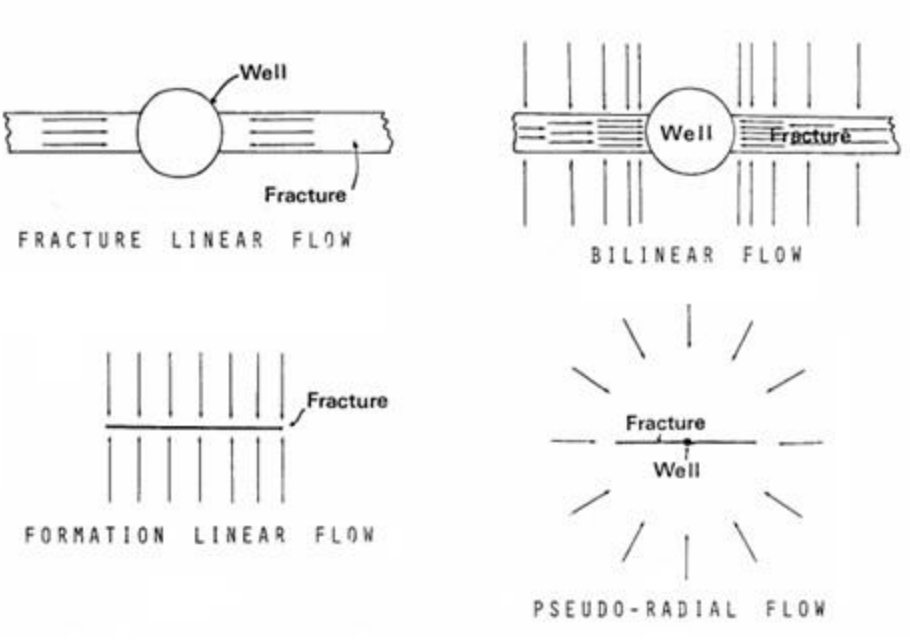

Figure 2.2: Different flow regimes in hydraulically fractured reservoirs, (Cinco-Ley and Samaniego, 1981)

Bennett et al. (1985) and Camacho et al. (1987) presented their models for the hydraulically fractured wells producing from different layers. Bennet et al. (1985) study considered equal fracture lengths, while the Camacho et al. (1987) model is applicable for unequal hydraulic fracture lengths. They also stated that if two different layers connect to each other, it will positively affect the cumulative production performance.

Cinco-Ley and Meng (1988) outlined their work on transient flow period of a well with a finite conductivity fracture. Differently from other models, they proposed a naturally fractured (dual porosity) reservoir with a hydraulically fractured well. In order

to represent a dual porosity reservoir, they used pseudo steady state (Warren and Root, 1963) and transient (de Swaan O., 1976 and Kazemi, 1969) dual porosity models. In that work they proposed a model named trilinear model which incorporates the flow in matrix blocks, natural fractures and hydraulic fractures. They also proposed the flow regime identification method and provided the appropriate type curves for each flow regime.

Raghavan et al. (1997) developed a mathematical model stating that their idea was "…creating a system whose long-time response will be identical to that of a single fracture of length equal to the spacing between the outermost fractures". For this purpose they used the effective well-radius concept, and dimensionless conductance of the system. Figure 2.3 represents their type curve for different number of hydraulic fractures (n). In order to calculate the flow rate of the multi-fractured well, one can find the effective wellbore radius from the type curve and plug it into well deliverability equation for horizontal wells. They further stated that mechanical or reservoir conditions might create an unequal fracture spacing conditions, so they proposed a type curve for unequal fracture spacing condition as well.

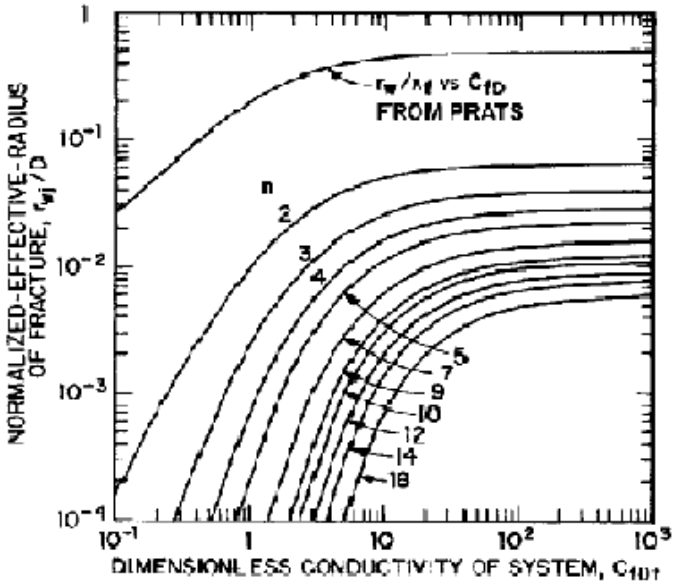

Figure 2.3: Conductivity curve of multiply fractured horizontal wells, (Raghavan et al. 1997)

Al-Kobaisi et al. (2006) studied a hybrid reservoir model which combines a numerical hydraulic fracture model with an analytical reservoir model. They stated that their objective was to remove simplifying assumptions for hydraulic fracture flow. An advantage of the numerical hydraulic fracture model is that the hydraulic fracture properties such as shape, width, and variable conductivity can be modeled numerically, while the reservoir flow model is still analytical and keeps the computational work manageable.

Mederios et al. (2006) developed a semi-analytical reservoir model for horizontal wells in layered reservoirs. Reservoir heterogeneity is considered, along with local gridding, and grid boundaries are coupled analytically. Their semi-analytical model is more advantageous than the analytical models when reservoir heterogeneity is considered.

In 2009, Brown et al. and Ozkan et al. presented their trilinear model. This model incorporates the flow into three different flow regions: the zone beyond the fracture tips, the zone between two adjacent hydraulic fractures, and the hydraulic fracture zone. They used Laplace transformation to obtain solution for their model. It is a common knowledge that hydraulic fracturing operation creates stress induced natural fracture network in tight formations, such as shale. This naturally fractured zone can be implemented in the trilinear model by using pseudo-steady state or transient dual porosity models; model details are given under the related section in this thesis.

Patzek et al. (2013) presented a simplified solution for production from unconventional reservoirs. In his study, the gas diffusivity equation is solved analytically, and the pseudo-pressure approach is used to linearize the gas diffusivity equation; model details will be given under the related section in this thesis.

2.2 Analytical Dual Porosity Models

Hydraulic fracturing treatment in tight formations creates stress induced fracture network and also triggers the existing natural fractures. Existing dual porosity models in literature are employed to model this natural fracture network in analytical reservoir models. Dual porosity models consist of reservoir matrix and natural fracture network. Reservoir parameters can be defined as an average value of matrix and fracture properties (bulk properties), or intrinsic properties of matrix and natural fractures. Additionally, the storativity and the transmisivity ratios are important parameters for dual porosity models, and need to be explained. The storativity gives the ratio of natural fracture storage capacity to total storage capacity of the medium. The transmisivity ratio in turn measures the flow capacity from matrix to natural fractures.

Warren and Root (1963) defined naturally fractured reservoir as a permeable medium which consists of two parts; part one (matrix) contributes to the pore volume capacity, but negligible flow capacity, while the part two (fracture) contributes to the fluid flow capacity. Figure 2.4 represents the model considered in Warren and Root (1963) dual porosity model. This model is known in literature as the "sugar cube" model. As a customary assumption, flow occurs only through the fractures to the wellbore, while the matrix provides fluid to natural fractures. Warren and Root (1963) model considers unsteady state flow from matrix to fractures. Their model's parameters are defined as bulk properties.

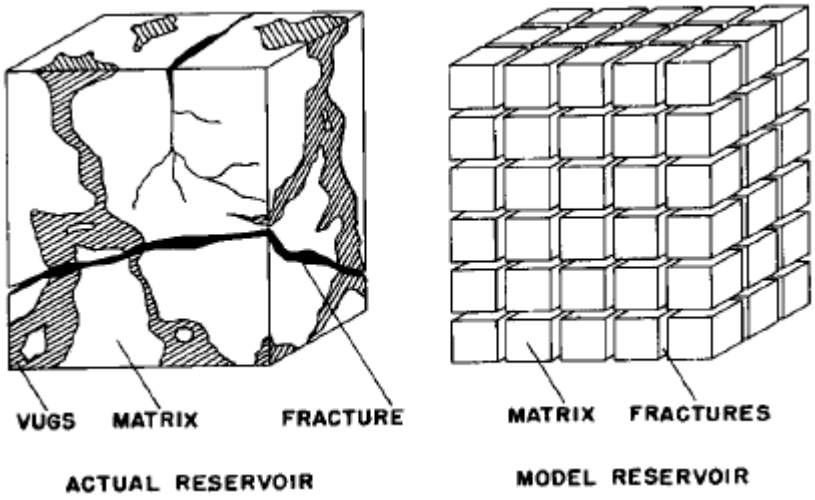

Figure 2.4: Warren and Root's dual porosity idealization, (Warren and Root, 1963)

Kazemi's (1969) dual porosity model extends the Warren and Root (1963) "sugar cube" dual porosity model by considering transient flow from matrix to fractures and from fractures to the wellbore. Kazemi's dual porosity model also represents a new dual porosity geometry, which is also known as a slab model; Figure 2.5 shows the Kazemi's slab model. His model assumes homogeneous and isotropic matrix properties. In addition, it is assumed that fluid flow to the wellbore only occurs through the natural

fractures. Kazemi (1969) and Warren and Root (1963) dual porosity models give identical responses except the transition time which occurs when the fluid flow from matrix to fractures starts. In 1976, Kazemi et al. developed a naturally fractured reservoir model that considers water-oil (multiphase) flow by defining a new matrix shape factor.

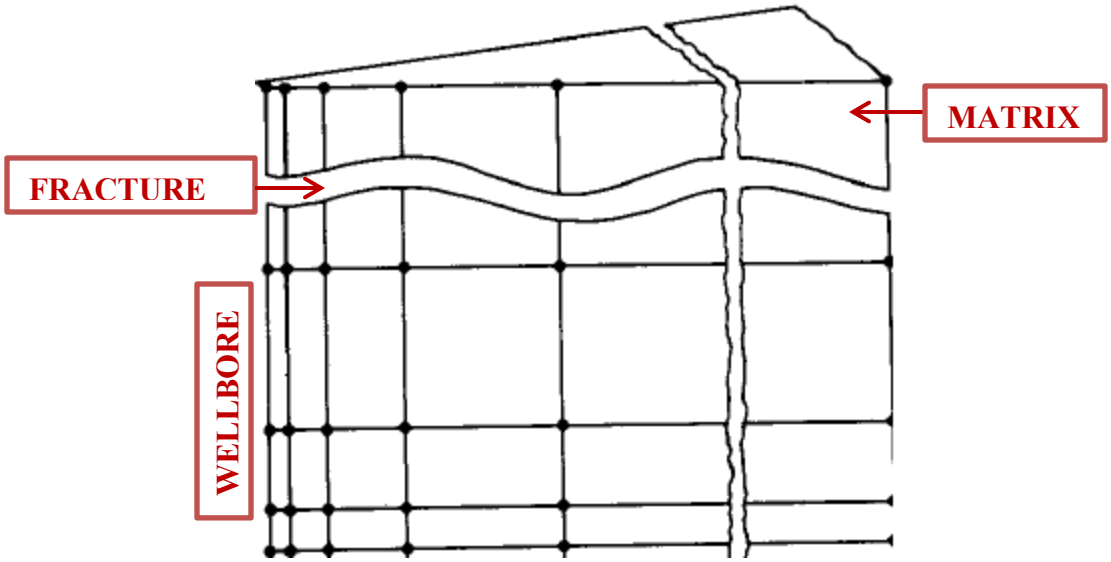

Figure 2.5 Kazemi's dual porosity idealization, (Kazemi, 1969)

de Swaan O., (1976) proposed another dual porosity model which considers transient flow from matrix to the fracture network. His transient model can be defined by intrinsic properties of matrix and natural fractures. Although the slab matrix shape is considered in his model, spherical matrix block solution is also presented in the same study.

Serra et al. (1983) demonstrated a new dual porosity model which is identical to the de Swaan O., (1976) model but with different storativity and transmisivity definitions. They used the intrinsic parameters of matrix and fracture medium, instead of bulk properties which modified the definition of key parameters.

Apaydin (2012) developed two new dual porosity models specific to naturally fractured unconventional reservoirs. His models consider sphere matrix geometry, (given in Figure 2.6) and transient fluid transfer from the matrix to the natural fracture. His first model consists of macro-fractures, micro-fractures on the sphere matrix block, and the core of matrix block. Fluid is first transferred from the matrix core to the micro-fracture networks, then from micro-fracture network to macro-fracture network. Basically, micro-fracture network enhances the permeability of surface layer of matrix block. Results show that the micro-fracture network excessively contributes to the unconventional reservoir performance.

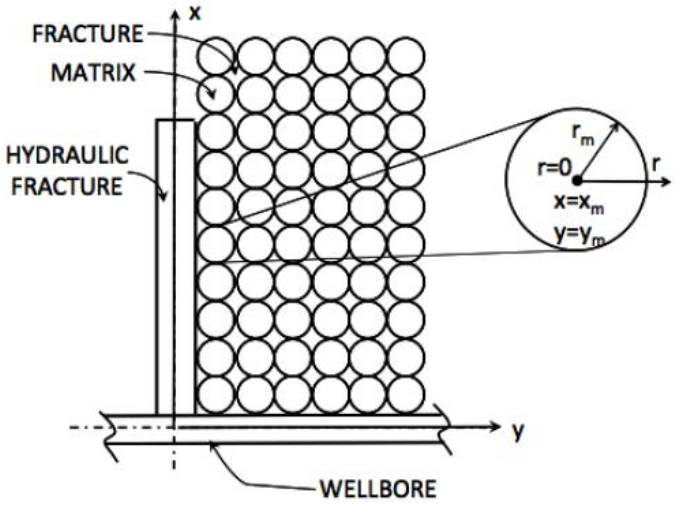

Figure 2.6 Apaydin's dual porosity idealization, (Apaydin, 2012)

Furthermore, slip flow, which is an important phenomenon especially for shale reservoirs, is taken into account in Apaydin's (2012) dual porosity model. This model also considers stress dependent natural fracture permeability. A combination of slip flow and stress dependent natural fracture permeability can be handled by the new transfer function. He stated that both of his models can be incorporated with analytical and numerical reservoir flow models.

2.3 EXPERIMENTAL STUDIES ON STRESS DEPENDENT PERMEABILITY

Permeability is the reservoir parameter which measures the ability of the rock to flow a reservoir fluid. Analytical and numerical reservoir models treat permeability as a static parameter most of the time. However, this assumption may not be true, because of the changing stress conditions in reservoir. Thus, experimental studies are conducted to shed light on the relationship between permeability and changing stress conditions. Experimental researches on stress-dependent permeability are presented herein.

In 1985, Barton et al. experimentally studied the behavior of solid rock samples with natural unfilled joints under the stress loading/unloading conditions. They considered interlocking joints and mismatched joints, and five different rock types. They studied the normal closure of joints, and shear displacement under different stress conditions. As a result of their experiments, they proposed a hyperbolic model for the normal deformation of natural fractures.

Soeder (1988) analyzed the core samples from Middle Devonian Age Marcellus shale. Although the prior goal of their work is to obtain data for Devanian shale reservoir simulation study, surprisingly they specified the factors controlling the gas production from organic rich formations. Presence of natural fractures, organic content of the medium and thermal maturity is the main controlling mechanisms in organic rich formations according to Soeder (1988). In the same study, he stated that the gas permeability showed excessive stress dependence.

Wilbur and Amadei (1990) conducted an experiment on natural and artificial fractures transmissivity behavior with changing normal stresses. They stated that the hydraulic conductivity and normal stress relationship is non-linear. Based on their stress unloading cycles, they further claimed that permeability of fracture non-recoverably

reduces, and the stress history of the fracture also affects the hydraulic conductivity of the fracture.

Luffel et al. (1993) published an experimental study conducted on shale matrix permeability measurement. Their study identified that some of the micro-fractures remained open under the net overburden stress. Later, these micro fractures are considered in the dual porosity models which are developed for shale reservoirs.

Makurat and Gutierrez (1996) stated that the natural fracture existence in the reservoir may affect hydrocarbon production performance positively or negatively. Natural fractures may increase the permeability of the system; they may also behave as barriers against the matrix flow and reduce the production. Because of this, they conducted experiments on fracture flow and fracture permeability. Based on their research they claimed that the stress dependent fracture aperture, tortuosity, roughness, and the fracture normal stress are the main factors that control the permeability of fractures.

Fredd et al. (2000) conducted an experimental research on fracture conductivity changes especially for the water fracturing treatments. They considered aligned and displaced fracture faces, and reported fracture conductivities for different stress conditions. Their results show that increasing the stress applying on the fractures reduces the permeability of the rock.

Gutierrez et al. (2000) experimentally investigated the natural fracture permeability in shale. Natural fracture permeability behavior with changing stress conditions and whether the natural fractures are completely closed with the excessive normal stress are two main questions answered in their study. Gutierrez et al. (2000) observed that the natural fracture permeability decreases remarkably, but never

completely closed unless cementation occurred. It is concluded that natural fractures are the main conduits for fluid flow, even under high normal stress.

Kwon et al. (2004) conducted an experimental study on clay content and anisotropy effects on shale permeability. They also studied the relation between permeability and effective stress, and based on their experiments they proposed a cubic-law correlation between shale permeability and effective pressure. They noted that increasing clay content reduces the permeability of shale.

Eshkalak et al. (2013) investigated the geo-mechanical properties of Marcellus shale. They generated a common source for securing these rock mechanical properties, geomechanical well logs, and studied various characteristics such as minimum horizontal stress, Young, bulk shear modulus, as well as Poison's ratio that play an important role in defining the stress profiles of an unconventional reservoir. Moreover, having access to rock's geo-mechanical properties enhances the understanding of parameters such as conductivity and pressure dependency of permeability (Eshkalak M. O., 2013).

Cho et al. (2013) presented changes in natural fracture permeability of shale with altering stress conditions, and its impact on production. They examined permeability measurement experiments with shale core samples under the various stress conditions. In order to represent natural fracture in shale, they created saw-cut fractures on shale core specimens. They observed reduction in permeability with increasing effective stress conditions. They used their natural fracture experimental data to see the applicability of the pressure dependent permeability correlations existing in literature. They provided the pressure dependent permeability correlation coefficients in their study for their sample cores. Most of the selected correlations handle the natural fracture permeability reduction with increasing effective stress. They further studied the effect of natural fracture permeability reduction in shale with the trilinear model (Brown et al. (2009). Based on

their model results, they stated that even though the permeability reduction in natural fractures is significant, the permeability of fractures is still enough to conduct the hydrocarbon flow from reservoir to hydraulic fracture. This conclusion is in agreement with Gutierrez et al. (2000) comments on natural fractures; as it is stated earlier in this chapter, they concluded that natural fractures do not completely close. Since the matrix permeability is too low to compare to natural fracture permeability, the remaining permeability of natural fractures can sustain the necessary conductivity for fluid flow.

2.4 Coupled Pressure Dependent Permeability and Fluid Flow Models

Experiments concerning matrix and fracture permeability reduction with changing stress conditions are well studied in the literature. In order to illustrate the permeability reduction effects on production, fluid flow models must be coupled with stress dependent permeability. To address this issue, there are several analytical and numerical approaches available in the literature as given below.

Ostensen (1986) modified gas pseudo-pressure in order to implement pressure dependent permeability in gas well testing. He stated that as production continues; pressure dependent permeability becomes important and also drawdown behavior is more sensitive to stress dependent permeability rather than build-up.

Pedrosa (1986) analytically coupled stress dependent permeability with fluid flow. He proposed the permeability modulus approach to solve this problem. He also developed type curves to analyze build-up and draw-down responses of reservoirs with stress dependent permeability.

Celis et al. (1994) published a model which characterized unsteady-state or pseudo steady state flow of pressure sensitive naturally fractured reservoirs. This model also employs permeability modulus concept to consider pressure dependent permeability,

as well as fluid flow in dual porosity medium (matrix block to fracture) modeled by De Swaan (1976).

Bai et al. (1999) presented a model which is numerically coupled fluid flow and fracture deformation. They considered a dual porosity medium to model the naturally fractured reservoir. They concluded that depending on rock properties, fracture deformation may be important and affects the reservoir production performance.

Chin et al. (2000) numerically coupled geomechanical effects with fluid flow in order to see its effects on production from stress sensitive reservoirs. The finite element method is used to develop the model. Pore pressure depletes with continuing production, consequently increases the stress applied on the fracture. This dynamic process also reduces the fracture permeability. For that reason, Chin et al. (2000) related fracture permeability to the pore pressure. They embedded pressure dependent permeability functions into gas pseudo pressure transform. They also developed a type curve demonstrating the differences between pressure dependent permeability case and constant permeability case. The effect of pressure dependent permeability on production may be insignificant, if the initial permeability is high.

Franquet et al. (2004) evaluated the importance of pressure dependent permeability in tight gas reservoirs. For this purpose, they used the exponential permeability vs. pore pressure drop correlation that embedded this correlation into gas pseudo pressure transform. Their aim was to find the impact of pressure dependent permeability on apparent permeability and skin factor calculations.

Zhao and Chen (2006) incorporated geomechanical effects with fluid flow in naturally fractured reservoirs. Contribution of their model is an anisotropic naturally fractured (modeled with dual porosity concept) medium that can be modeled consistently.

Bagheri and Settari (2008) presented a numerical solution for geomechanics in naturally fractured reservoirs with coupled fluid flow. The core difference between their work and previous works is that they solved matrix and fracture geomechanics individually, and then coupled them with fluid flow using dynamic permeability tensor.

Cipolla et al. (2010) used Fredd et al.'s (2000) laboratory experiments for pressure dependent fracture conductivity in their reservoir simulator. From this they analyzed that which circumstances required pressure dependent natural fracture conductivity needs to be accounted for. According to their findings, they stated that shale with a relatively higher Young's Modulus ($5x10^6$ psi), such as the Barnett shale, does not cause significant production loss.

Tao et al. (2010) investigated the pressure dependent fracture permeability in naturally fractured reservoirs with fully coupled reservoir flow and the fracture deformation model. They stated that the natural fractures are the main flow channels in a naturally fractured reservoir environment; therefore, they focused on fracture permeability changes and its effect on production. They further claimed that matrix deformation is insignificant compared to fractures in a naturally fractured medium. They used the Barton-Bandis joint deformation model (Bandis et al., 1983) and Barton et al., 1985) to construct a relationship between the effective stress and fracture deformation. They concluded that the fracture permeability reduces with production under the isotropic stress condition.

In 2013, Moinfar et al. coupled geomechanics and flow simulation for a naturally fractured reservoir. Their work is among the first to incorporate geomechanics and reservoir flow with an embedded discrete fracture model. They also used Barton-Bandis joint deformation model in order to consider geomechanical effects in the discrete fracture network. They extended their studies by evaluating geomechanical effects on

hydraulic fractures by using a particular effective stress–fracture conductivity table. Their results show insignificant cumulative production difference between the dynamic and static fracture conductivity conditions for an example case.

Aybar et al. (2014) modified the Apaydin (2012) and Cho (2012) dual porosity model to investigate pressure dependent natural fracture permeability effects on production performance. They used the trilinear model and proposed an average reservoir pressure calculation to couple the dual porosity model with the reservoir flow model. Their approach is able to simulate constant bottom hole pressure production scenarios.

Eshkalak et al. (2014) proposed their model with incorporating all the pressure dependent phenomena in a simple reservoir model. The importance of their study is to show which pressure dependent parameter needs to be taken in to account in unconventional reservoir modeling. Results of their study proved that the minimum ingredients required to model shale gas reservoirs are: (1) desorption phenomena and (2) pressure-dependent permeability for hydraulic and induced-fractures. Consequently, it is unnecessary to add more mechanisms and nonlinearity into the model.

Chapter 3: Analytical Models for Hydraulically Fractured Homogeneous Unconventional Reservoirs

The objective of this chapter is to investigate two analytical models, which were developed for hydraulically fractured unconventional reservoirs. Namely, the simplified model for gas production from a hydraulically fractured unconventional reservoir, developed by Patzek et al. (2013), and the trilinear flow model, proposed by Ozkan et al. (2009) and Brown et al. (2009), are outlined in this chapter. A comprehensive description of the flow models and the assumptions associated with the models are provided. Derivations of the equations used in the models to calculate the gas production rate are stated. Results of these two analytical models for a synthetic case are compared with the results obtained from a commercial reservoir simulator (CMG, IMEX 2012). Lastly, two analytical models and the commercial reservoir simulator are used to conduct a sensitivity analysis for practical ranges of reservoir and well parameters. Such an analysis is essential since it provides a better understanding of parameters that are dominating the well performance in different time periods.

3.1 The Simplified Model for Gas Production from a Hydraulically Fractured Unconventional Reservoir

Patzek et al. (2013) developed a nonlinear analytical model for multiply fractured horizontal wells in unconventional reservoirs. The model solves the gas diffusivity equation numerically, and provides an approximate solution for forecasting the unconventional reservoirs production performance. Patzek et al. (2013) demonstrated that such a solution is practical and enables us to make analysis with different combination of parameters that are influencing the performance of hydraulically fractured wells. Figure 3.1 depicts the hydraulic fractures and the horizontal well schematic used in the

simplified model (Patzek et al., 2013). Here we will present the linearized version of the Patzek et al. (2013) model.

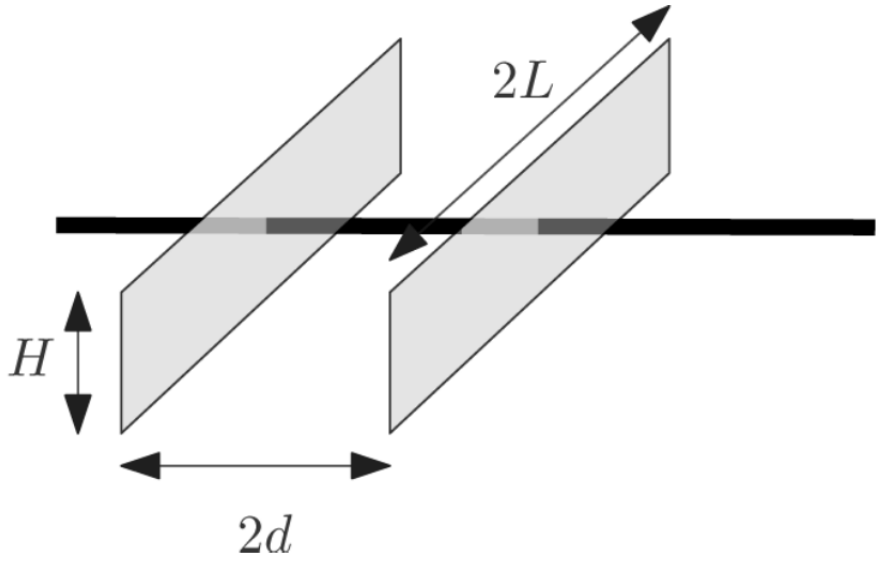

Figure 3.1: Schematic of the Simplified Model, (Patzek et al., 2013)

3.1.1 Assumptions for the Simplified Model

Assumptions for the simplified model for gas production from a hydraulically fracture unconventional reservoirs are highlighted as follows:

1. Linear flow

   The model assumes linear and horizontal single gas phase flow.

2. Constant gas diffusivity coefficient

   The simplified model incorporates Al-Hussainy et al. (1966) pseudo-pressure approach to linearize the gas diffusivity equation. In addition, the gas diffusivity coefficient is assumed as a constant in order to obtain an approximate analytical solution. This includes a constant temperature for the control volume under the study, a constant viscosity, permeability, and compressibility.

3. Infinite hydraulic fracture conductivity

The simplified model considers infinite hydraulic fracture conductivity.

4. Fracture height treated to be equal to formation height

The model considers the zone between two adjacent hydraulic fractures as a homogeneous reservoir and an identical formation and hydraulic fracture height.

5. Darcy flow

Darcy flow is considered for the flow of gas. In addition, desorption/adsorption of gas in the system is neglected in this study.

3.1.2 Formulation of the Simplified Model

The model solves the gas diffusivity equation in the time domain with using the method of separation of variables proposed by Carslaw and Jaeger (1959). There are several steps taken before arriving to the gas diffusivity equation. In this section, these steps are outlined following the same lines as Patzek et al. (2013). Firstly, the gas material balance is applied for the unit flow area to obtain Eqn. 3.1, and Darcy's law (Eqn. 3.2) substituted in Eqn. 3.1 to arrive to Eqn. 3.3.

$$-\frac{\partial(\rho_g u_g)}{\partial x} = \frac{\partial[S_g \phi \rho_g + (1-\phi)\rho_a]}{\partial t}, \qquad \text{(Eqn. 3.1)}$$

where,

u_g – Darcy (superficial) velocity of gas

S_g – Gas saturation

ρ_g – Free gas density, kg/m^3

ρ_a – Adsorbed gas density, kg gas / m^3 solid

ϕ – Rock porosity

$$u_g = -\frac{k}{\mu_g}\frac{\partial p}{\partial x}, \qquad \text{(Eqn. 3.2)}$$

where,

$\mathrm{k} - \text{Absolute premeability of the rock}, \mathrm{m}^2$

$\mu_g - \text{Gas Viscosity}, \mathrm{Pa} - \mathrm{s}$

$$\frac{\partial}{\partial x}\left(\frac{k\rho_g}{\mu_g}\frac{\partial p}{\partial x}\right) = S_g\phi\frac{\partial \rho_g}{\partial p}\frac{\partial p}{\partial t} + (1-\phi)\frac{\partial \rho_a}{\partial \rho_g}\frac{\partial \rho_g}{\partial p}\frac{\partial p}{\partial t}. \qquad \text{(Eqn. 3.3)}$$

As a customary approach, the gas density can be obtained by the equation of state for real gases, which is given by Eqn. 3.4.

$$\rho_g = \frac{M_g p}{Z_g R T}, \qquad \text{(Eqn. 3.4)}$$

where,

P – Pressure, Pa

Z_g – Compressibility factor of gas

M_g – Pseudo molecular mass of gas, kg/mol

R – Universal gas constant, 8.314 J/(K mol)

T – Temperature, K.

The isothermal compressibility of gas and the differential equilibrium portioning coefficient of gas are given by Eqn. 3.5 and Eqn. 3.6, respectively.

$$c_g = \frac{1}{\rho_g}\left(\frac{\partial \rho_a}{\partial \rho_g}\right)_{T=constant} = \frac{1}{p} - \frac{1}{Z_g}\frac{\partial Z_g}{\partial p}, \qquad \text{(Eqn. 3.5)}$$

$$K_a = \left(\frac{\partial \rho_a}{\partial \rho_g}\right)_{T=constant}. \qquad \text{(Eqn. 3.6)}$$

Substituting Eqns. 3.5 and 3.6 into Eqn. 3.3, the transient gas flow equation for a horizontal and linear flow is derived (Eqn. 3.7).

$$\frac{\partial}{\partial x}\left(\frac{k\rho_g}{\mu_g}\frac{\partial p}{\partial x}\right) = \left[S_g\phi + (1-\phi)K_a\right]c_p\rho_g\frac{\partial p}{\partial t}. \quad \text{(Eqn. 3.7)}$$

Patzek et al. (2013) stated that $(1-\phi)K_a$ term can be neglected (specifically for the Barnett shale), because this gas adsorption term is much smaller than $S_g\phi$ term. Finally, using Al-Hussainy et al. (1966), the real gas pseudo-pressure approach in Eqn. 3.7, the gas diffusivity equation is obtained in terms of pseudo-pressure and is given in Eqn. 3.8.

$$\frac{\partial^2 m(p)}{\partial x^2} = \left(\frac{S_g\phi\mu_g c_g}{k}\right)\frac{\partial m(p)}{\partial t} = \frac{1}{\alpha}\frac{\partial m(p)}{\partial t}. \quad \text{(Eqn. 3.8)}$$

This is a partial differential equation showing pseudo pressure m as a dependent of two independent variables x (location) and t (time).

3.1.2.1 Definitions of the Dimensionless Variables in the Simplified Flow Model

This section outlines the definition of dimensionless variables used in the simplified model with following the same lines presented by Patzek et al. (2013). Starting with dimensionless pseudo-pressure (Eqn. 3.9), all other dimensionless parameters are provided below:

$$\widetilde{m} = \frac{m_i - m}{m_i}, \quad \text{(Eqn. 3.9)}$$

where,

$\widetilde{m}$ – Dimensionless pseudo-pressure

m_i – Initial reservoir pseudo-pressure, psi^2/cp

$$\tilde{t} = \frac{t}{t_r}, \quad \text{(Eqn. 3.10)}$$

where,

$\tilde{t}$ – Dimensionless time

t_r – Characteristic time of diffusion, sec

$$t_r = \frac{d^2}{\alpha_r}, \quad \text{(Eqn. 3.11)}$$

d – Half distance between two hydraulic fractures, m

α_r – Reference value of the hydraulic diffusivity of gas, m^2/sec

$$\alpha_r = \frac{k}{S_g \phi (\mu_g c_g)_r}, \quad \text{(Eqn. 3.12)}$$

$$\tilde{x} = \frac{x}{d}, \quad \text{(Eqn. 3.13)}$$

$\tilde{x}$ – Dimensionless distance

x – Dimensional distance in the x-direction, m

Substituting these dimensionless variables into Eqn. 3.8, Eqn. 3.14 is obtained.

$$\frac{\partial \tilde{m}}{\partial \tilde{t}} = \frac{\alpha}{\alpha_r} \frac{\partial^2 \tilde{m}}{\partial \tilde{x}^2}. \quad \text{(Eqn. 3.14)}$$

Initial and boundary conditions for Eqn. 3.14 are given in Eqn. 3.15 and Eqn. 3.16, respectively.

$$\tilde{m}(\tilde{x}, \tilde{t} = 0) = 0. \quad \text{(Eqn. 3.15)}$$

Initial condition given Eqn. 3.15 shows that the initial pressure is "zero" dimensionless pseudo-pressure according to its definition.

$$\tilde{m}(\tilde{x} = \pm 1, \tilde{t} > 0) = \widetilde{m_f} = 1. \quad \text{(Eqn. 3.16)}$$

Boundary condition given Eqn. 3.16 means that the constant pressure at hydraulic fractures is “one” dimensionless pseudo-pressure according to dimensionless pseudo-pressure definition.

3.1.2.2 Solution for the Simplified Model for Gas Production from a Hydraulically Fractured Unconventional Reservoir

Once the gas diffusivity equation is derived, the model calculates the pseudo-pressure distribution between two adjacent hydraulic fractures. Constant bottom-hole pressure condition is considered as a production scenario, and all the hydraulic fractures have an identical pseudo-pressure.

The production rate of each hydraulic fracture at down-hole condition can be obtained by the multiplication of hydraulic fracture surface area with the superficial velocity of the gas. Note that if the midpoint between two hydraulic fractures assumed as origin, then the hydraulic fractures are placed in between +d and –d.

$$q_R(t) = 2A_f u(x = 0, t) = -\frac{A_f k Z_f}{p_f}\left(\frac{\partial m}{\partial x}\right)_{x=\pm d}, \qquad \text{(Eqn. 3.17)}$$

where,

$$A_f = 2HL, \qquad \text{(Eqn. 3.18)}$$

where,

A_f – The total surface area of the hydraulic fractures, m^2

H – Height of the hydraulic fractures, m

L – Hydraulic fracture half-length, m.

In order to linearize Eqn. 3.14 with respected boundary conditions, the model assumes diffusivity constant α equals to α_r (Eqn. 3.12). The model uses the separation of variables technique to solve the partial differential equation given by Eqn. 3.14 and the result is given by Eqn. 3.19

$$\frac{\widetilde{m}}{\widetilde{m_f}} = \widetilde{m} = 1 - \frac{4}{\pi}\sum_{n=0}^{\infty}\frac{(-1)^n}{2n+1}e^{(-2n+1)^2\pi^2\tilde{t}/4)}\cos\left(\frac{(2n+1)\pi\tilde{x}}{2}\right). \qquad \text{(Eqn. 3.19)}$$

Patzek et al. (2013) stated that the right hand side of Eqn. 3.19 can be differentiated separately in order to differentiated the left hand side, because of the exponential factor in this series converges uniformly for all x(t>0). The average pseudo-pressure in the reservoir is an exponential function of time and given by Eqn. 3.20.

$$\frac{1}{2}\int_{-1}^{1}\widetilde{m}(\tilde{x}', t')d\tilde{x}' = 1 - \frac{4}{\pi}\sum_{n=0}^{\infty}\frac{(-1)^n}{2n+1}e^{(-2n+1)^2\pi^2\tilde{t}/4)}. \qquad \text{(Eqn. 3.20)}$$

The average reservoir pseudo-pressure can be calculated by using Eqns. 3.21 and 3.22.

$$\frac{1}{2}\int_{-1}^{1}(-1)^n\cos\left(\frac{(2n+1)\pi\tilde{x}}{2}\right)d\tilde{x}' = \frac{2}{(2n+1)\pi} \quad \text{for n} = 0,1 \ldots, \qquad \text{(Eqn. 3.21)}$$

$$\langle m(t)\rangle = m_i\frac{8}{\pi^2}\sum_{n=0}^{\infty}\frac{1}{(2n+1)^2}e^{\left[-(2n+1)^2\pi^2 t\alpha_r/(4d^2)\right]}. \qquad \text{(Eqn. 3.22)}$$

Using the dimensionless variables, the model calculates the pseudo-pressure gradient at the hydraulic fracture by Eqn. 3.23:

$$\frac{4}{\pi}\sum_{n=0}^{\infty}(-1)^n e^{(-2n+1)^2\pi^2\tilde{t}/4)}\sin\left(\frac{(2n+1)\pi}{2}\right). \qquad \text{(Eqn. 3.23)}$$

Patzek (2013) stated that for all n values the sinus term goes to "1", since,

$$(-1)^n\sin\left(\frac{(2n+1)\pi}{2}\right) = 1. \qquad \text{(Eqn. 3.24)}$$

Finally Eqn. 3.23 becomes

$$\frac{\partial \tilde{m}}{\partial \tilde{x}} = 2\sum_{n=0}^{\infty} e^{(-2n+1)^2\pi^2\tilde{t}/4)}. \qquad \text{(Eqn. 3.25)}$$

The dimensional form of pressure gradient is given by Eqn. 3.26

$$\frac{\partial m}{\partial x} = -\frac{m_i}{d}\frac{\partial \tilde{m}}{\partial \tilde{x}}\,. \qquad \text{(Eqn. 3.26)}$$

Substituting the Eqn. 3.26 back in the gas flow rate equation (Eqn. 3.17) at down-hole conditions Eqn. 3.27 is obtained. Note that gas flows from both sides of the hydraulic fracture, therefore factor of two comes into the gas flow rate equation

$$q_R(\tilde{t}) = 2\frac{A_f k Z_f m_i}{p_f d}\sum_{n=0}^{\infty} e^{(-2n+1)^2\pi^2\tilde{t}/4)}. \qquad \text{(Eqn. 3.27)}$$

The model uses the gas expansion factor (Eqn. 3.28) to represents the produced gas at stock tank conditions

$$E_g = \frac{V_{gas\ in\ fracture}}{V_{gas\ in\ stock\ tank}} = \left(\frac{p_{ST}}{T_{ST}}\right)\frac{Z_f T}{p_f}\,, \qquad \text{(Eqn. 3.28)}$$

where,

P_{ST} – Pressure at standard conditions, 1 atm

T_{ST} – Temperature at standard conditions, 60 °F.

Incorporating the gas expansion factor with the gas flow rate equation for each hydraulic fracture is given in Eqn. 3.27; stock tank condition production rate for each hydraulic fracture can be obtained (Eqn. 3.29).

$$q_{ST}(t) = 2\frac{A_f k m_i}{p_{ST} d}\frac{T_{ST}}{T_i}\sum_{n=0}^{\infty} e^{(-2n+1)^2\pi^2\tilde{t}/4)} \qquad \text{(Eqn. 3.29)}$$

where,

T_i – Temperature at reservoir conditions, °F

Here the summation of the series in Eqn. 3.29 includes the integration stated in Eqn. 3.30

$$\int_0^t e^{\left[-(2n+1)^2\pi^2\check{t}\widetilde{\alpha_r}/(4d^2)\right]}dt' = \frac{4d^2}{\pi^2(2n+1)^2\alpha_r}\left(1 - e^{\left[\frac{-(2n+1)^2\pi^2\check{t}\widetilde{\alpha_r}}{4d^2}\right]}\right) . \qquad \text{(Eqn. 3.30)}$$

The cumulative gas production is a function of gas flow rate and the production time and can be calculated by Eqn. 3.31

$$Q_{ST} = \int_0^t q_{ST}(t')dt' . \qquad \text{(Eqn. 3.31)}$$

In light of Eqns. 3.29, 3.30 and 3.31, the cumulative production from each hydraulic fracture can be calculated by Eqn. 3.32

$$Q_{ST}(t) = \frac{A_f d\phi S_g(\mu_g c_g)_r m_i}{p_{ST}} \frac{T_{ST}}{T_i}\left(1 - \frac{8}{\pi^2}\sum_{n=0}^{\infty}\frac{1}{(2n+1)^2}e^{\left[-(2n+1)^2\pi^2 t\alpha_r/(4d^2)\right]}\right) .$$

(Eqn. 3.32)

Since the summation term on the right hand side shares the same parameters with average reservoir pressure equation (Eqn. 3.22), the cumulative production equation can be represented by Eqn. 3.33

$$Q_{ST}(t) = \frac{A_f(2d)\phi S_g(\mu_g c_g)_r}{2p_{ST}} \frac{T_{ST}}{T_i} \left(m_i - \langle m(t)\rangle\right) . \qquad \text{(Eqn. 3.33)}$$

In order to simplify Eqn. 3.33, the model defines the hydrocarbon in place by Eqn. 3.34. It must be noted that these equations are derived for a single hydraulic fracture, so in

order to obtain the cumulative production of the horizontal well, number of hydraulic fractures must be multiplied by the single hydraulic fracture cumulative production.

$$HCPV = V_b S_g \phi \,, \qquad \text{(Eqn. 3.34)}$$

where,

V_b – Bulk volume, m^3

Finally, Eqn. 3.33 can be presented as follows:

$$Q_{ST}(t) = \frac{HCPV(\mu_g c_g)_r}{2p_{ST}} \frac{T_{ST}}{T_i} \left(m_i - \langle m(t) \rangle\right) . \qquad \text{(Eqn. 3.35)}$$

All of the necessary equations for gas production performance forecasting are stated above as proposed by Patzek et al. (2013). The results of simplified model implemented in a synthetic unconventional reservoir case will be discussed later.

3.2 THE TRILINEAR FLOW MODEL

Ozkan et al. (2009) and Brown et al. (2009) proposed an analytical flow model for a hydraulically fractured horizontal well in unconventional reservoirs. The zone beyond the hydraulic fracture tips, the inner reservoir zone which is placed between two adjacent hydraulic fractures (Simulated Reservoir Volume, SRV) and the hydraulic fracture flow are analytically combined with the trilinear model. These three different regions may have different properties. Figure 3.2 represents the well and reservoir schematic considered in the trilinear model (Brown, 2009). Although the model is developed for a single representative hydraulic fracture, multiple hydraulic fracture cases can be investigated by this trilinear model.

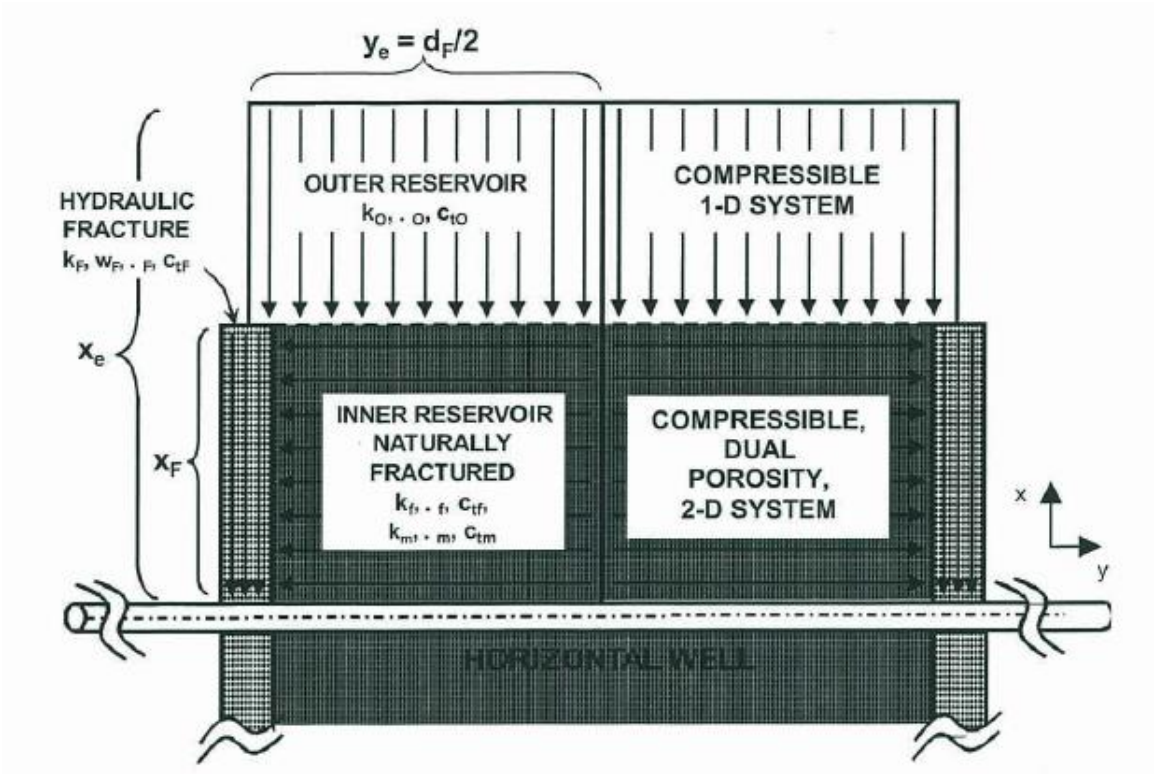

Figure 3.2: Schematic of the Trilinear Model, (Brown, 2009)

3.2.1 Assumptions for the Trilinear Model

Assumptions for the trilinear model are as follows:

1. Linear flow

   Ozkan et al. (2009) and Brown et al. (2009) indicated that the lifespan of unconventional reservoirs are dominated by the linear flow. Therefore, the trilinear model assumed linear flow regime for all three regions.

2. Extremely low matrix permeability

   Extremely low matrix permeability (10^{-9} – 10^{-6} Darcy), which is a characteristic of an unconventional reservoir, is also assumed in the trilinear model.

3. Finite hydraulic fracture conductivity

Hydraulic fracture conductivity is another important aspect of the hydraulically fractured reservoir models as it controls how fast the hydraulic fracture transmits reservoir fluid to the wellbore. The trilinear model assumes finite hydraulic fracture conductivity, which means that the hydraulic fracture properties have an impact on production performance. It is also assumed that the hydraulic fractures are evenly distributed along the horizontal well length, and the hydraulic fracture properties are identical to each other.

4. Equal fracture height to the formation height

   The model also assumes equal hydraulic fracture and formation heights. One dimensional (in the x-direction) flow is assumed in the hydraulic fractures. Flow choking skin proposed by Mukherjee and Economides (1991) is used to overcome the radial flow convergence issue at the intersection of the hydraulic fracture and horizontal well.

5. No flow boundary in the middle of the adjacent hydraulic fractures

   The trilinear model assumes no flow boundary in the middle of the adjacent hydraulic fractures. As can be seen in Figure 3.3, the symmetry element represents the ¼ of the rectangular reservoir with a hydraulic fracture in the middle of y-direction. The model solves the fluid flow problem for one hydraulic fracture; however the cumulative production of the horizontal well can be calculated by multiplying the number of hydraulic fractures with production of the representative hydraulic fracture.

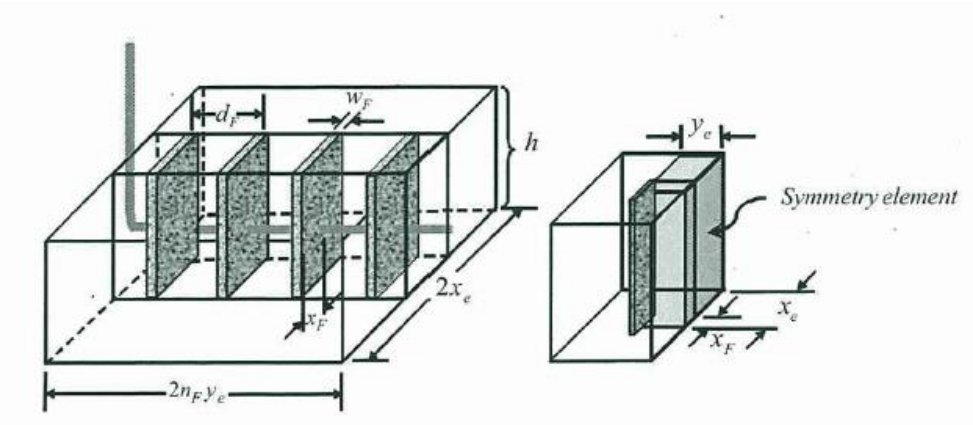

Figure 3.3: Multiply fractured horizontal well and symmetry element considered in the model, (Brown, 2009)

An advantage of the trilinear model is that the simulated reservoir volume (SRV) can be modeled with the dual porosity concepts in order to represent natural or stress induced fracture network. Such a modeling is beneficial because current studies (Cho et al., 2013) claim that the hydraulic fracturing treatment creates stress induced natural fracture network in tight formations, such as shale.

3.2.2 Formulation of the Trilinear Model

This section highlights the definitions of the dimensionless variables, mathematical derivation of the model, and the pertinent equations used in the computational code. The trilinear flow model is derived in terms of dimensionless variables, and the fluid flow equations for three different flow regions are solved and coupled with Laplace transformation domain. Eventually, the trilinear model calculates the dimensionless wellbore pressure (in Laplace domain) for corresponding dimensionless time step. Stehfest (1970) numerical algorithm is employed to convert the solution back to time domain.

The original trilinear model was developed for a constant compressibility fluid such as oil for simplicity purposes. Since gas properties are pressure dependent, the gas diffusivity equation becomes a non-linear equation. Following Al-Hussainy et al. (1966) procedure, the real gas pseudo-pressure approach, the diffusivity equation for real gas flow can be linearized (Brown et al. 2011). In this thesis, the flow of real gases is considered in the derivations.

3.2.2.1 Definitions of the Dimensionless Variables in the Trilinear Model

This section outlines the definition of dimensionless variables used in the trilinear flow model as presented by Brown et al. (2011) and Ozkan et al. (2011). Starting with the dimensionless wellbore pressure (Eqn. 3.36), all other dimensionless parameters are given in the followings:

$$m_{wD} = \frac{k_I\, h}{1422\, q_{F,sc}\, T}\, [m(p_i) - m(p_{wf})]\,, \qquad \text{(Eqn. 3.36)}$$

where,

$\mathrm{m_{wD}} -$ Dimensionless wellbore pseudopressure

$\mathrm{k_I} -$ Inner reservoir permeability, md

$\mathrm{h} -$ Formation thickness, ft

$\mathrm{q_{F,sc}} -$ Hydraulic fracture flow rate, Mscf/d

$\mathrm{T} -$ Reservoir temperature, Rankine

$\mathrm{m(p_i)} -$ Initial reservoir pseudopressure, psi^2/cp

$\mathrm{m(p_{wf})} -$ Flowing wellbore pseudopressure, psi^2/cp

$$m(p) = 2\, \int_{p*}^{P} \frac{p'dp'}{\mu\, z}\,, \qquad \text{(Eqn. 3.37)}$$

where,

$m(p)$ − Pseudopressure transformation, psi^2/cp

P − Pressure, psi

P^* − Reference pressure which can be fracture pressure, psi

μ − Gas viscosity, cp

z − Gas compressibility factor

$$t_D = \frac{2.637\ x\ 10^{-4}\ x\ \eta_I\ x\ t}{x_F^2}, \qquad \text{(Eqn. 3.38)}$$

where,

t_D − Dimensionless time

t − Time, hours

η_I − Inner reservoir diffusivity, ft^2/hr

x_F − Hydraulic fracture half length, ft

$$\eta_I = \frac{k_I}{(\phi c_t)_I\ \mu}, \qquad \text{(Eqn. 3.39)}$$

where,

ϕ_I − Inner reservoir porosity

c_t − Inner reservoir total compressibility, psi^{-1}

$$x_D = \frac{x}{x_F}, \qquad \text{(Eqn. 3.40)}$$

where,

x_D − Dimensionless distance in the x direction, perpendicular to wellbore

x − Distance in the x direction, perpendicular to wellbore, ft

$$y_D = \frac{y}{x_F}, \qquad \text{(Eqn. 3.41)}$$

where,

y_D − Dimensionless distance in the y direction, perpendicular to hydraulic fracture

y − Distance in the y direction, perpendicular to hydraulic fracture, ft

$$C_{FD} = \frac{k_F\, w_F}{\tilde{k}_I\, x_F}, \qquad \text{(Eqn. 3.42)}$$

where,

C_{FD} − Dimensionless fracture conductivity

k_F − Hydraulic fracture permeability, md

w_F − Hydraulic fracture width, ft

$\tilde{k}_I$ − Effective inner reservoir permeability for dual porosity SRV region, md

$$\tilde{k}_I = \frac{k_f\, h_{ft}}{h}, \qquad \text{(Eqn. 3.43)}$$

where,

k_f − Natural fracture permeability, md

h_{ft} − Total thickness of natural fractures, ft

$$C_{RD} = \frac{\tilde{k}_I\, x_F}{k_O\, y_e}, \qquad \text{(Eqn. 3.44)}$$

where,

C_{RD} − Dimensionless reservoir conductivity

k_O − Outer reservoir permeability, md

y_e − Inner reservoir length along the y direction perpendicular to fracture, ft

$$\eta_{FD} = \frac{\eta_F}{\eta_I}, \qquad \text{(Eqn. 3.45)}$$

where,

η_{FD} − Dimensionless hydraulic fracture diffusivity

$\eta_{F,I}$ − Hydraulic fracture and inner reservoir diffusivity, ft^2/hr

$$\eta_{OD} = \frac{\eta_O}{\eta_I}, \quad \text{(Eqn. 3.46)}$$

where,

η_{OD} − Dimensionless outer reservoir diffusivity

η_O − Outer reservoir diffusivity, ft^2/hr

$$\eta_{F,O} = 2.637\ x\ 10^{-4}\ \frac{k_I}{(\phi c_t)_{I,O}\ \mu}, \quad \text{(Eqn. 3.47)}$$

where,

$\eta_{F,O}$ − Fracture and outer reservoir diffusivity, ft^2/hr .

Summary of the derivations for three different flow regions is presented in the next section. The outer reservoir solution is outlined first, and then inner reservoir region (SRV) which can be homogeneous or naturally fractured and hydraulic fracture solution are provided respectively. We note that the over bar ($\bar{}$) represents the Laplace transform domain, and $\underline{s}$ is the Laplace transform parameter with respect to dimensionless time (t_D) in the following sections.

3.2.2.2 The Outer Reservoir Solution

The outer reservoir description in the trilinear model refers to the zone beyond the hydraulic fracture tips. This condition occurs when the reservoir size in the x-direction (perpendicular to the wellbore) is longer than the hydraulic fracture half length. However, Brown et al. (2011) stated that the contribution from outer reservoir is very limited

compared to the simulated reservoir region. The model assumes that the outer reservoir is homogeneous, and fluid flows linearly in the x direction (perpendicular to the wellbore); pressure is not a function of the y direction. Diffusivity equation for the outer reservoir is given by Eqn. 3.48 with dimensionless variables in Laplace transformation domain.

$$\frac{d^2\bar{m}_{OD}}{dx_D^2} - \frac{s}{\eta_{OD}}\bar{m}_{OD} = 0 \,, \qquad \text{(Eqn. 3.48)}$$

where,

$\bar{m}_{OD}$ – Dimensionless outer reservoir pseudopressure in Laplace domain .

The outer boundary of the outer reservoir is subject to a no flow condition, and given by Eqn. 3.49.

$$\left(\frac{d\bar{m}_{OD}}{dx_D}\right)_{x_D = xe_D} = 0 \,. \qquad \text{(Eqn. 3.49)}$$

The inner boundary condition of the outer reservoir is equal to the outer boundary condition of the inner reservoir and given by Eqn. 3.50.

$$\bar{m}_{OD}\Big|_{x_D=1} = \bar{m}_{ID}\Big|_{x_D=1} \,. \qquad \text{(Eqn. 3.50)}$$

Finally, the solution for the outer reservoir flow is given by

$$\bar{m}_{OD} = \bar{m}_{ID}\Big|_{x_D=1} \frac{\cosh\left[\sqrt{\frac{s}{\eta_{OD}}}\,(x_{eD} - x_D)\right]}{\cosh\left[\sqrt{\frac{s}{\eta_{OD}}}\,(x_{eD} - 1)\right]} \,. \qquad \text{(Eqn. 3.51)}$$

3.2.2.3 The Inner Reservoir Solution

The inner reservoir description in the trilinear model refers to the zone between the two adjacent hydraulic fractures. The inner reservoir region can be homogeneous or naturally fractured. The original trilinear model used pseudo-steady dual porosity model (Warren and Root, 1963) or transient dual porosity model (Kazemi, 1969, de Swaan-O, 1976, Serra et al., 1983) with slab matrices for naturally fractured inner reservoir conditions. Brown et al. (2011) stated that since the matrix permeability is extremely low, transient dual porosity approach is the favorable dual porosity model. As a customary assumption for dual porosity models, fluid flow from matrix to the wellbore and matrix to the hydraulic fracture is negligible. Fluid flows to the hydraulic fracture through the natural fractures only in the y direction, so pressure is not a function of the x direction. It must be noted that in this chapter, homogeneous inner reservoir condition is considered. Diffusivity equation for the inner reservoir is given by Eqn. 3.52 with dimensionless variables in Laplace transformation domain.

$$\frac{d^2\,\bar{m}_{ID}}{dy_D^2} + \left(\frac{1}{y_{eD}C_{RD}}\right)\frac{d\,\bar{m}_{OD}}{dx_D}\Big|_{x_D=1} - u\bar{m}_{ID} = 0\,, \qquad \text{(Eqn. 3.52)}$$

where,

$$u = s\,f(s)\,, \qquad \text{(Eqn. 3.53)}$$

where,

$f(s)$ is the transfer function from matrix to natural fracture.

For homogeneous inner reservoir: $f(s) = 1$ (Eqn. 3.54)

For transient dual-porosity inner reservoir:

$$f(s) = 1 + \sqrt{\lambda\omega/(3s)}\tanh(\sqrt{3\omega s/\lambda}\,, \qquad \text{(Eqn. 3.55)}$$

where,

$$\lambda = 12\,\left(\frac{{x_F}^2}{h_m^2}\right)\left(\frac{k_m\,h_m}{k_f\,h_f}\right), \qquad \text{(Eqn. 3.56)}$$

where,

$\lambda -$ Transmissivity ratio

$k_{m,f} -$ Matrix and fracture permeabilities, md

$h_{m,f} -$ Matrix and fracture thickness, ft

$$\omega = \frac{(\phi c_t)_m}{(\phi c_t)_f}\,, \qquad \text{(Eqn. 3.57)}$$

where,

$\omega -$ Storativity ratio .

Taking the derivative of Eqn. 3.50 with respect to X_D, Eqn. 3.58 can be obtained,

$$\frac{d\,\bar{m}_{OD}}{dx_D}\,\Big|_{x_D=1} = -\beta_O \bar{m}_{ID}\,\Big|_{x_D=1}\,, \qquad \text{(Eqn. 3.58)}$$

where,

$$\beta_O = \sqrt{s/\eta_{OD}}\tanh\left[\sqrt{\frac{s}{\eta_{OD}}}\,(x_{eD}-1)\right]. \qquad \text{(Eqn. 3.59)}$$

Since the inner reservoir pseudo-pressure is not a function of the x-direction, Eqn. 3.52 becomes:

$$\frac{d^2\,\bar{m}_{ID}}{dy_D^2} - \alpha_O \bar{m}_{ID} = 0\,, \qquad \text{(Eqn. 3.60)}$$

where,

$$\alpha_O = \frac{\beta_O}{C_{RD}\, y_{eD}} + u \ . \qquad \text{(Eqn. 3.61)}$$

The model assumes no flow boundary condition in the middle of two adjacent hydraulic fractures. Therefore, outer boundary of the inner reservoir is treated as no flow boundary. Inner boundary of the inner reservoir is equal to the outer boundary condition of hydraulic fracture. Outer and inner boundary conditions of the inner reservoir are given by Eqn. 3.62 and Eqn. 3.63, respectively.

$$\left(\frac{d\bar{m}_{ID}}{dy_D}\right)_{yD=ye_D} = 0 \ , \qquad \text{(Eqn. 3.62)}$$

$$\bar{m}_{ID}\Big|_{yD=wD/2} = \bar{m}_{FD}\Big|_{yD=wD/2} \ . \qquad \text{(Eqn. 3.63)}$$

Finally, solution for the inner reservoir is given by Eqn. 3.64.

$$\bar{m}_{ID} = (\bar{m}_{FD}\Big|_{yD=\frac{wD}{2}}) \frac{\cosh[\sqrt{\alpha_O}\ (y_{eD} - y_D)]}{\cosh[\sqrt{\alpha_O}\ (y_{eD} - w_D/2)]} \ . \qquad \text{(Eqn. 3.64)}$$

There are several points that must be stressed for the naturally fractured inner reservoir condition. Transient and pseudo steady state dual porosity models are available for the naturally fractured inner reservoir modeling. As stated earlier, the transient dual porosity model is more appropriate due to low permeability characteristics of unconventional reservoirs. For the transient dual porosity model the inner reservoir parameters must be defined as fracture properties such as $k_I = k_f$, but the dimensionless conductivities (CFD and CRD) must be calculated by using the bulk properties. For

instance, effective permeability equation which is given by Eqn. 3.43 must be used in order to calculate $\tilde{k}_I$ and plugged back into CFD and CRD calculations which are given by Eqn. 3.42 and Eqn. 3.44, respectively.

3.2.2.4 Hydraulic Fracture Solution

Hydraulic fracture solution is the last step in their model which combines flow equations in all three regions, and calculated the dimensionless wellbore pressure. Hydraulic fracture solution assumes fluid flow in the x-direction only (1D), so pressure is not a function of the y-direction. Diffusivity equation for the flow in hydraulic fracture is given by Eqn. 3.65 with dimensionless variables in the Laplace domain.

$$\frac{d^2\,\bar{m}_{FD}}{dx_D^2} + \left(\frac{2}{C_{FD}}\right)\frac{d\,\bar{m}_{ID}}{dy_D}\Big|_{y_D=wD/2} - \frac{s}{\eta_{FD}}\bar{m}_{FD} = 0\,. \qquad \text{(Eqn. 3.65)}$$

Taking the derivative of Eqn. 3.64 with respect to y_D,

$$\frac{d\,\bar{m}_{ID}}{dy_D}\Big|_{y_D=wD/2} = -\beta_F \bar{m}_{FD}\Big|_{y_D=wD/2}\,, \qquad \text{(Eqn. 3.66)}$$

where,

$$\beta_F = \sqrt{\alpha_O}\tanh\left[\sqrt{\alpha_O}(y_{eD} - wD/2)\right]\,. \qquad \text{(Eqn. 3.67)}$$

Since the hydraulic fracture pseudo-pressure is not a function of y_D, Eqn. 3.65 becomes:

$$\frac{d^2\,\bar{m}_{FD}}{dX_D^2} - \alpha_F \bar{m}_{FD} = 0\,, \qquad \text{(Eqn. 3.68)}$$

where,

$$\alpha_F = \frac{2\beta_F}{C_{FD}} + \frac{s}{\eta_{FD}} \qquad \text{(Eqn. 3.69)}$$

The model assumes no flow at the hydraulic fracture tips, so the boundary conditions represented by

$$\left(\frac{d\bar{m}_{FD}}{dx_D}\right)_{xD=1} = 0\,, \qquad \text{(Eqn. 3.70)}$$

$$\bar{m}_{FD}\Big|_{xD=0} = \frac{-\pi}{C_{FD}s}\,. \qquad \text{(Eqn. 3.71)}$$

Finally by solving the second order ordinary differential equation (Eqn. 3.68), the wellbore pseudo-pressure with dimensionless variables in the Laplace domain is given by

$$\bar{m}_{wD} = \bar{m}_{FD}(x_D = 0) = \frac{\pi}{C_{FD}s\sqrt{\alpha_F}\tanh(\sqrt{\alpha_F})} + \frac{S_c}{s}\,. \qquad \text{(Eqn. 3.72)}$$

Eqn. 3.72 is the final equation of the trilinear model developed by Ozkan et al. (2009) and Brown et al. (2009). Lastly, adding the flow chocking equation, which is proposed by Mukherjee and Economidies (1991), completes the solution.

$$s_c = \frac{k_I\, h_I}{k_F\, w_F}\left[ln\left(\frac{h}{2r_w}\right) - \frac{\Pi}{2}\right]\,, \qquad \text{(Eqn. 3.73)}$$

where,

w_F – Width of the hydraulic fracture, ft

r_w – Wellbore radius, ft .

Stehfest's (1970) numerical algorithm is employed in the computational code to convert the dimensionless wellbore pressure back to time domain. Once the dimensionless wellbore pressure is obtained in the time domain, one can substitute dimensionless wellbore pressure into the Eqn. 3.35 to calculate the flowing bottom-hole pressure (for constant rate scenario). Following Van Everdingen and Hurst (1949), constant bottom hole pressure scenario can be modeled as well, but dimensionless wellbore pressure in the Laplace domain must be converted to the dimensionless flow rate again in Laplace domain by Eqn. 3.74. Dimensionless cumulative production can be obtained by Eqn. 3.75.

$$\bar{q}_{wD} = \frac{1}{s^2\,\bar{m}_{wD}}, \qquad \text{(Eqn. 3.74)}$$

where,

$\bar{q}_{wD}$ – Dimensionless gas flow rate in Laplace domain

$$\bar{Q}_{wD} = \frac{1}{s^3\,\bar{m}_{wD}}, \qquad \text{(Eqn. 3.75)}$$

where,

$\bar{Q}_{wD}$ – Dimensionless cumulative gas production in Laplace domain.

Once the dimensionless flow rate and dimensionless cumulative production calculated with using Eqn. 3.74 and Eqn. 3.75, dimensional flow rate and cumulative gas production can be calculated by Eqn. 3.76 and Eqn. 3.77, respectively.

$$q_g = \frac{n_F kh[m(p_i) - m(p_{wf})]q_{wD}}{1422\,T} \qquad \text{(Eqn. 3.76)}$$

where,

n_F – Number of hydraulic fractures

T – Reservoir temperature, Rankine.

$$Q_g = \frac{n_F kh[m(p_i) - m(p_{wf})]Q_{wD}}{1422\,T} x \frac{\phi c_t \mu\, x_F^2}{63.288\ 10^{-4}}, \qquad \text{(Eqn. 3.77)}$$

where,

Q_g – Cumulative gas production, Mscf.

3.3 IMPLEMENTATION OF ANALYTICAL MODELS

In this section, a synthetic data set for an unconventional multiply fractured reservoir is evaluated with the simplified and the trilinear models. In addition to these two analytical models, a commercial reservoir simulator (CMG, IMEX 2012) is employed for the same data set, and the results are compared with the analytical solutions. Lastly, a sensitivity analysis of certain reservoir and well parameters are performed with using the simplified model, the trilinear model, and CMG. Cumulative gas production performances for different time periods are also investigated thoroughly with these models, and the results are discussed in detail.

3.3.1 Comparison of Analytical Models with CMG for Base Case

In order to handle the sensitivity analysis, the main objective of this chapter, a synthetic data set is designed for an unconventional multiply fractured reservoir. This data set is provided in Table 3.1 as the Base Case.

Table 3.1: The Base Case input parameters

Parameter	Value(s)	Unit
The model dimensions	4,000 (length), 425 (half-width), 200 (height)	ft
Initial reservoir pressure	3500	psi
BHP	600	psi
Production time	30	year
Reservoir temperature	200	^{o}F
Initial Gas viscosity	0.0184	cp
Initial gas saturation	1	fraction
Total compressibility	$5x10^{-4}$	psi^{-1}
Matrix permeability	0.0006	md
Matrix porosity	0.06	fraction
Fracture conductivity	10	md-ft
Fracture half length	425	ft
Fracture stage spacing	300	ft
Fracture height	200	ft
Horizontal well length	4,000	ft
Number of well	1	number

CMG (IMEX, 2012) commercial reservoir simulator is used to create the reservoir model for base case input parameters. 2-D and 3-D views of this model are given in Figures 3.4 and 3.5, respectively. Local grid refinement method is applied to represent hydraulic fractures in the reservoir model (CMG, IMEX, 2012). Figure 3.4 (a) represents the well condition considered in the Base Case (14 hydraulic fractures), and Figure 3.5 (b) depicts the details of hydraulic fracture created in CMG (IMEX, 2012).

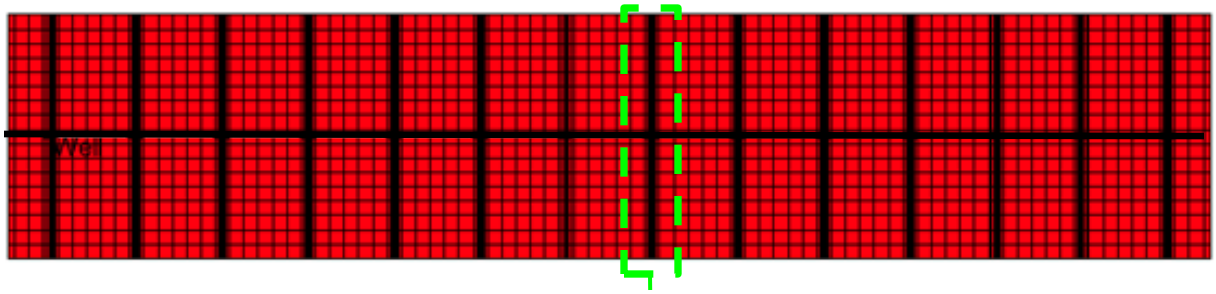

(a) CMG Model for the Base Case

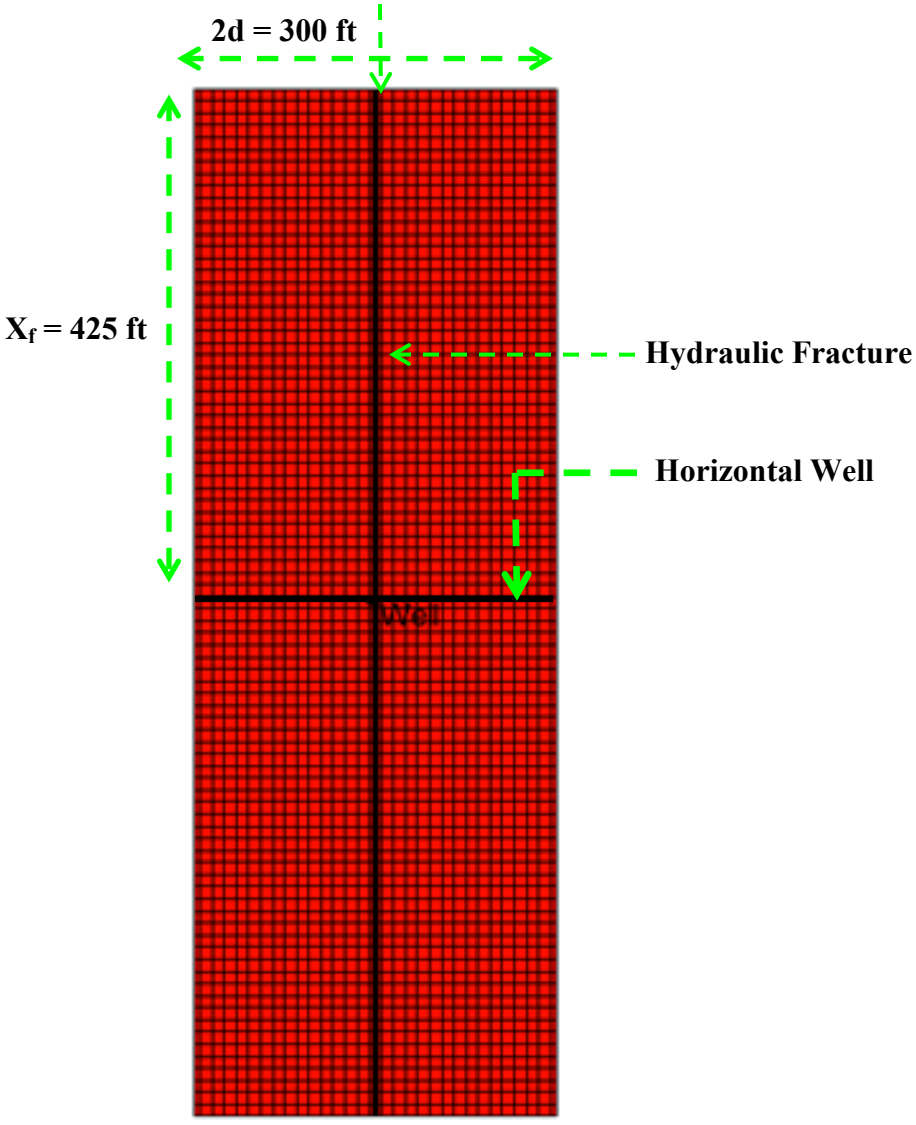

(b) Local grid refinement for hydraulic fractures

Figure 3.4: 2-D view of the Base Case, (CMG, IMEX 2012)

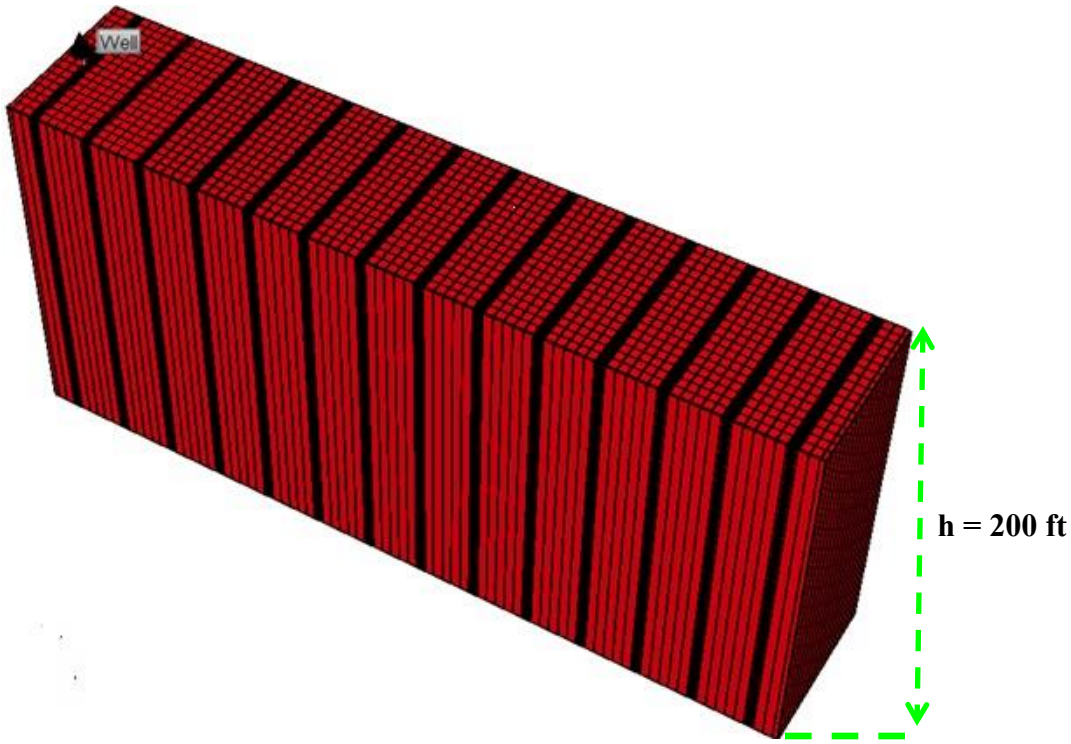

Figure 3.5: 3-D view of the Base Case, (CMG, IMEX 2012)

Simulations are performed using CMG (IMEX, 2012) and two analytical models for the reservoir considered in the base case. Figure 3.6 and 3.7 represent the gas flow rate and the cumulative production performance for the Base Case. It is observed that results attained from the analytical models and the commercial reservoir simulator (CMG, IMEX) show a good agreement for the Base Case model. However, the commercial reservoir simulator is computationally more expensive than the analytical models. These results verify that the analytical solutions capture the fundamental physics of fluid flow and give reliable results with minimum computational effort.

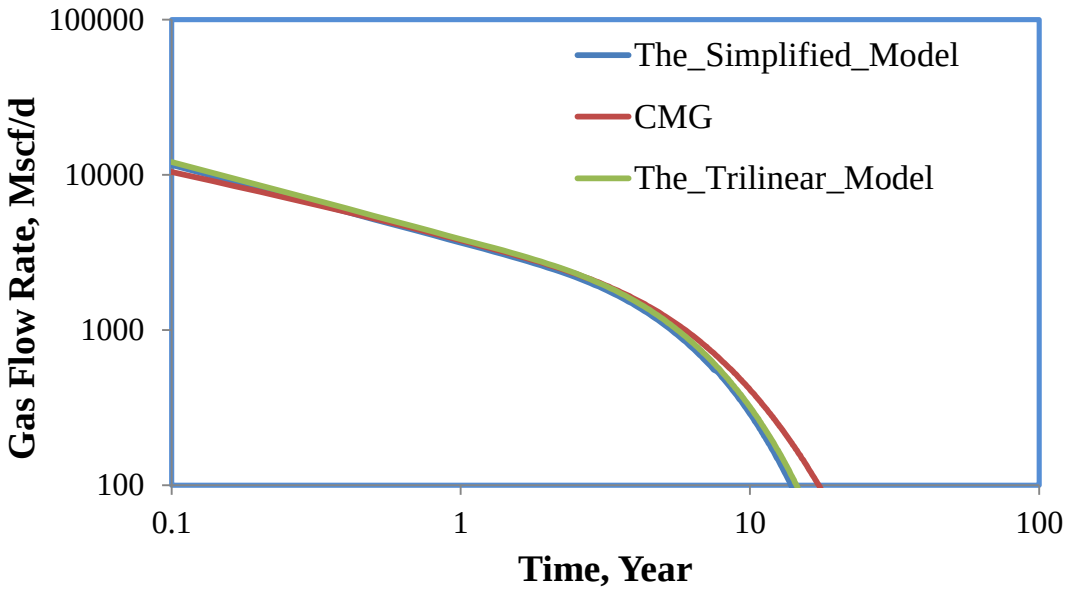

Figure 3.6: Gas flow rate results for the Base Case using The Simplified Model, The Trilinear Model and CMG

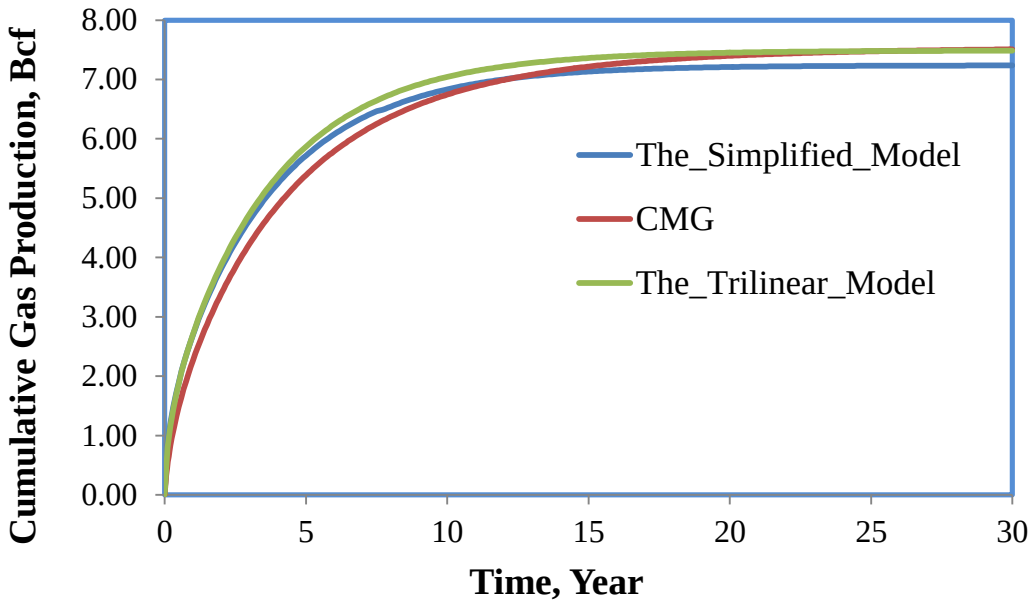

Figure 3.7: Cumulative gas production performances for the Base Case using The Simplified Model, The Trilinear Model and CMG

3.3.2 Sensitivity analysis for a Synthetic Unconventional Multiply Fractured Reservoir Case

Sensitivity analysis is an investigative process of mathematical model robustness that contains changing input variables and parameters. Sensitivity analysis has a wide application in engineering problems, and usage of sensitivity analysis can be grouped as follows (Pannell, 1997):

- Robustness of mathematical model can be tested.
- Sensitive and important parameters can be identified.
- Critical values and thresholds can be determined.
- Recommendations become more understandable and credible.
- Lack of commitment to any single strategy problem can be solved.
- The risk factors can be evaluated widely.

In light of this information, sensitivity analysis for a synthetic unconventional multiply fractured homogeneous reservoir is performed. Two analytical reservoir models and a commercial reservoir simulator (CMG, IMEX, 2012) are employed for this sensitivity analysis. In order to accomplish the sensitivity analysis with analytical models, MATLAB computational code is developed for both models. This sensitivity analysis is conducted for certain reservoir and well parameters, and results are evaluated based on cumulative production performance. It must be noted that some parameters, such as matrix permeability and porosity, are beyond an engineer's control and result in uncertainty. In addition to these parameters, there are some design parameters such as hydraulic fracture spacing and hydraulic fracture half-length that can be used for well production performance optimization. Both uncertainty and design parameters are considered and the results are evaluated accordingly. Since the oil and gas production form unconventional reservoirs are long term projections, different time periods of

reservoir lifespan may be sensitive to different parameters, so different time periods sensitivity analysis are also assessed. For the Base Case inputs; see Table 3.1. For the sensitivity analysis parameters and their range; see Table 3.2 below.

Table 3.2: Sensitivity parameters used in this study

Parameter	Minimum		Mean		Maximum	Unit
Permeability	0.0002	0.0004	0.0006	0.0008	0.001	md
Porosity	0.02	0.04	0.06	0.08	0.1	fraction
Fracture half – length	300	350	400	415	425	ft
Fracture conductivity	2	4	6	8	10	md-ft
Fracture stage spacing	200	250	300	350	400	ft
Fracture height	100	150	200	250	300	ft
BHP	400	500	600	700	800	psi

3.3.2.1 Matrix Permeability Sensitivity Analysis

In this sensitivity study, we considered five different matrix permeability values in the nano-Darcy range. As expected, matrix permeability sensitivity analysis results manifests that the matrix permeability controls how fast the reservoir can be drained. For the early production time period, daily production rate increases with increasing matrix permeability. As time progresses the previously stated factor no longer applies, because the high permeability cases have already drained. Although the minimum permeability case (0.0002 md) could not reach the absolute production limit in 30 years period, cases with matrix permeabilities higher than 0.0002 md reach the same absolute production limits in 30 years. Both analytical models and CMG results show similar responses for matrix permeability sensitivity analysis (Figures 3.8 through Figure 3.13).

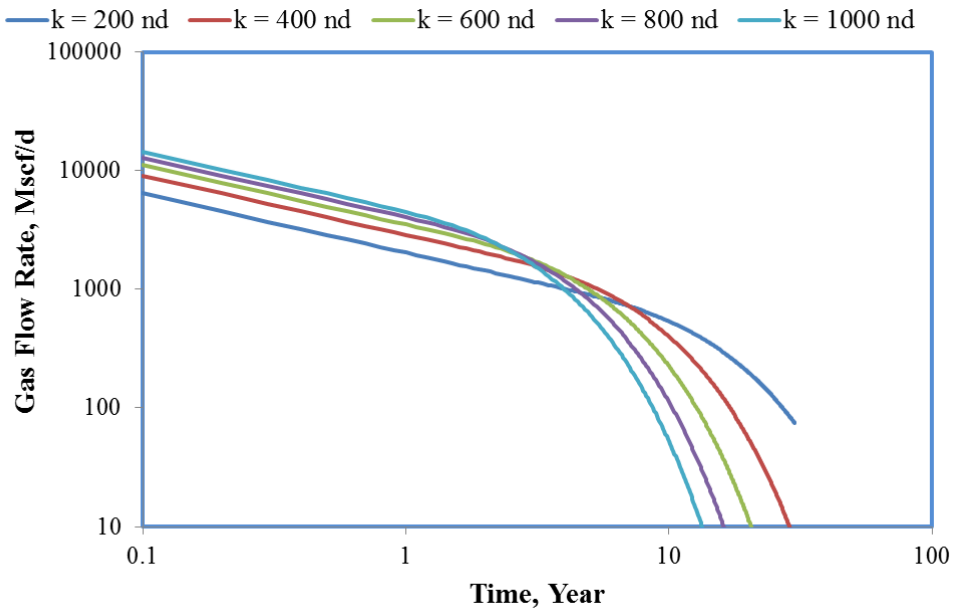

Figure 3.8: The Simplified Model gas flow rate results for permeability sensitivity analysis

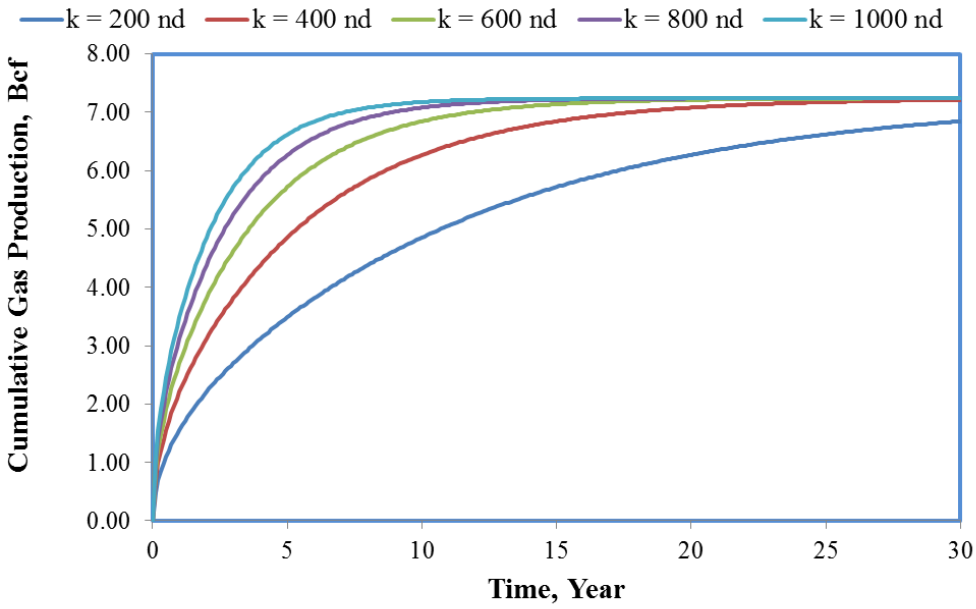

Figure 3.9: The Simplified Model cumulative gas production performance for permeability sensitivity analysis

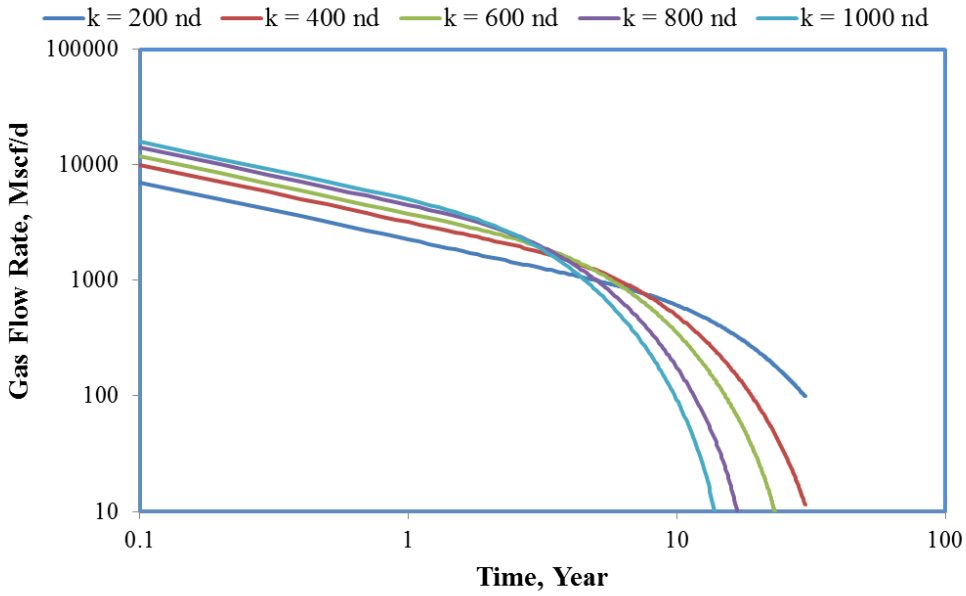

Figure 3.10: The Trilinear Model gas flow rate results for permeability sensitivity analysis

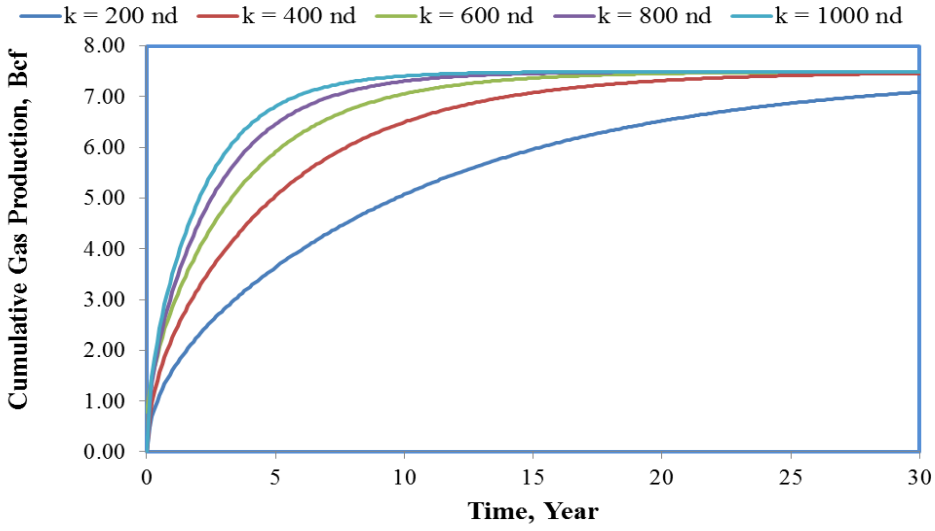

Figure 3.11: The Trilinear Model cumulative gas production performance for permeability sensitivity analysis

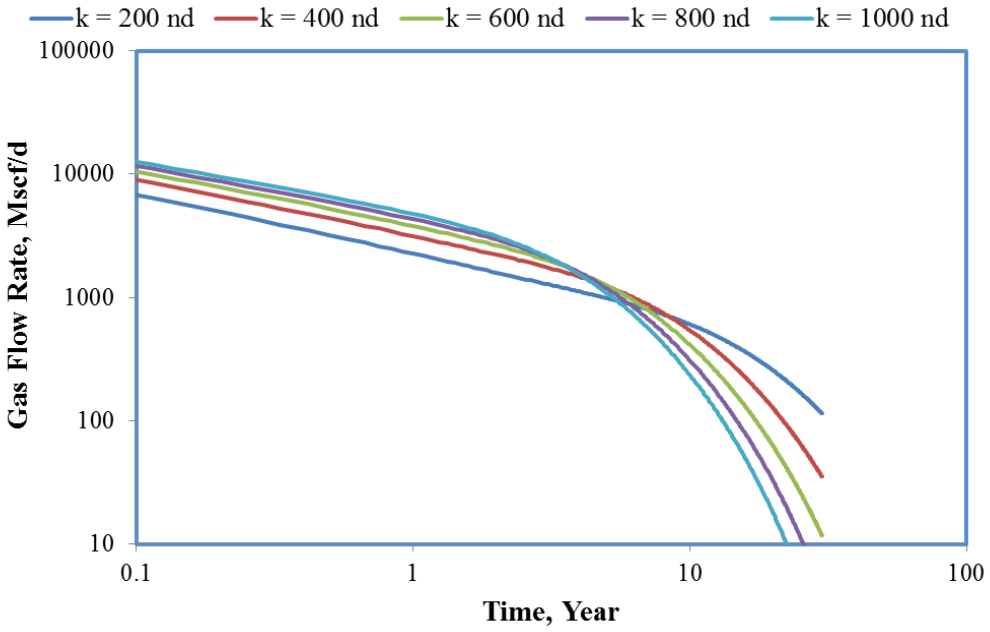

Figure 3.12: CMG gas flow rate results for permeability sensitivity analysis

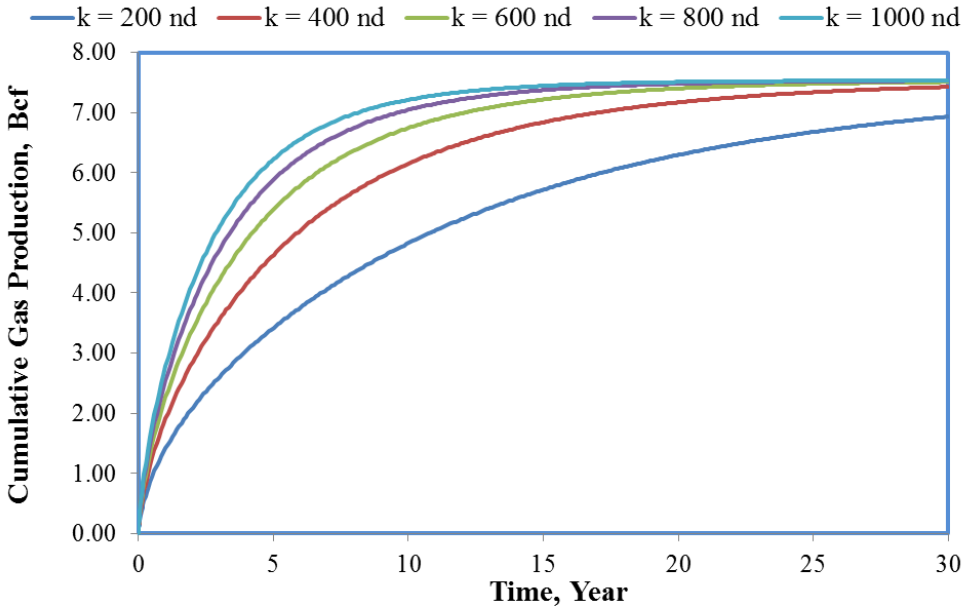

Figure 3.13: CMG cumulative gas production performance for permeability sensitivity analysis

3.3.2.2 Matrix Porosity Sensitivity Analysis

It is obvious that the matrix porosity controls the original gas in place; due to this reason increasing matrix porosity results in higher cumulative production in 30 year time period. For the early production time all cases have similar daily production. However, the late time production rates differ from each other, because the reservoirs with lower porosity depletes faster than the higher porosity cases. The two analytical model results show a good agreement with CMG for porosity sensitivity analysis (Figures 3.14 through Figure 3.19).

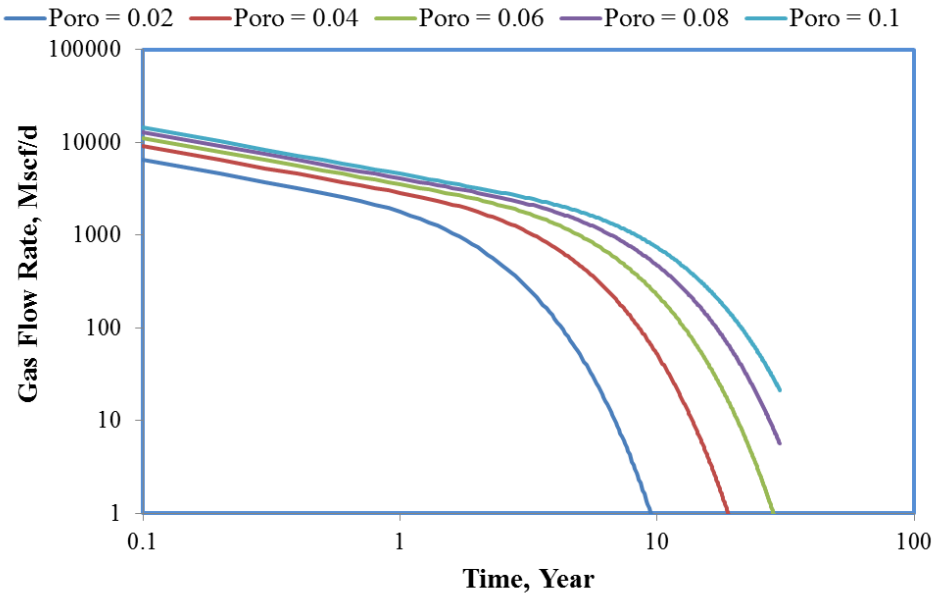

Figure 3.14: The Simplified Model gas flow rate results for porosity sensitivity analysis

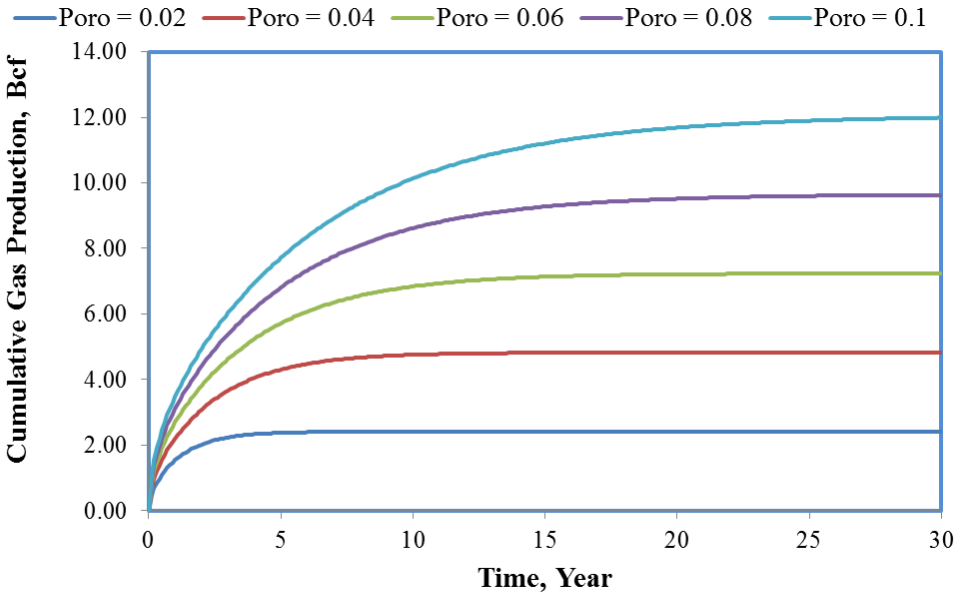

Figure 3.15: The Simplified Model cumulative gas production performance for porosity sensitivity analysis

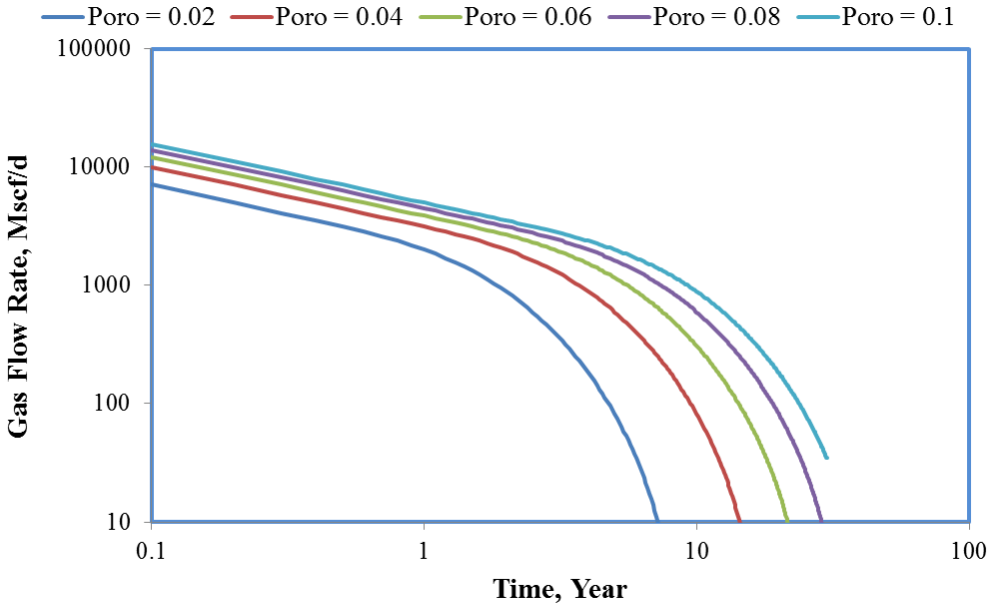

Figure 3.16: The Trilinear Model gas flow rate results for porosity sensitivity analysis

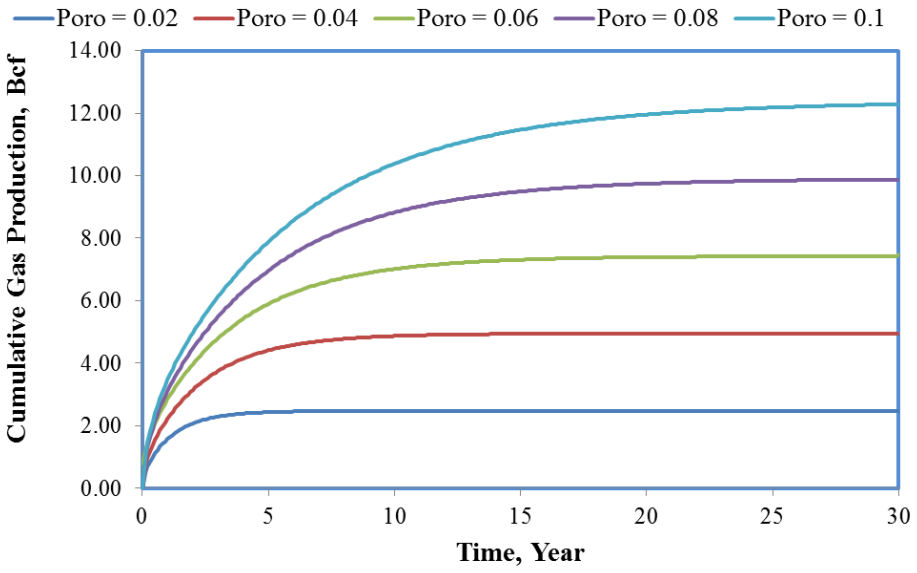

Figure 3.17: The Simplified Model cumulative gas production performance for porosity sensitivity analysis

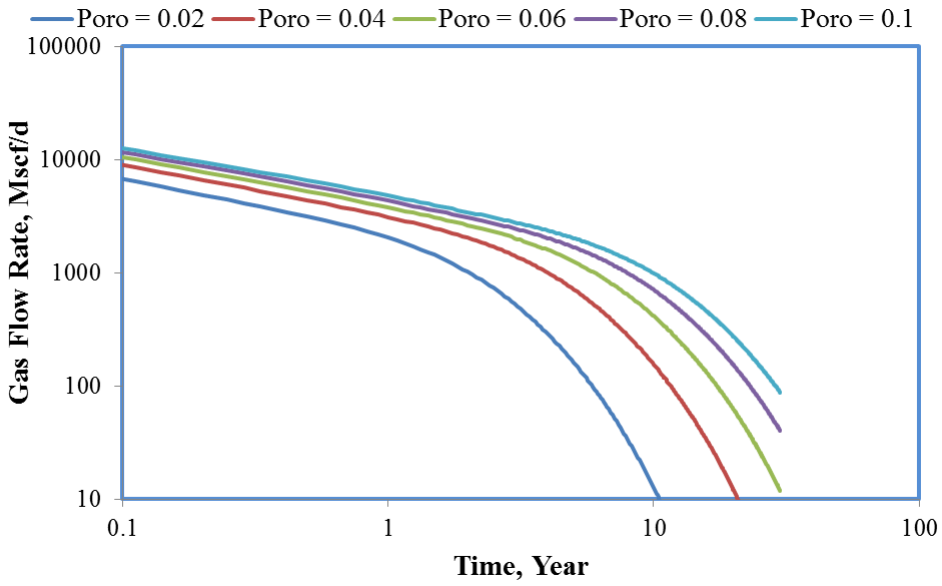

Figure 3.18: CMG gas flow rate results for porosity sensitivity analysis

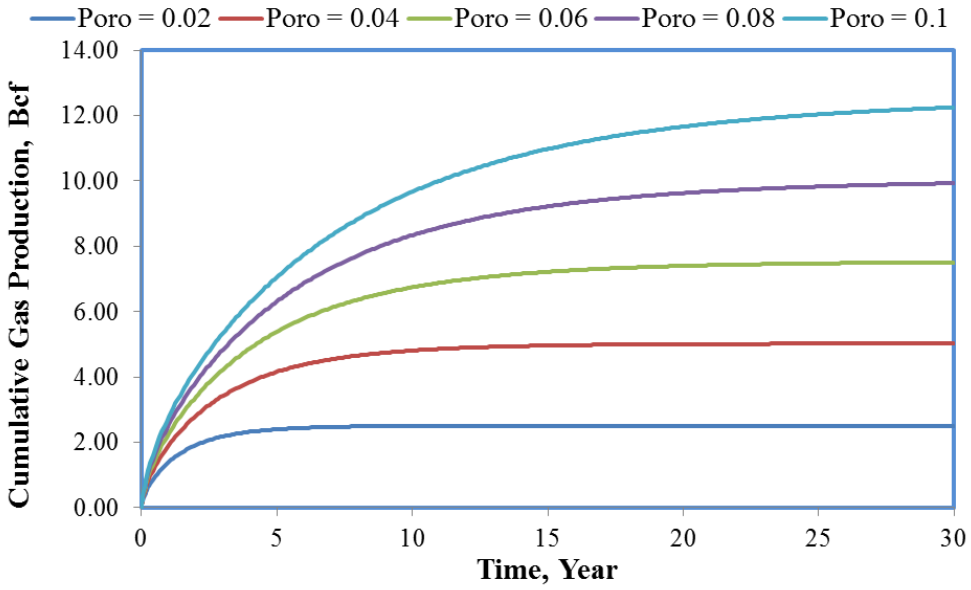

Figure 3.19: CMG cumulative gas production performance for porosity sensitivity analysis

3.3.2.3 Hydraulic Fracture Half Length Sensitivity Analysis

In this study the same reservoir width (425 ft.) is considered for five different hydraulic fracture half lengths for the trilinear model and CMG. It must be noted that the simplified model considers the reservoir size perpendicular to the wellbore is equal to the hydraulic fracture half length, so the hydraulic fracture half-length effects the original gas in place volume and the cumulative production performance results for the simplified model differs from the trilinear model and CMG behavior. However, the daily production rate responses show the same trend for the two analytical models and CMG. Cumulative production performances of the trilinear model and CMG agree with each other (Figures 3.20 through Figure 3.25).

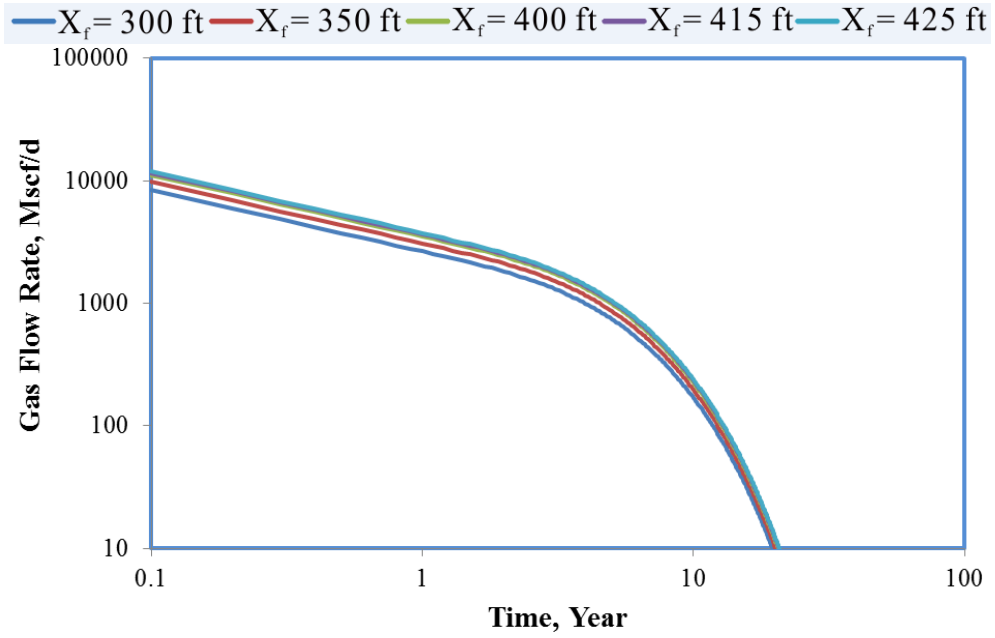

Figure 3.20: The Simplified Model gas flow rate results for hydraulic fracture half length sensitivity analysis

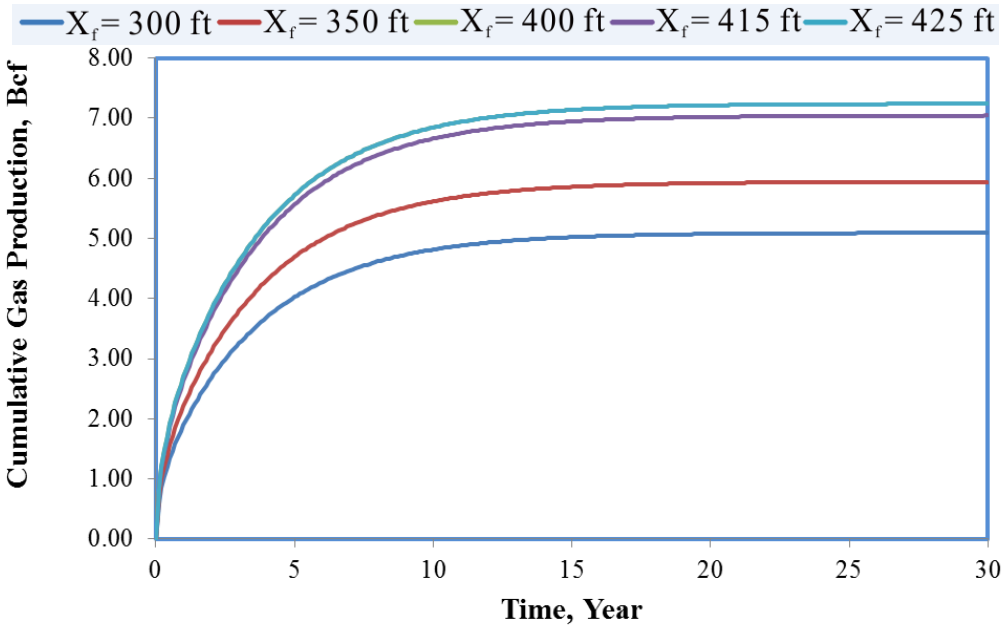

Figure 3.21: The Simplified Model cumulative gas production performance for hydraulic fracture half length sensitivity analysis

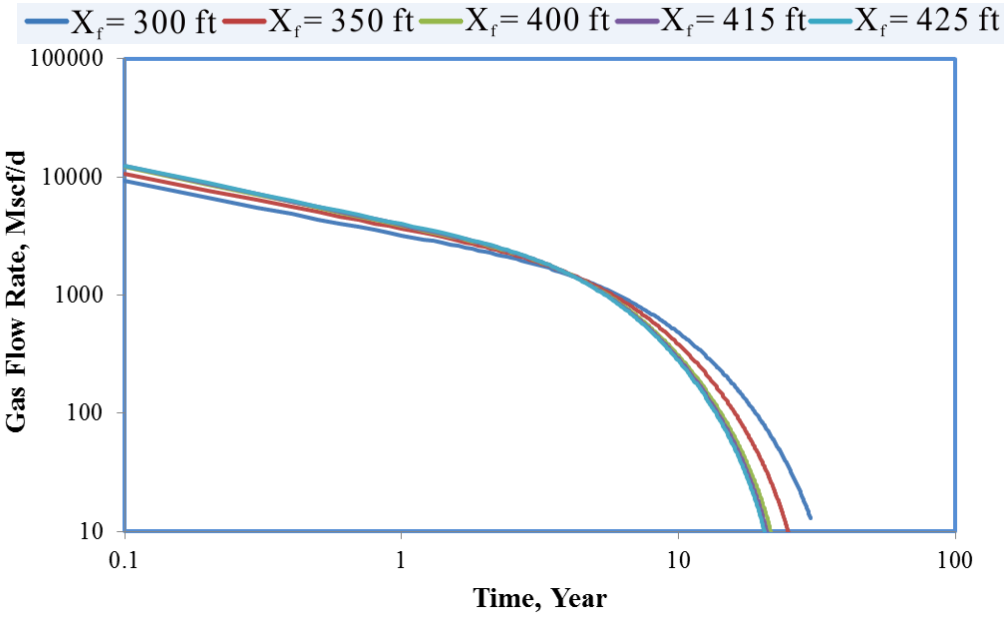

Figure 3.22: The Trilinear Model gas flow rate results for hydraulic fracture half length sensitivity analysis

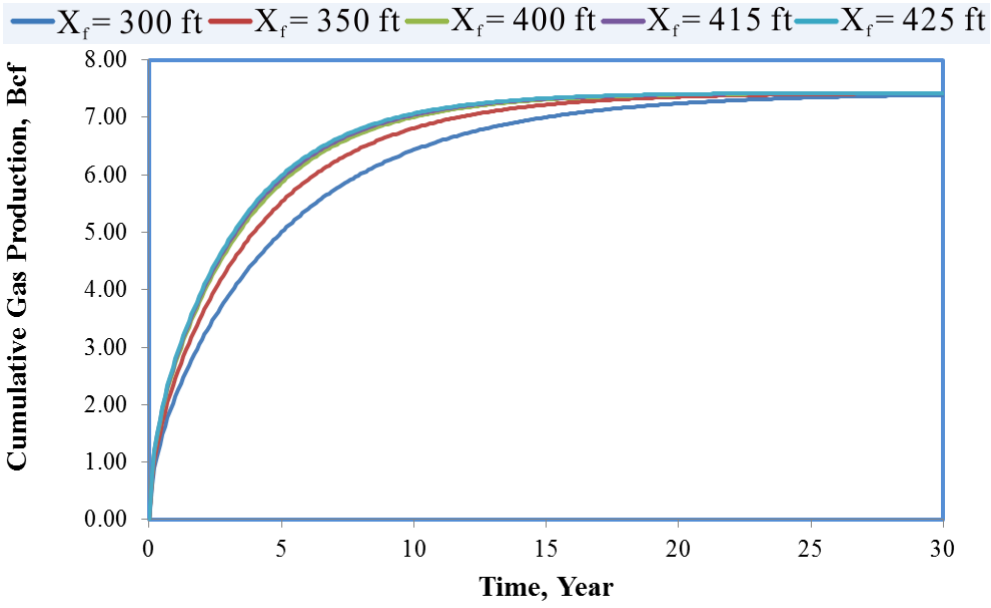

Figure 3.23: The Trilinear Model cumulative gas production performance for hydraulic fracture half length sensitivity analysis

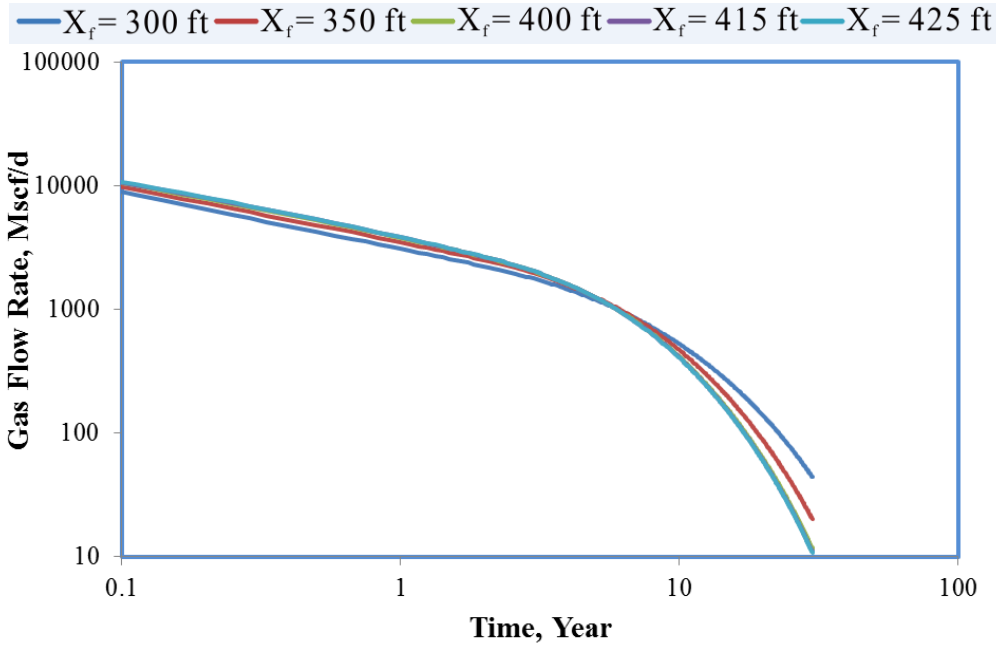

Figure 3.24: CMG gas flow rate results for hydraulic fracture half length sensitivity analysis

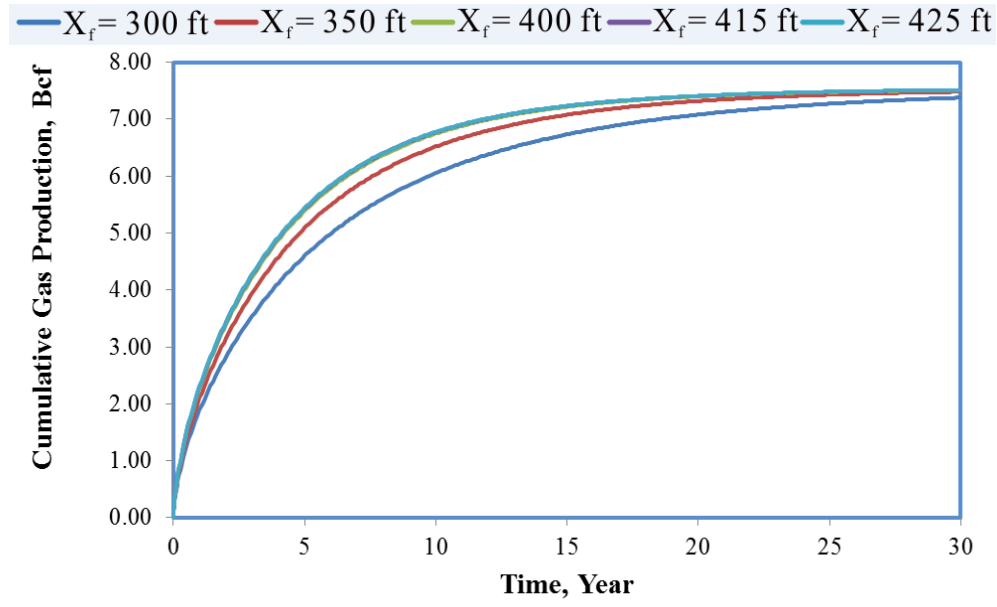

Figure 3.25: CMG cumulative gas production performance for hydraulic fracture half length sensitivity analysis

3.3.2.4 Hydraulic Fracture Stage Spacing Sensitivity Analysis

Hydraulic fracture stage spacing is an important design parameter for hydraulic fracture treatment, which is under an engineer's control. Dense hydraulic fracture treatment means shorter stage spacing which results in more hydraulic fractures and better production performances. On the other hand, since the hydraulic fracture is an expensive treatment, applying more treatment stages costs more, so it is necessary to optimize the stage spacing while keeping well performance at a reasonable level. In this sensitivity analysis the same horizontal well length (4,000 ft) is considered with five different hydraulic fracture stage spacings; see Table 3.2. Hydraulic fracture stage spacing sensitivity analysis shows that the hydraulic fracture spacing remarkably affects the production performance of the well, but for a 30 year period this effect diminishes, since the reservoir has been already depleted at that time. The simplified model, the trilinear model and the CMG results show a perfect agreement on hydraulic fracture stage spacing sensitivity analysis (Figures 3.26 through 3.31).

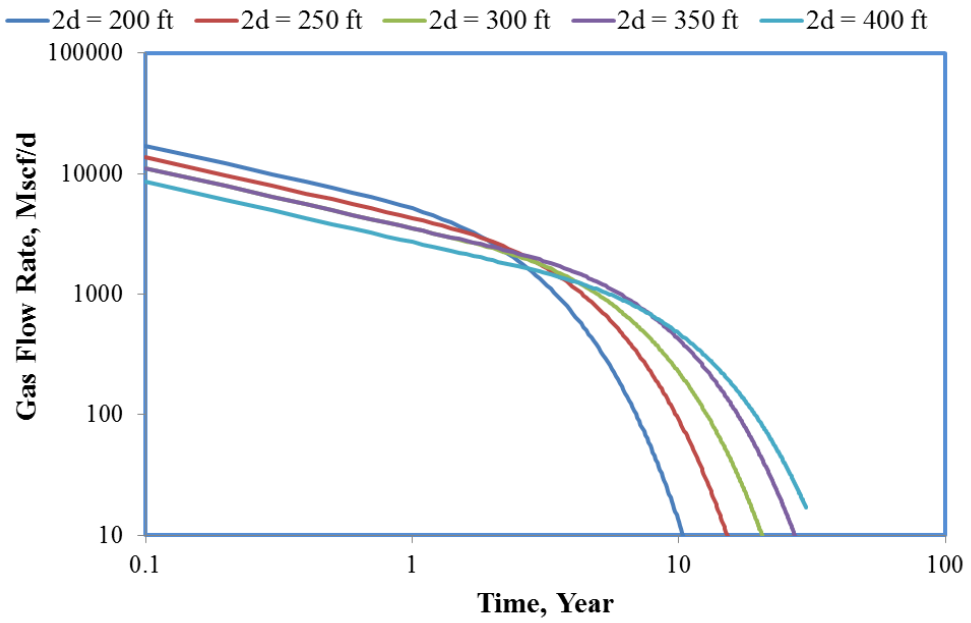

Figure 3.26: The Simplified Model gas flow rate results for hydraulic fracture stage spacing sensitivity analysis

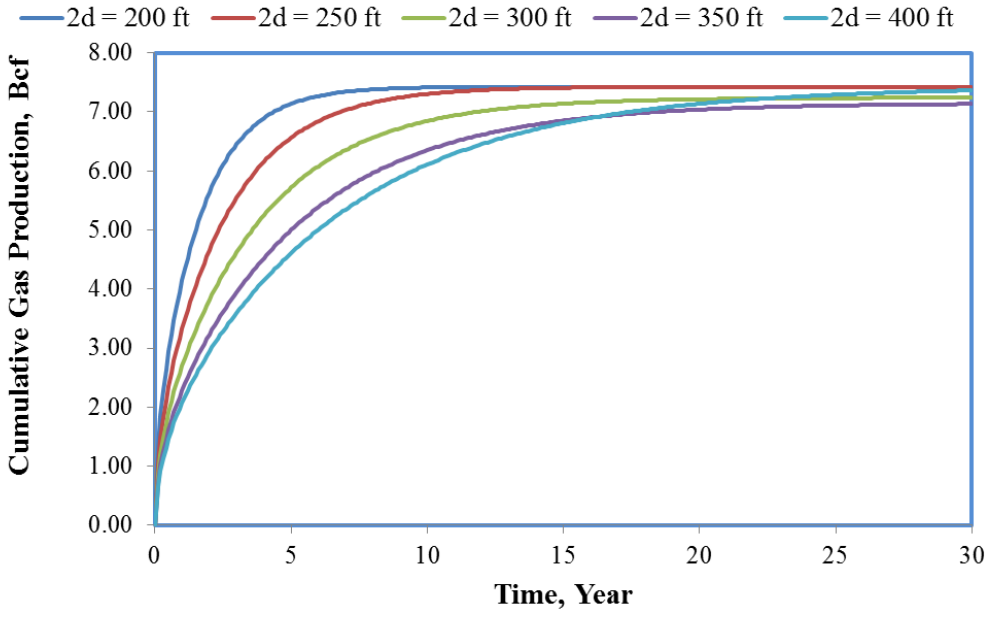

Figure 3.27: The Simplified Model cumulative gas production performance for hydraulic fracture stage spacing sensitivity analysis

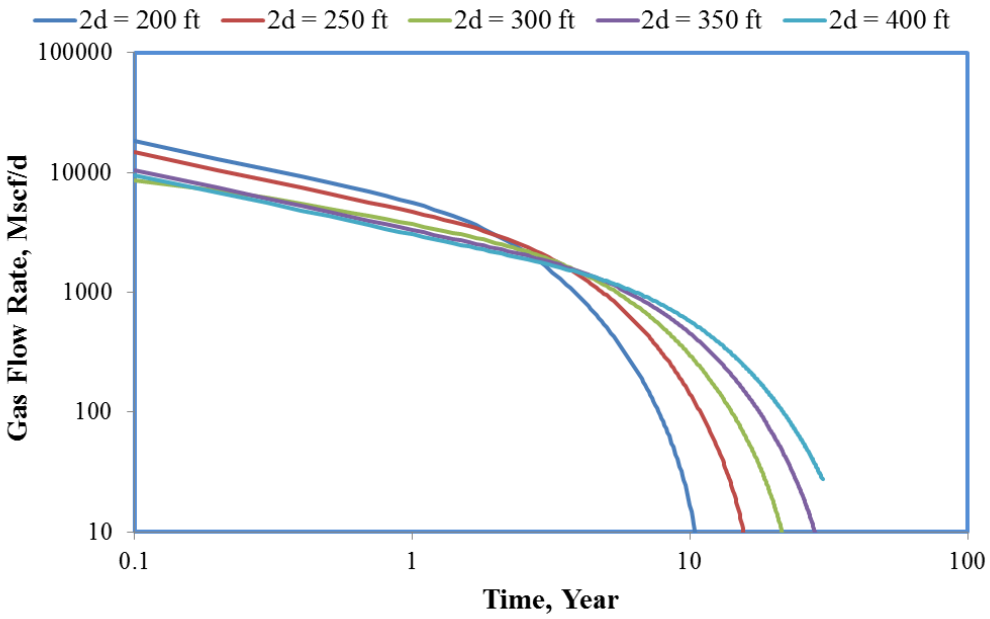

Figure 3.28: The Trilinear Model gas flow rate results for hydraulic fracture stage spacing sensitivity analysis

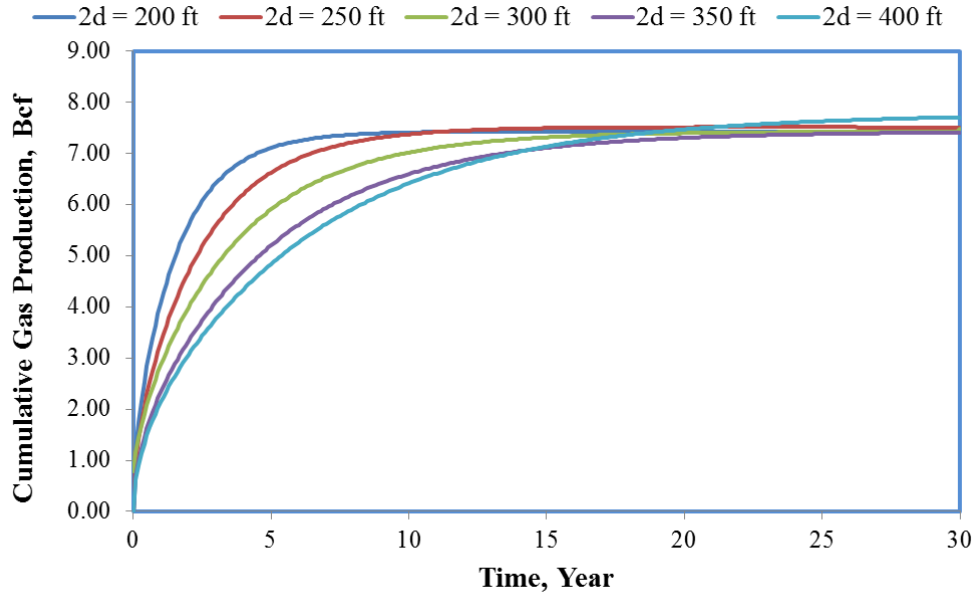

Figure 3.29: The Simplified Model cumulative gas production performance for hydraulic fracture stage spacing sensitivity analysis

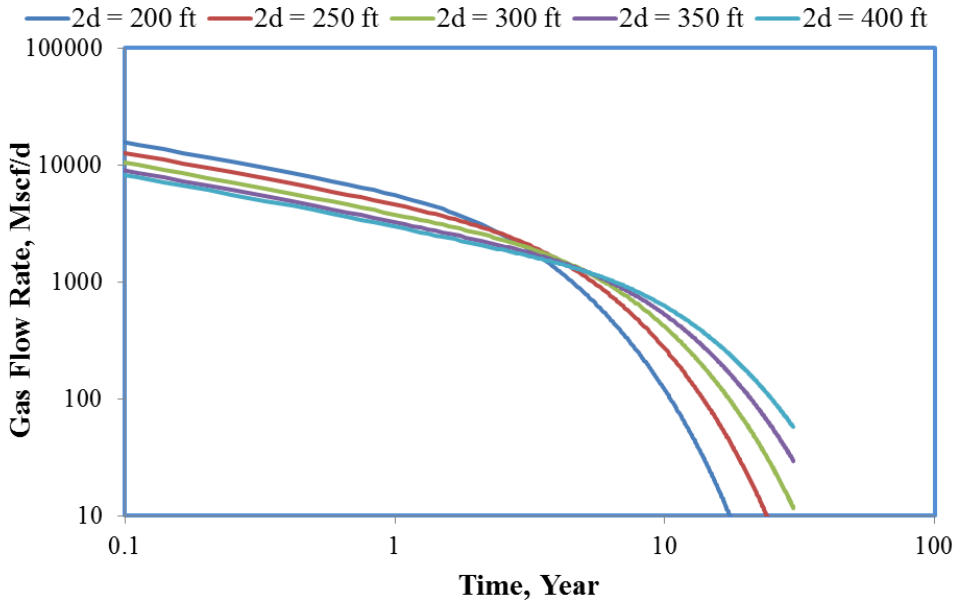

Figure 3.30: CMG gas flow rate results for hydraulic fracture stage spacing sensitivity analysis

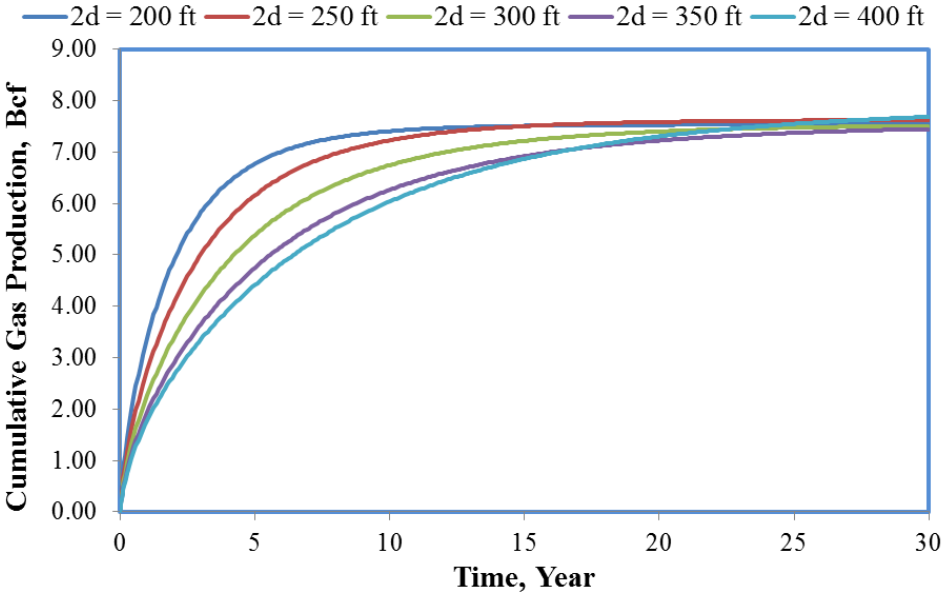

Figure 3.31: CMG cumulative gas production performance for hydraulic fracture stage spacing sensitivity analysis

3.3.2.5 Hydraulic Fracture Conductivity Sensitivity Analysis

Hydraulic fracture conductivity is the parameter that measures the ability of hydraulic fractures to transmit the hydrocarbon flow from reservoir to the wellbore, and it depends on the hydraulic fracture width and the hydraulic fracture permeability. Hydraulic fracture conductivity equation is given by Eqn. 3.77. In this equation, hydraulic fracture permeability is the parameter which can be controlled by the operator with propant selection. There is a threshold for conductivity after which hydraulic fractures act infinitely conductive, once the threshold is reached, increasing the hydraulic fracture permeability does not change the production performance. Therefore, before deciding the appropriate propant type an engineer must make an optimization study for different propant types.

Moving from the propant selection, it is important to note that the trilinear model considers finite hydraulic fracture conductivity, so the theoretical maximum value for hydraulic conductivity after which hydraulic fracture acts like an infinite conductivity for the trilinear model is determined. It is decided that 10 md-ft is the threshold for infinite acting hydraulic fracture conductivity for the trilinear model.

$$FC = w_{hydraulic\ fracture}\ x\ k_{hydraulic\ fracture}\ , \qquad \text{(Eqn. 3.77)}$$

where,

FC – Hydraulic fracture conductivity, md-ft

w – Hydraulic fracture width, ft

k – Hydraulic fracture permeability, md

Sensitivity results show that the minimum fracture conductivity case (2 md-ft) produces with lower flow rates than the other cases. However, there is no difference between the mean hydraulic fracture conductivity case (6 md-ft) and the maximum

hydraulic fracture conductivity case (10 md –ft) for 30 year time period (Figures 3.32 through Figure 3.35).

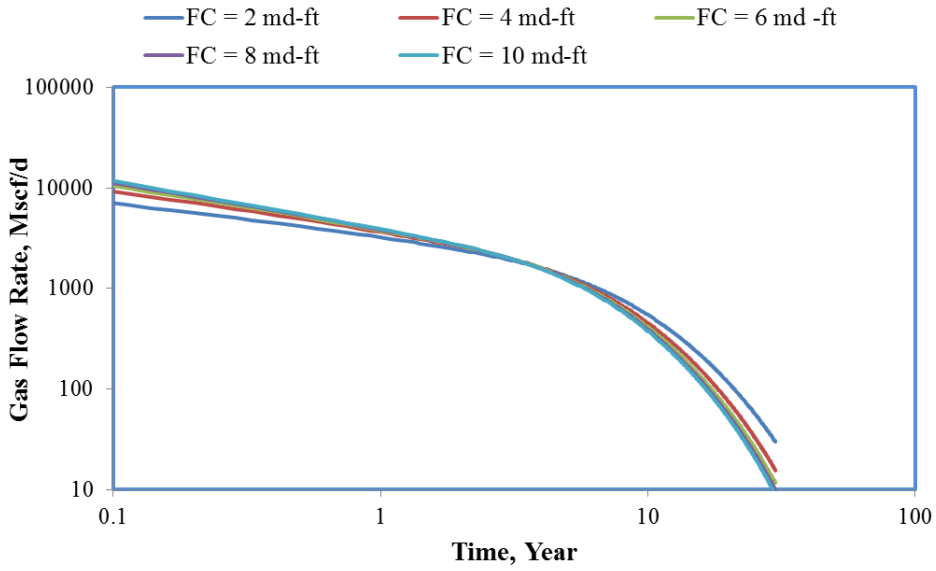

Figure 3.32: The Trilinear Model gas flow rate results for hydraulic fracture conductivity sensitivity analysis

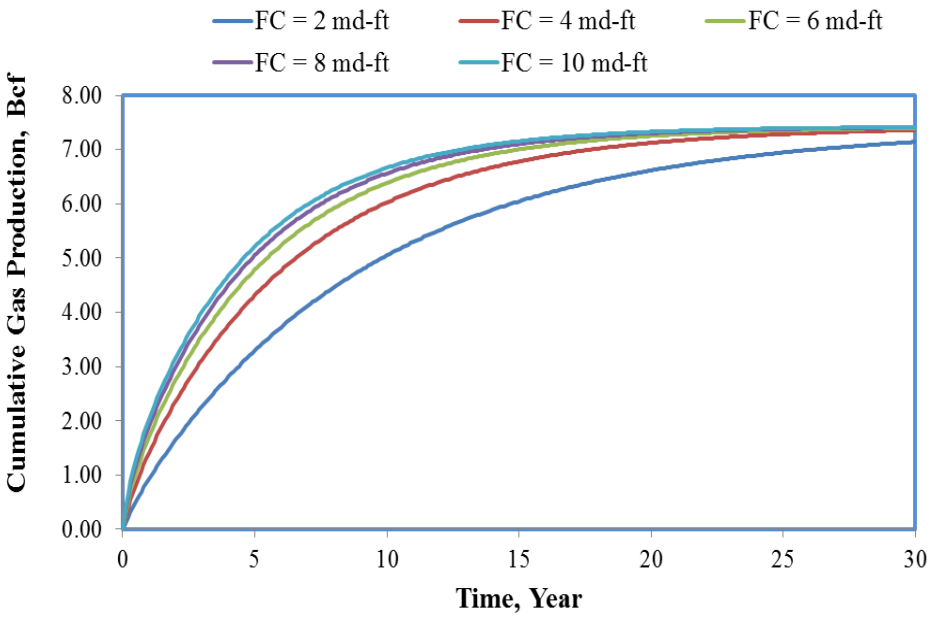

Figure 3.33: The Trilinear Model cumulative gas production performance for hydraulic fracture conductivity sensitivity analysis

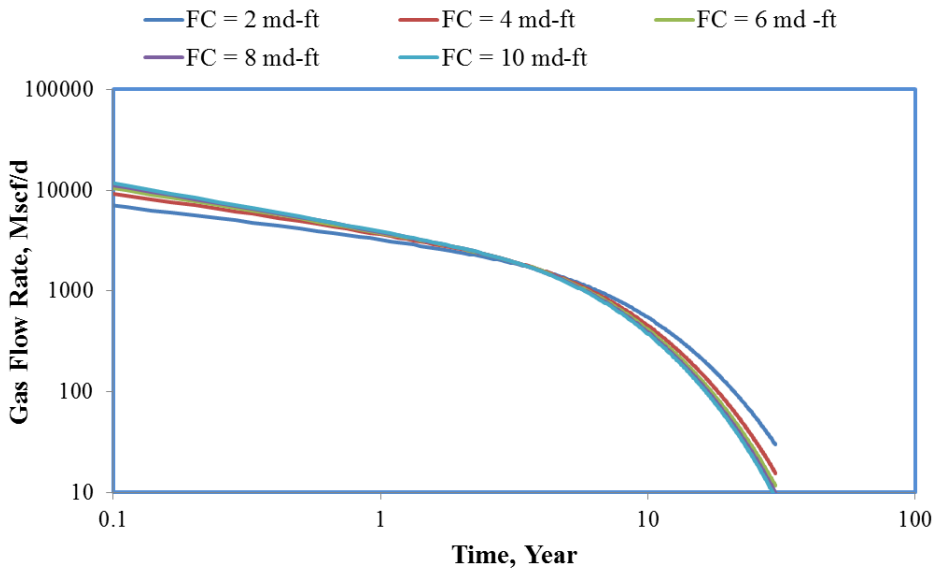

Figure 3.34: CMG gas flow rate results for hydraulic fracture conductivity sensitivity analysis

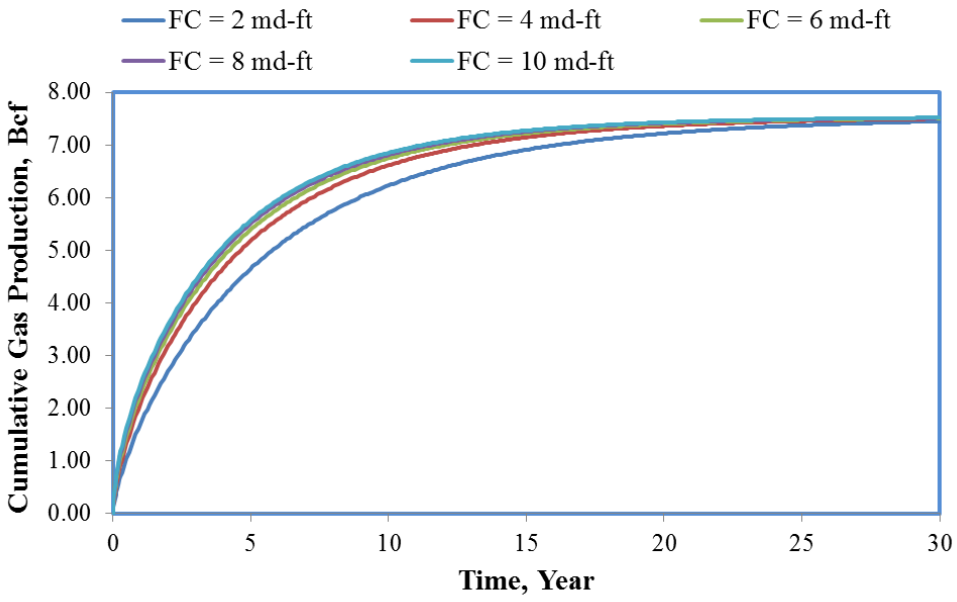

Figure 3.35: CMG cumulative gas production performance for hydraulic fracture conductivity sensitivity analysis

3.3.2.6 Hydraulic Fracture Height Sensitivity Analysis

The simplified and the trilinear model assume hydraulic fracture and formation heights are equal to each other. For a fair comparison, the model created in CMG also has an equal hydraulic fracture and formation thickness. Because of this assumption, hydraulic fracture height controls the initial gas in place volume. Daily production rates (Figures 3.36, 3.38, and 3.40) and cumulative production performances (Figures 3.37, 3.39, and 3.41) clearly show that the increasing fracture height positively affected the production performance. The two analytical models and CMG results show an identical behavior for formation height sensitivity analysis (Figures 3.31 through Figure 3.36).

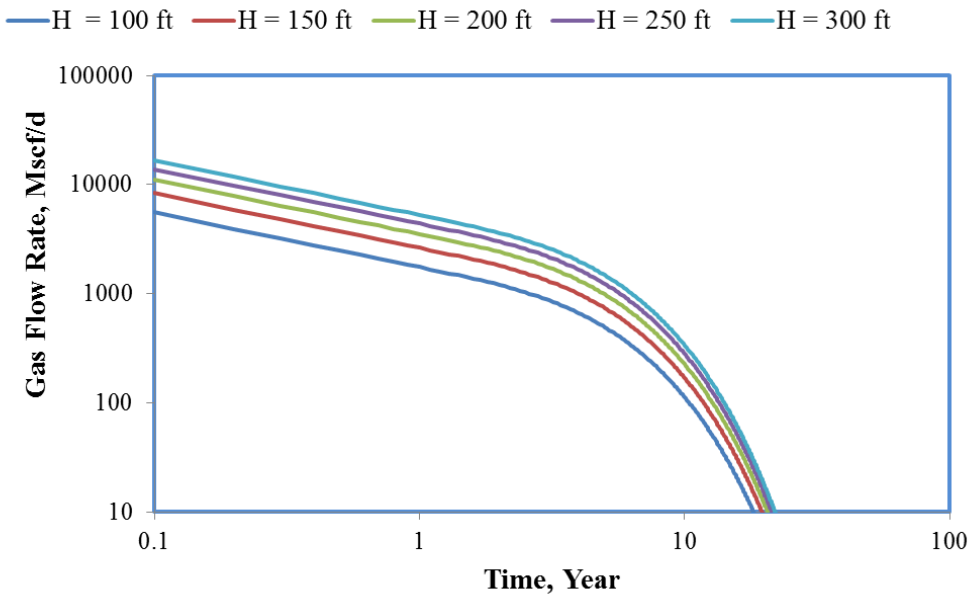

Figure 3.36: The Simplified Model gas flow rate results for hydraulic fracture height sensitivity analysis

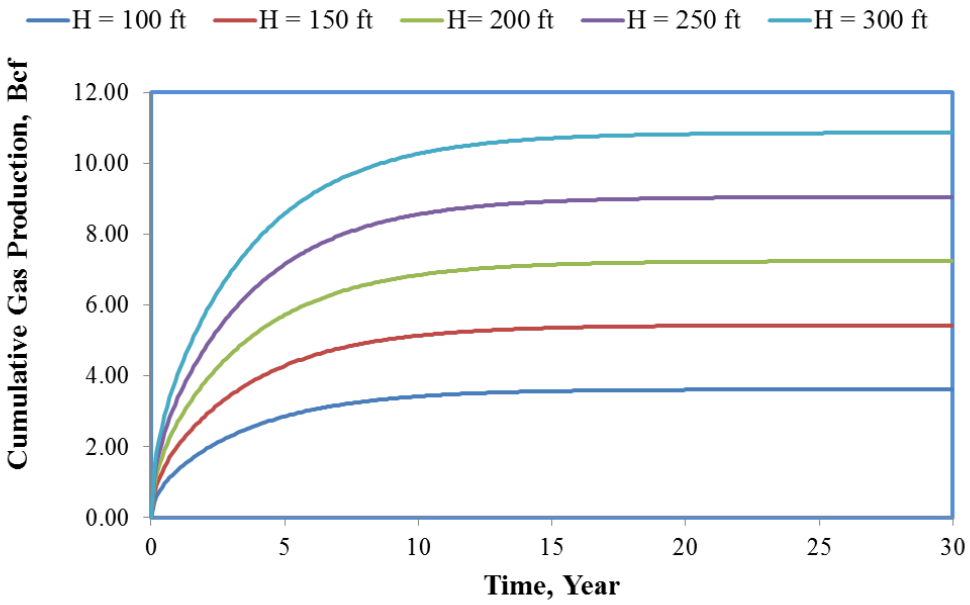

Figure 3.37: The Simplified Model cumulative gas production performance for hydraulic fracture height sensitivity analysis

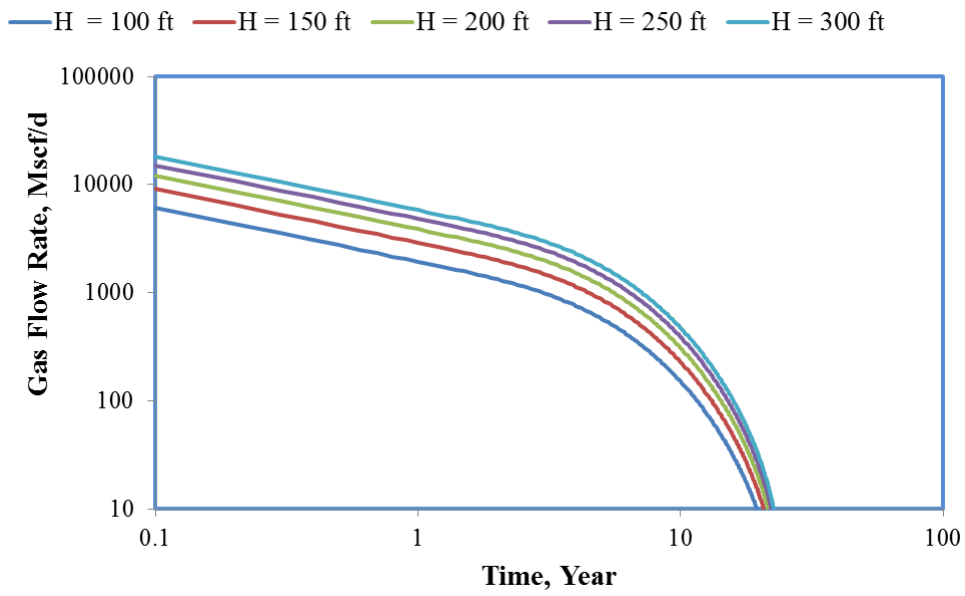

Figure 3.38: The Trilinear Model gas flow rate results for hydraulic fracture height sensitivity analysis

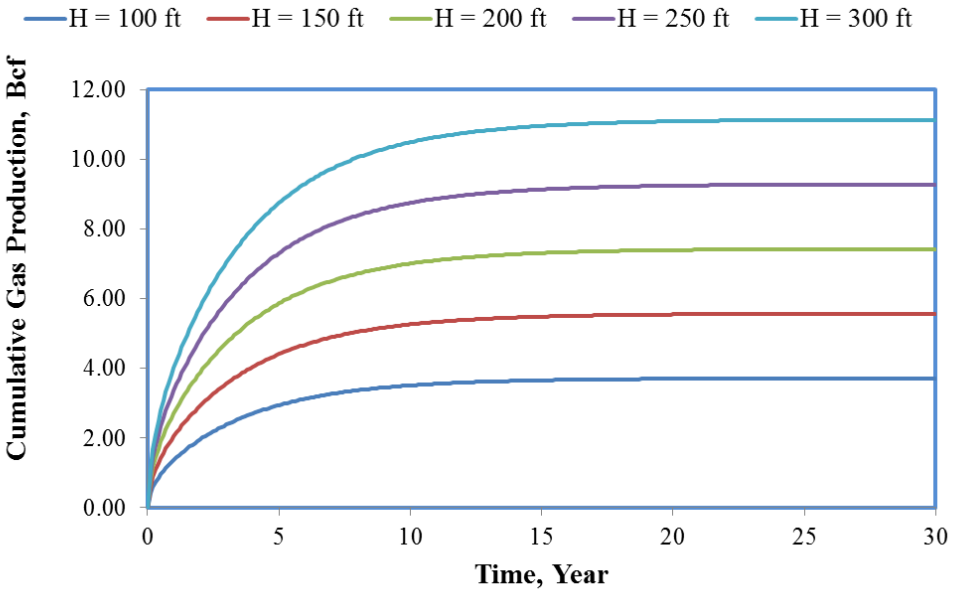

Figure 3.39: The Trilinear Model cumulative gas production performance for hydraulic fracture height sensitivity analysis

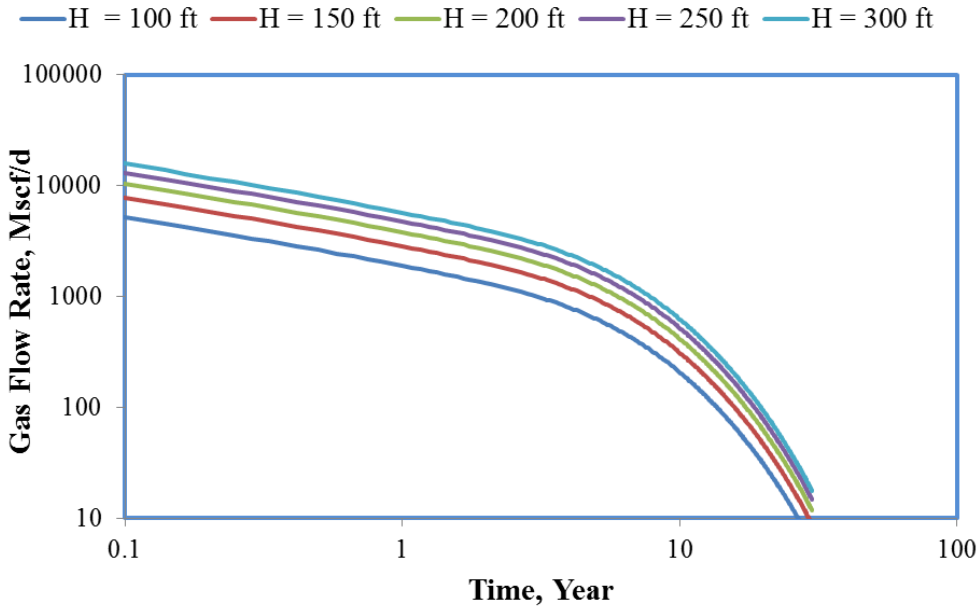

Figure 3.40: CMG gas flow rate results for hydraulic fracture height sensitivity analysis

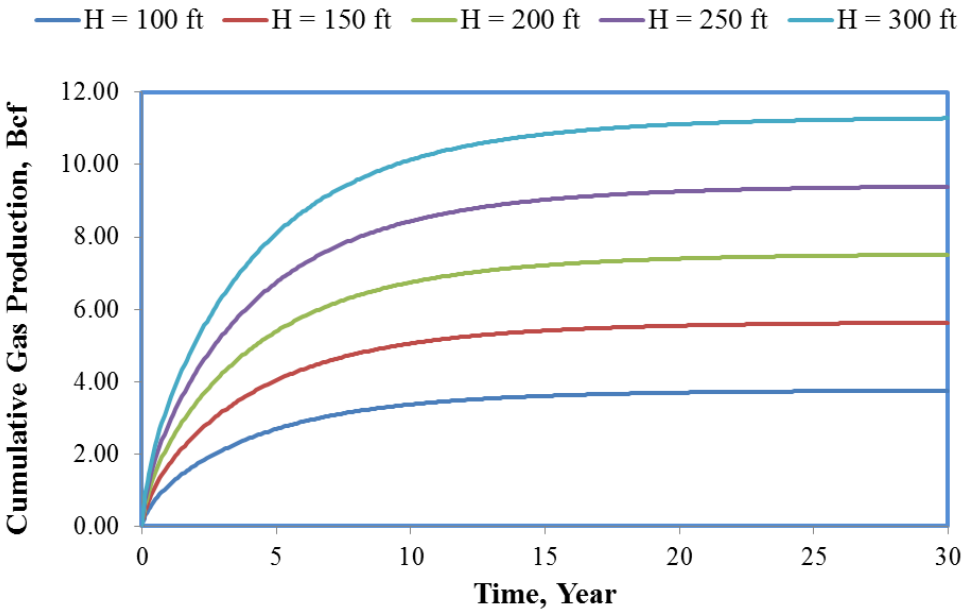

Figure 3.41: CMG cumulative gas production performance for hydraulic fracture height sensitivity analysis

3.3.2.7 Bottom Hole Pressure Sensitivity Analysis

Constant bottom-hole pressure and constant flow rate scenarios are the two options to control the well performance. Constant bottom-hole condition is considered in this sensitivity analysis, and five different bottom-hole pressures with 100 psi increments are evaluated. Daily production and cumulative production results show that the bottom-hole pressure effects on daily gas flow rate and cumulative production are insignificant (Figures 3.42 through Figure 3.47).

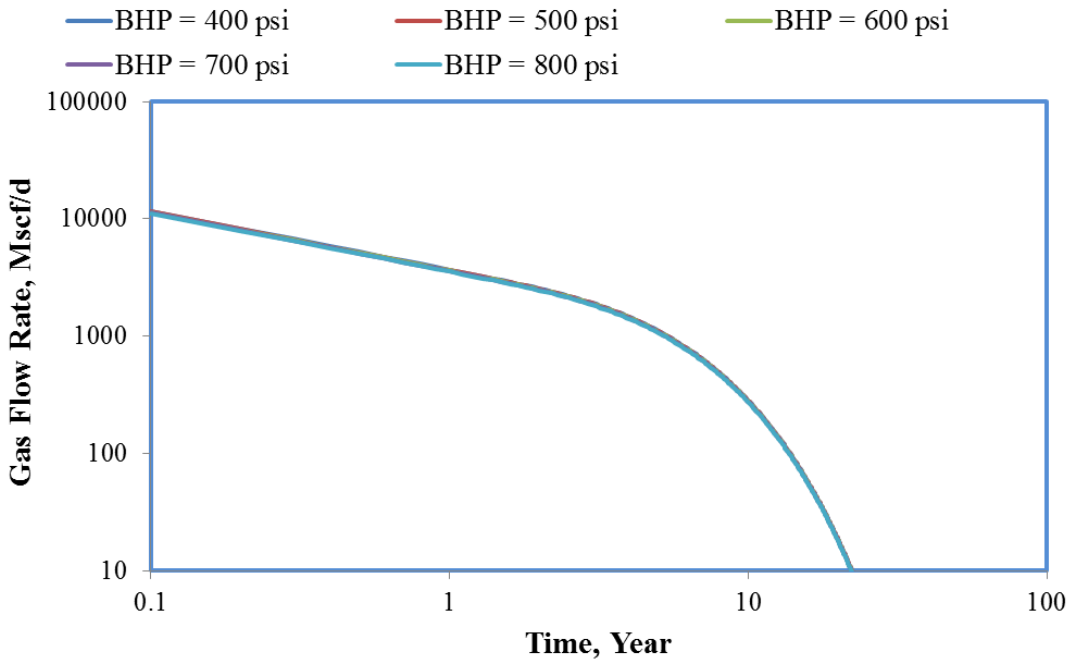

Figure 3.42: The Simplified Model gas flow rate results for BHP sensitivity analysis

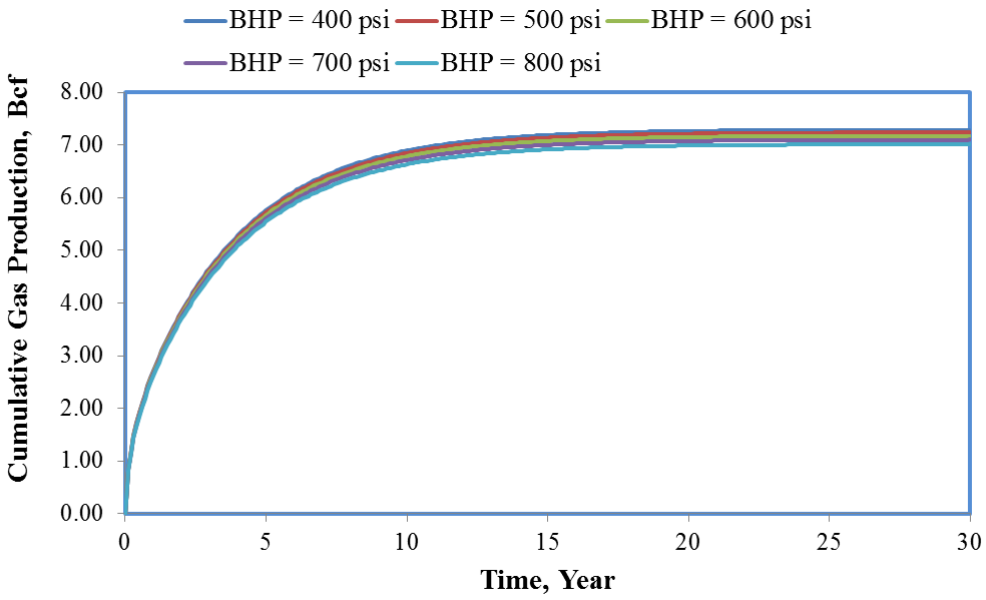

Figure 3.43: The Simplified Model cumulative gas production performance for BHP sensitivity analysis

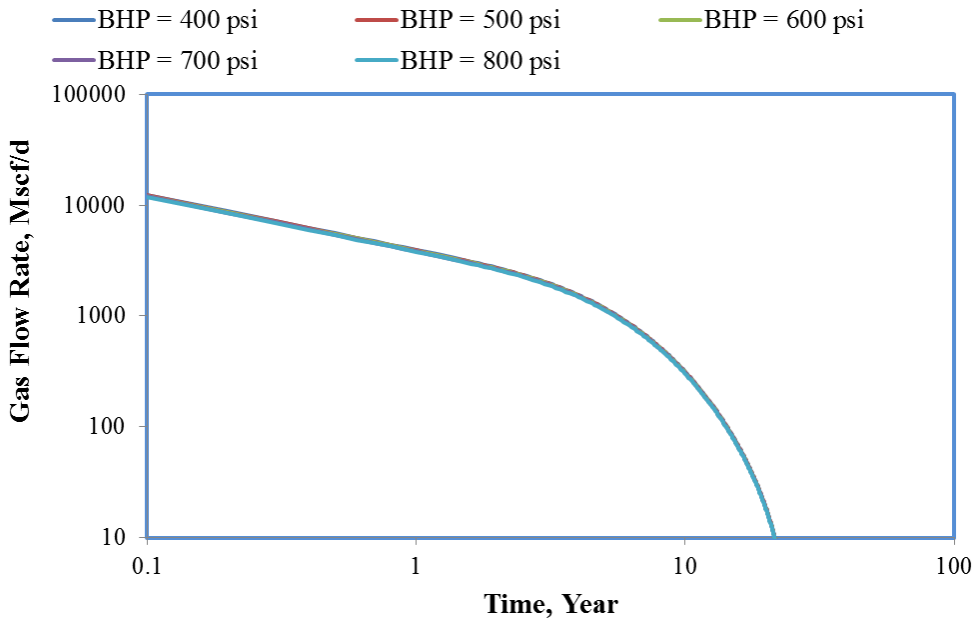

Figure 3.44: The Trilinear Model gas flow rate results for BHP sensitivity analysis

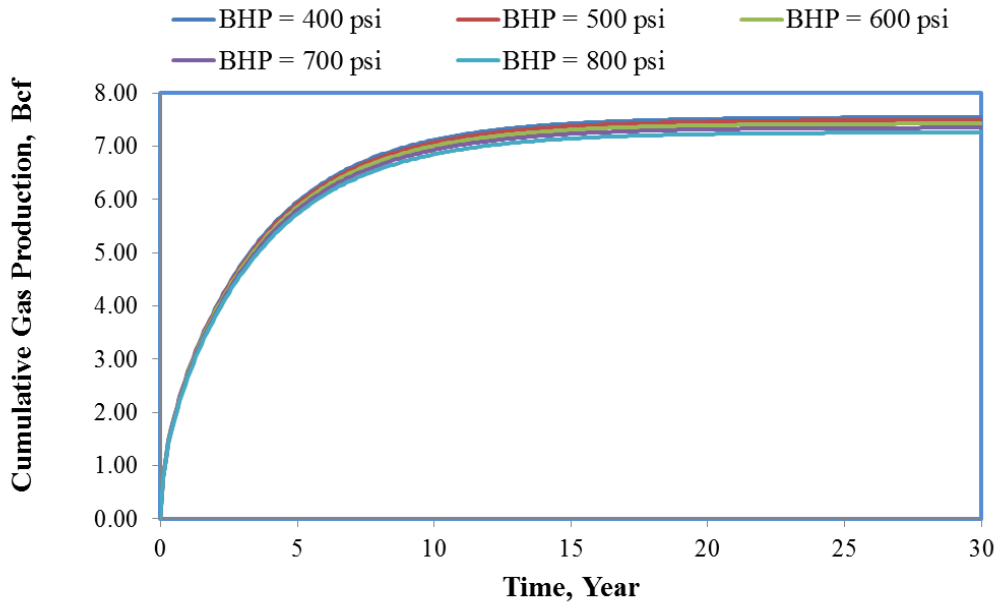

Figure 3.45: The Trilinear Model cumulative gas production performance for BHP sensitivity analysis

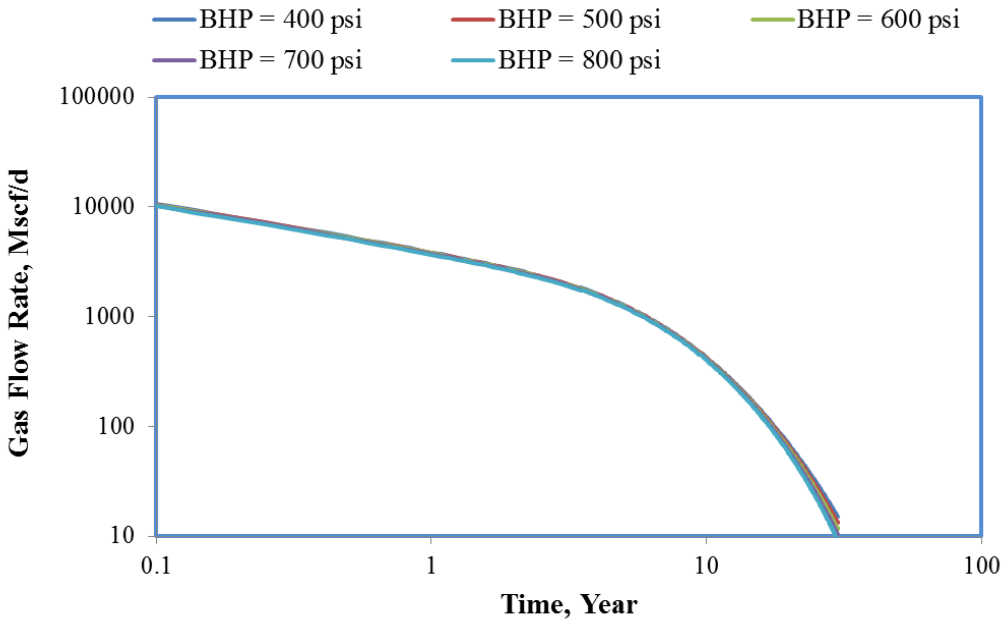

Figure 3.46: CMG gas flow rate results for BHP sensitivity analysis

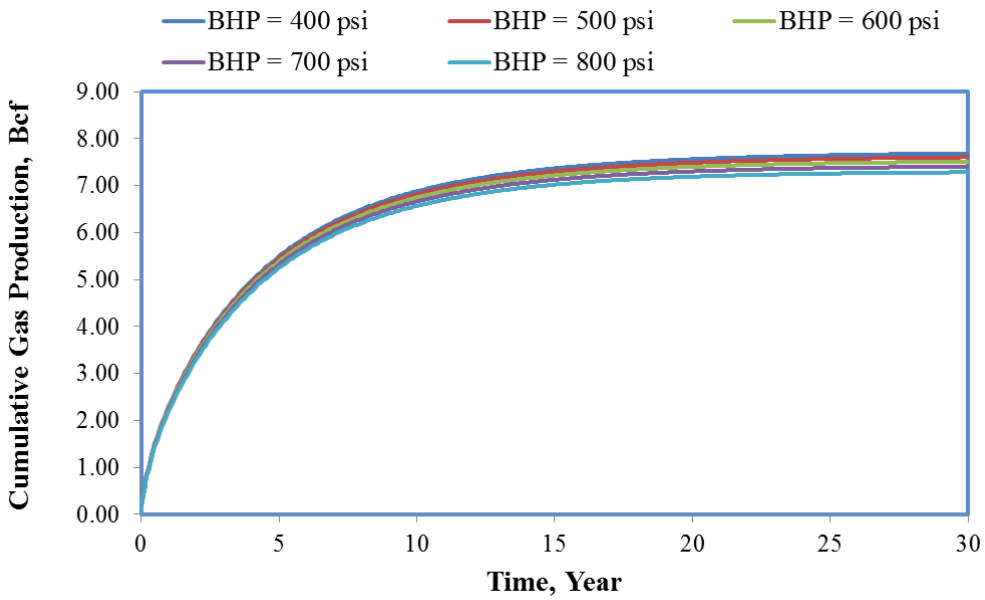

Figure 3.47: CMG cumulative gas production performance for BHP sensitivity analysis

3.3.3 Summary of the Sensitivity Analysis

This section summarizes the sensitivity analysis performed by using two analytical models and the commercial reservoir simulator for different production time periods. Wells in unconventional reservoirs are long-term investments. Depending on the operator and economic considerations, optimum well design can be obtained as a result of design parameter sensitivity analysis. Time is another fact that must be considered in such an analysis, because short, medium and long term periods might show different responses. In this study 5 year (short term), 10 year (medium term) and 30 year (long term) time periods are considered and evaluations are made based on cumulative production.

In order to organize sensitivity results obtained from analytical models and the commercial reservoir simulator tornado plots are used. Tornado plots are the chart types which listed sensitivity parameters with respect to their relative importance for a specific

reference point. For instance, in this section sensitivity parameters are listed based on cumulative production performances. In the below sections, the mid-line in the tornado plot indicates the Base Case parameters cumulative production performance, while the blue bar representing the minimum cumulative production and the red bar representing the maximum cumulative production performance. Short, medium, and long term evaluations are employed tornado plots, and results are discussed in detail.

3.3.3.1 Short Term Cumulative Production Performance Sensitivity Analysis

Short term sensitivity analyses are evaluated both for analytical models and the commercial reservoir simulator. Tornado plots obtained from short term sensitivity analysis from the simplified model, the trilinear model, and the commercial reservoir simulator (CMG) are given in Figures 3.49, 3.50 and 3.51, respectively. Detailed discussion given in this section attempts to interpret these tornado plots (Figures 3.49, 3.50 and 3.51) mainly.

Short term (5 year) cumulative production performance manifests that the fracture height and the matrix porosity are two main parameters that control the cumulative production performance, but these variables are specific to each reservoir and beyond an engineer's control. The third important parameter for cumulative production performance is hydraulic fracture stage spacing, which is under an engineer's control. For the same horizontal well length (4,000 ft.) shorter stage spacings improves the well's performance. This means in order to improve the well performance more hydraulic fracture stages must be applied and of course this fact increases the capital investment. Depending on capital investment and the rate of return, optimum stage spacing can be determined by an engineer based on the short term production performance. Matrix permeability is the fourth important parameter on the short term performance, which is again unique to each

reservoir and not a design parameter. Fracture conductivity is the fifth important parameter, which can be designed by an engineer to improve well performance, but again this kind of improvement costs more. The optimum hydraulic fracture conductivity can be determined by an engineer as a result of sensitivity studies and economic considerations. Hydraulic fracture half-length is the sixth important design parameter in this period (5 year term). There is a noticeable difference between the shortest and the longest fracture half length. Lastly, bottom hole pressure sensitivity analysis results show an insignificant difference between the highest and the lowest bottom hole pressure conditions. Sensitivity analysis results for the first five years of production are given in Figures 3.49, 3.50, and 3.51. It is observed that both analytical models and commercial reservoir simulator (CMG, IMEX) have identical sensitivity responses for the first five years of production. Figure 3.48 below shows the pressure distribution of a representative hydraulic fracture after 5 years of production. Pressure in the reservoir is still high, and only the zones near the hydraulic fracture are depleted in 5 years.

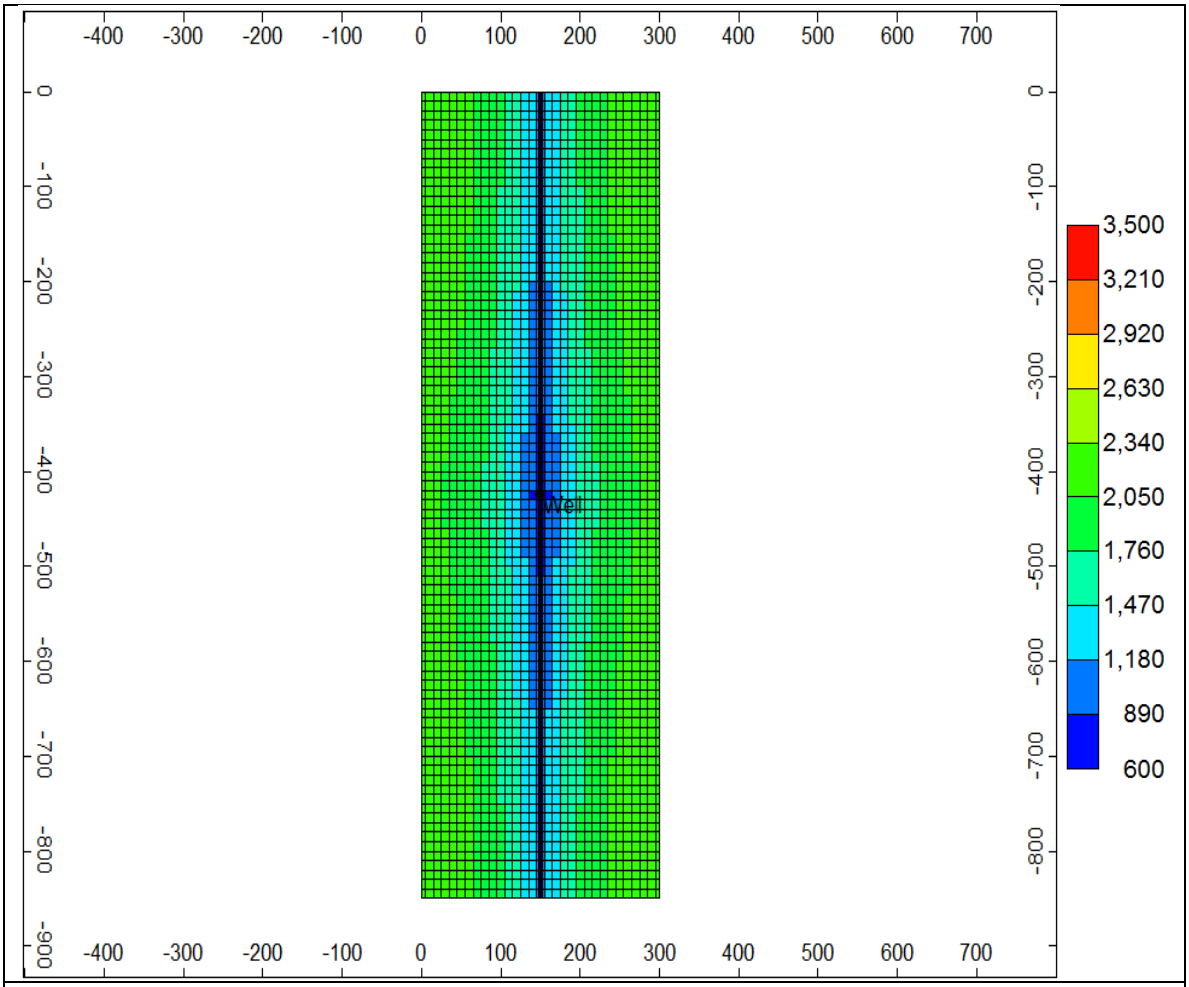

Figure 3.48: Pressure distribution after 5 years of production

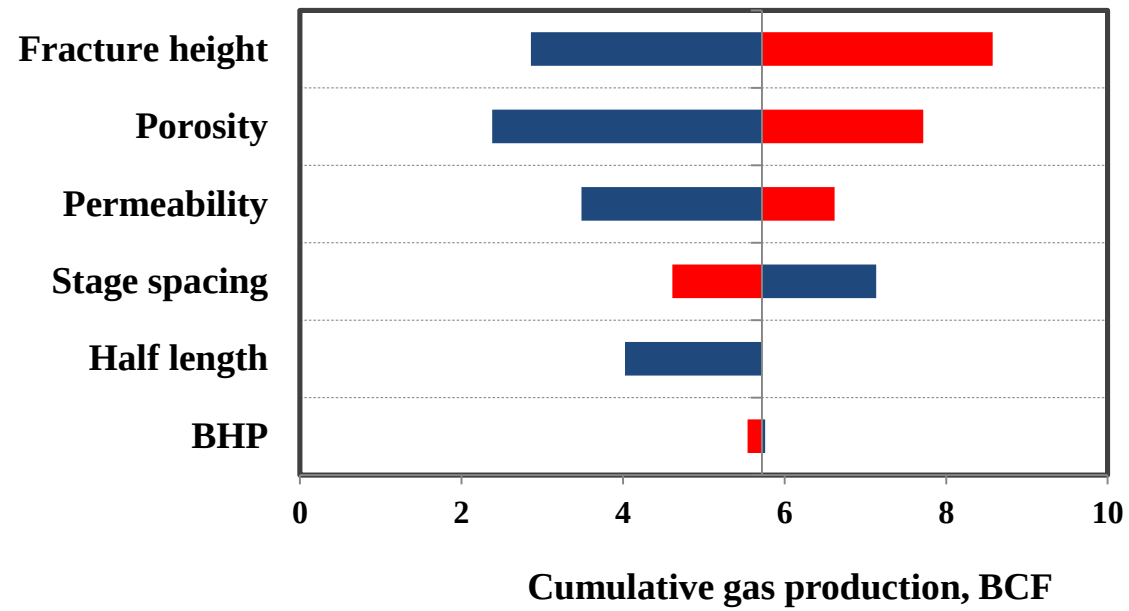

Figure 3.49: The Simplified Model Tornado Plot for 5 years

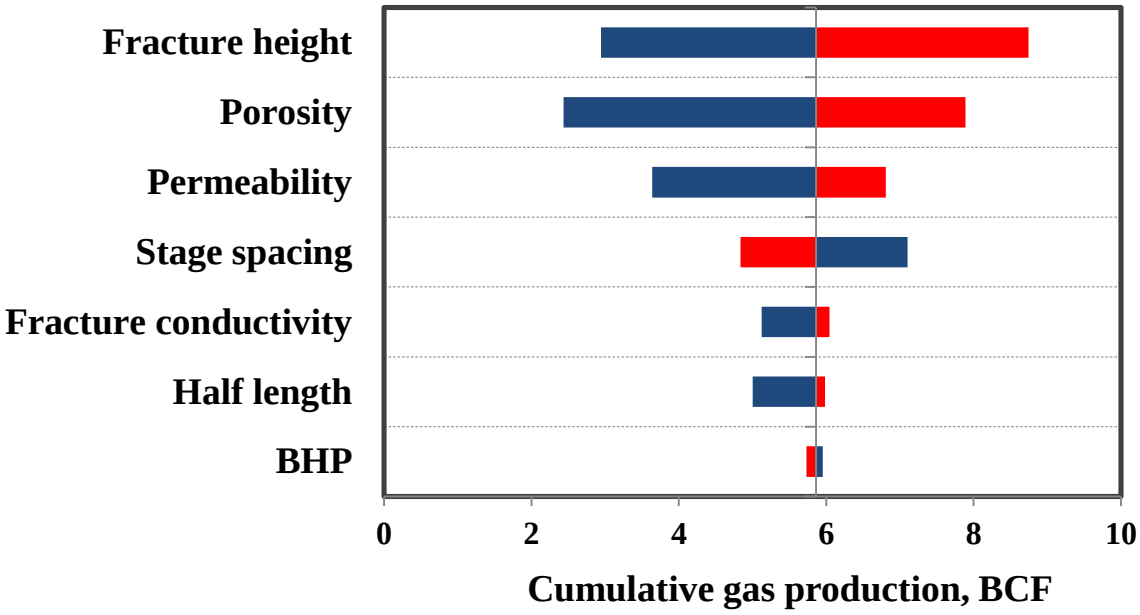

Figure 3.50: The Trilinear Model Tornado Plot for 5 years

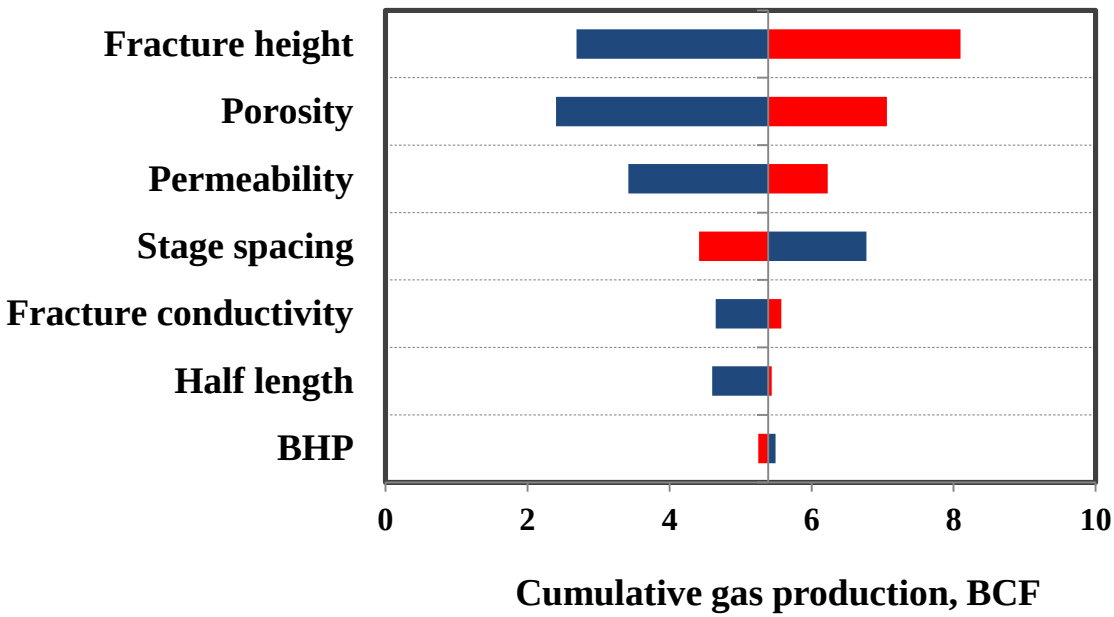

Figure 3.51: CMG Tornado Plot for 5 years

3.3.3.2 Medium Term Cumulative Production Performance Sensitivity Analysis

Sensitivity analysis for 10 years of production is evaluated in this section. Results for the simplified model, trilinear model, and the commercial reservoir simulator (CMG) are organized and provided in tornado plots in Figures 3.53, 3.54, and 3.55, respectively. Discussions in the below refers to those tornado plots.

Medium term (10 year) cumulative production performance results show that the matrix porosity and the fracture height are still two main parameters that controlling the cumulative production performance. The low matrix permeability characteristic shows its effect and importance for the first ten years of production performance. The simplified model sensitivity analysis differs from the others for medium term (10 year) sensitivity analysis, because the hydraulic fracture half-length, which controls the reservoir size in the simplified model, becomes the fourth important parameter as time progress for the simplified model analysis. Except the hydraulic fracture half-length, analytical models

and CMG show the same responses (Figures 3.53, 3.54, and 3.55). Moreover, the hydraulic fracture stage spacing still has a noticeable impact on cumulative production performance. Hydraulic fracture conductivity also continues its importance. The cumulative production difference between the highest and the lowest bottom-hole pressure conditions is insignificant for the medium term production scenario. Figure 3.52 below shows the pressure distribution of a representative hydraulic fracture after 10 years of production. Pressure distribution in the reservoir shows that the most parts of the reservoir feels the effect of production, but the zones away from hydraulic fracture still have high pressure compare to flowing bottom-hole pressure.

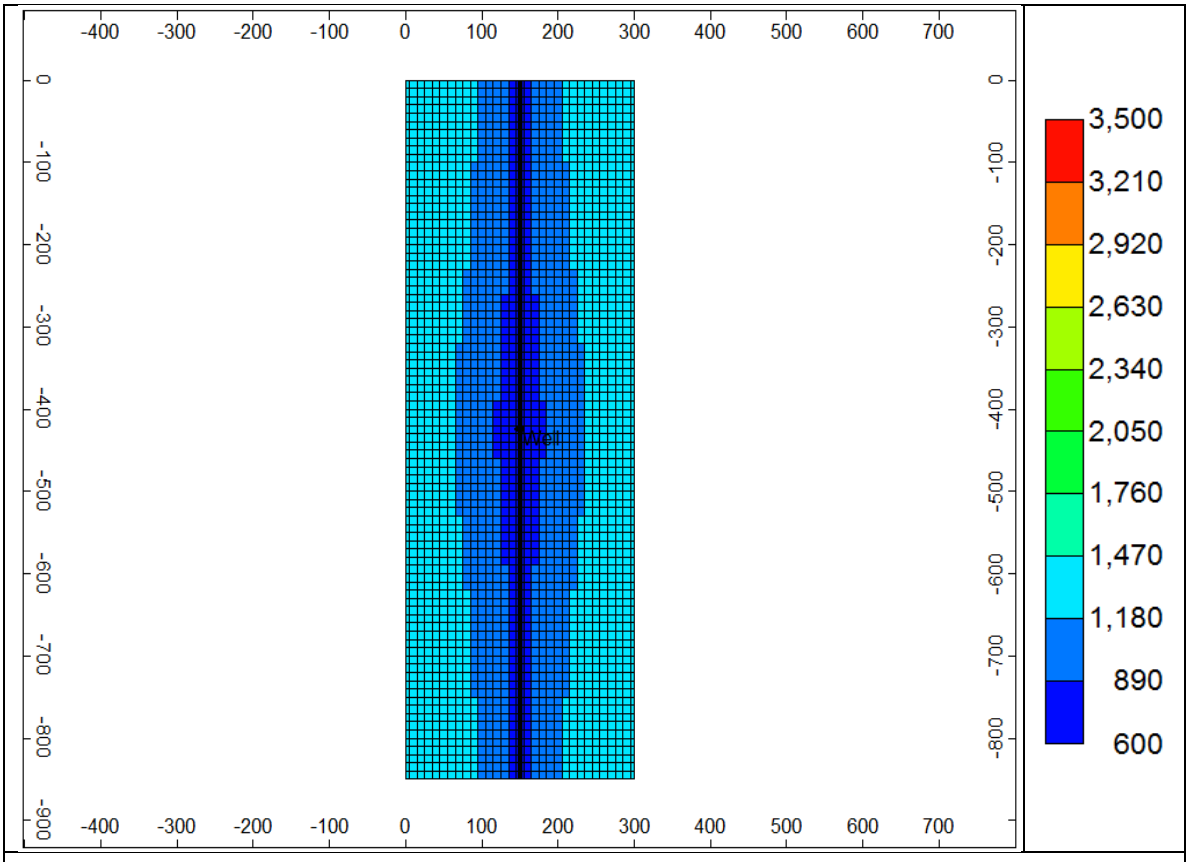

Figure 3.52: Pressure distribution after 10 years of production

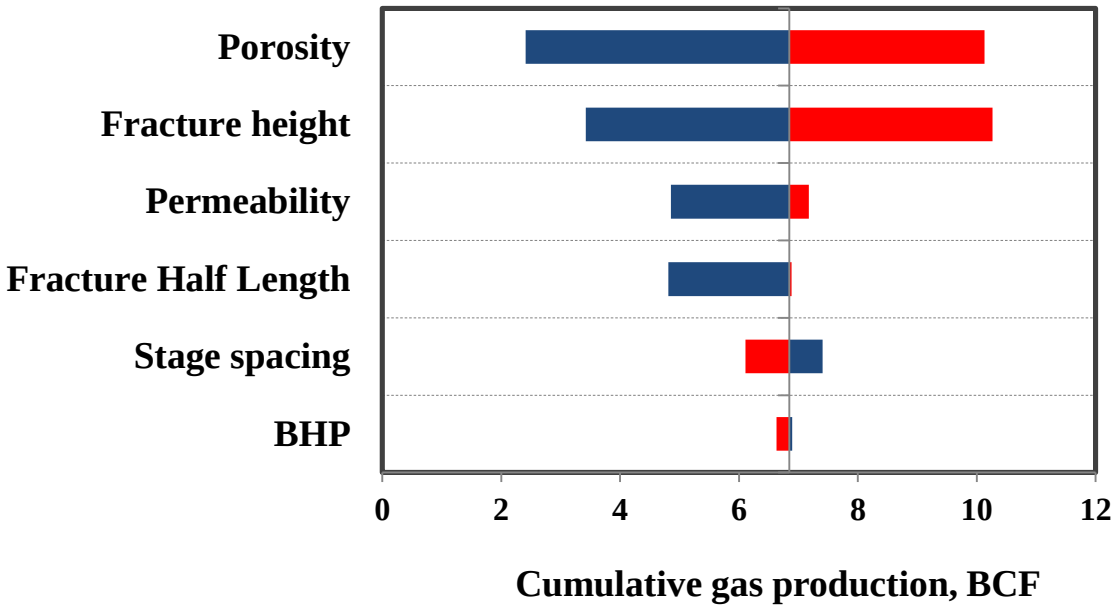

Figure 3.53: The Simplified Model Tornado Plot for 10 years

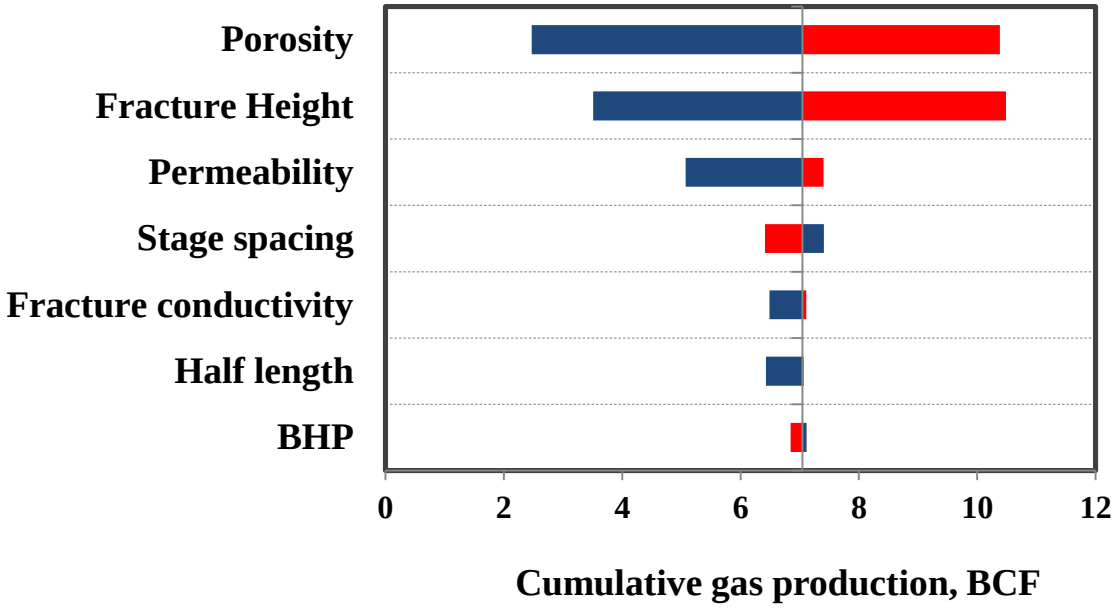

Figure 3.54: The Trilinear Model Tornado Plot for 10 years

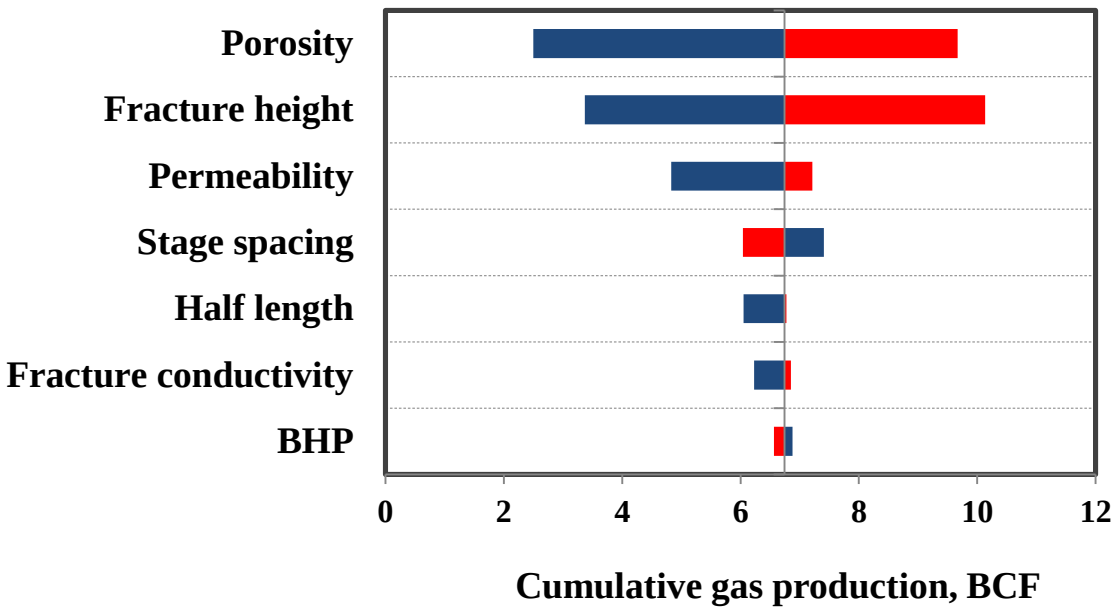

Figure 3.55: CMG Tornado Plot for 10 years

3.3.3.3 Long Term Cumulative Production Performance Sensitivity Analysis

Sensitivity analysis for long term (30 year) production is evaluated in this section. Results for the simplified model, trilinear model, and the commercial reservoir simulator (CMG) are organized and provided in tornado plots in Figures 3.57, 3.58, and 3.59, respectively. Discussions in the below mainly refers to those tornado plots.

As it is expected, the long term (30 year) cumulative production performance shows that the matrix porosity and the fracture height are two main parameters that control the cumulative production performance, since these two parameters control the original gas in place. It must be noted that the hydraulic fracture half-length in the simplified model also controls the original gas in place volume that is why the hydraulic fracture half-length is maintained its effect for 30 years performance. Other reservoir and design parameters lose their impacts on production for the long term analysis and each case reach the absolute cumulative production in 30 years (Figures 3.57, 3.58, and 3.59).

Figure 3.56 below shows the pressure distribution of a representative hydraulic fracture after 30 years of production. It is clear that the reservoir is completely depleted and reached flowing bottom-hole pressure (600 psi).

Briefly, short, medium and long term production performances are sensitive to different reservoir and design parameters, but all in all matrix porosity and reservoir height control the original gas in place and cumulative production performance eventually.

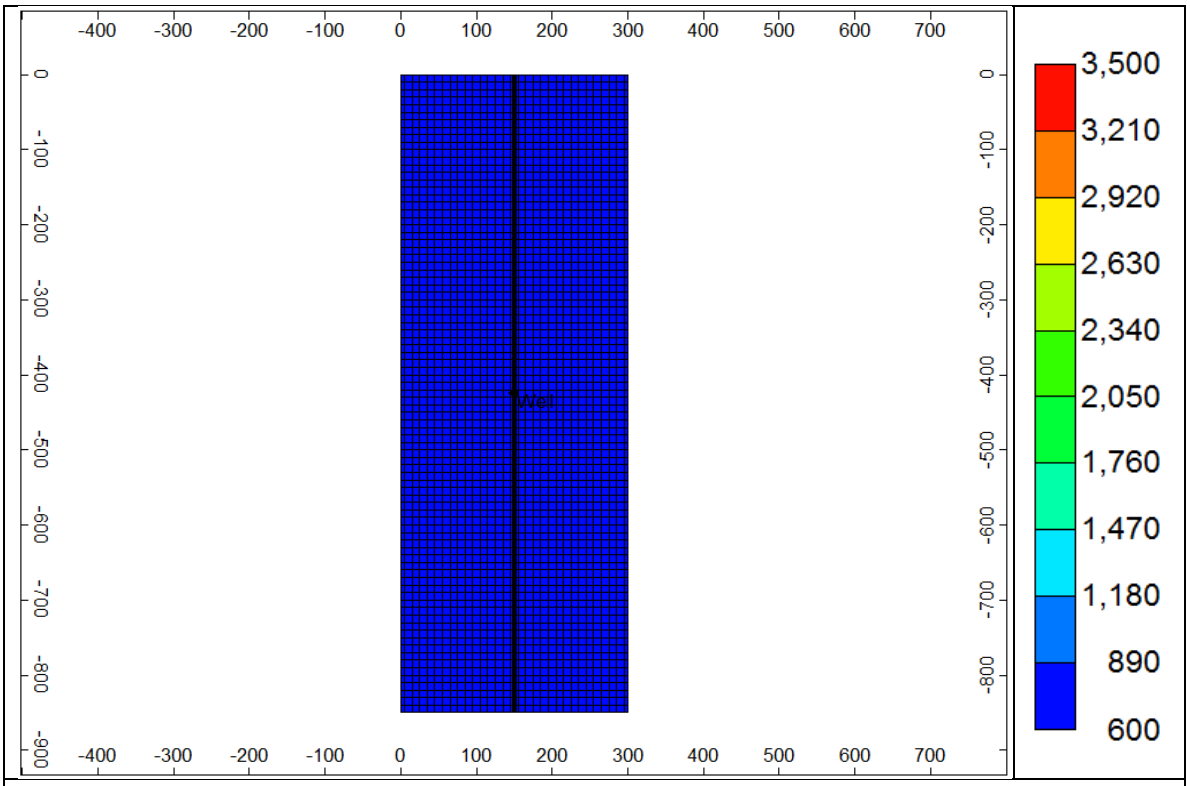

Figure 3.56: Pressure distribution after 30 years of production

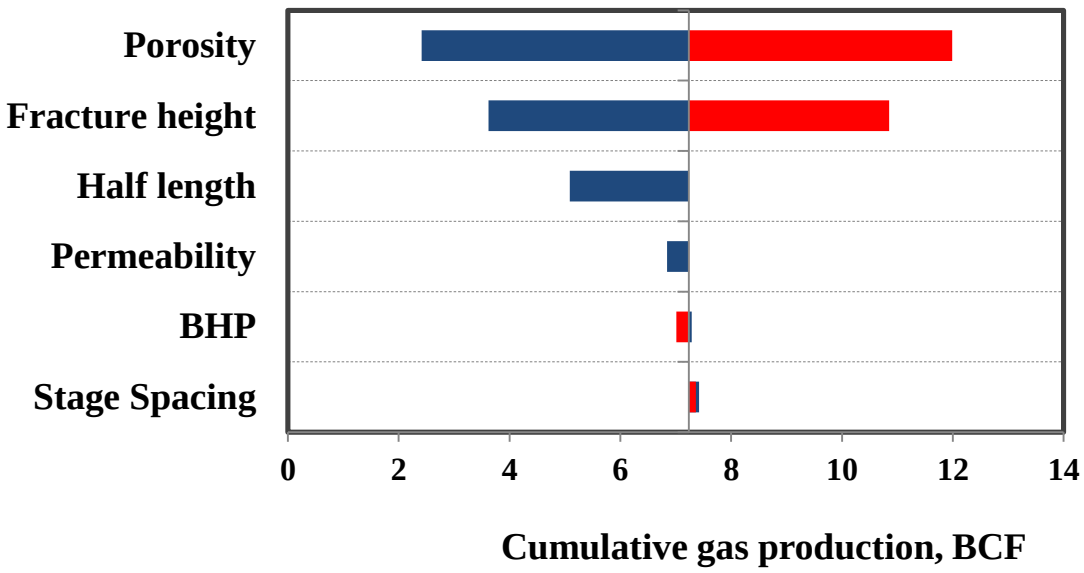

Figure 3.57: The Simplified Model Tornado Plot for 30 years

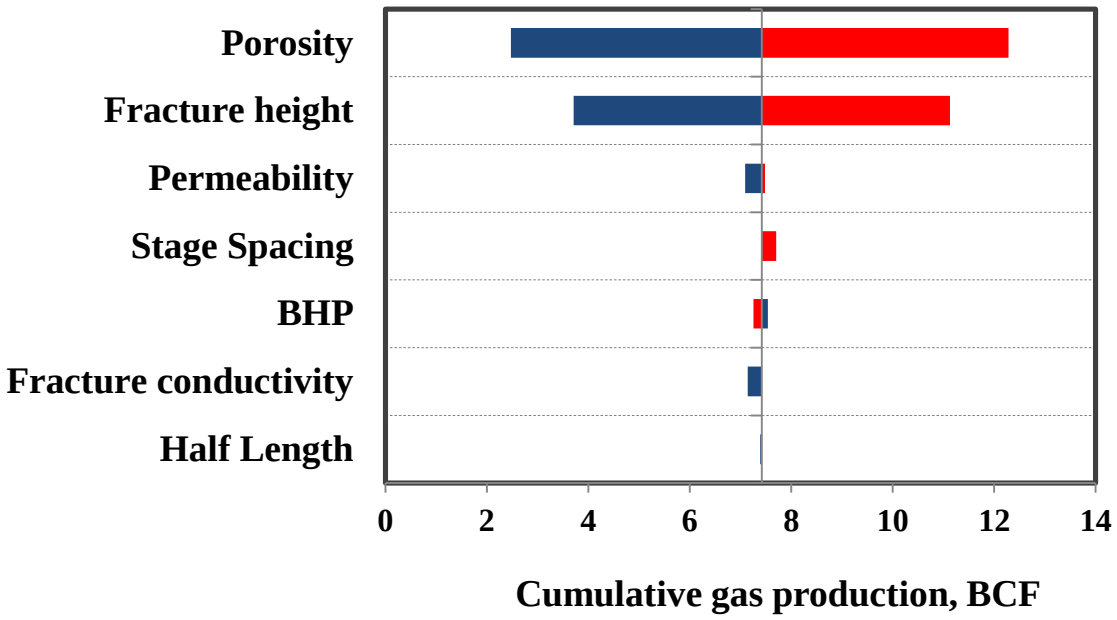

Figure 3.58: The Trilinear Model Tornado Plot for 30 years

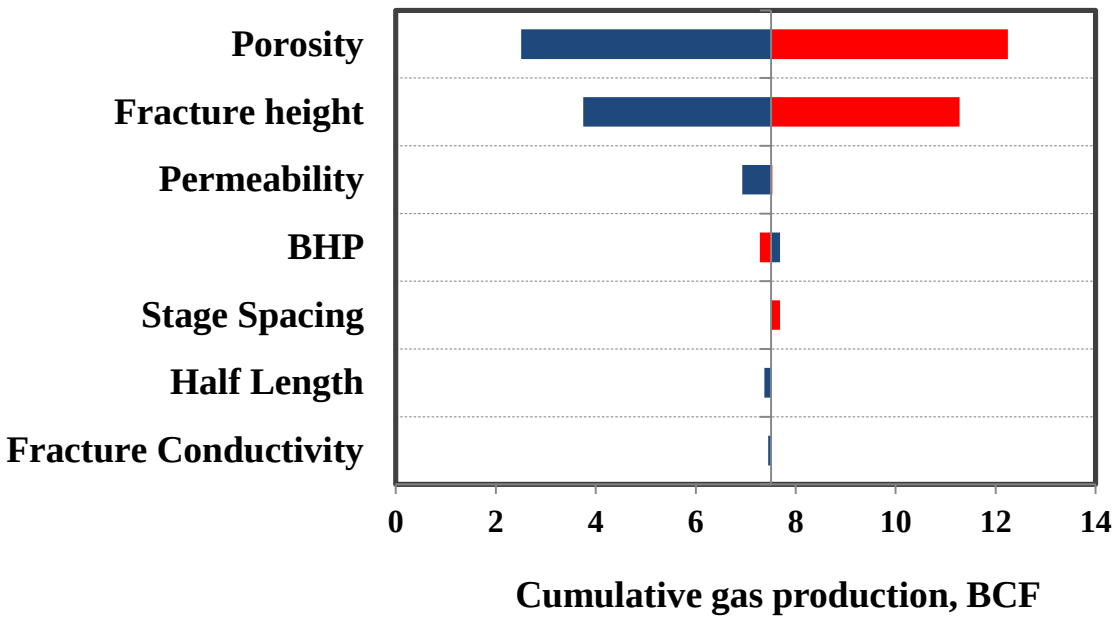

Figure 3.59: CMG Tornado Plot for 30 years

Chapter 4: Hydraulically and Naturally Fractured Unconventional Reservoir Models

The objective of this chapter is to investigate the production behavior of naturally and hydraulically fractured unconventional reservoirs incorporating the geomechanical effects. Hydraulic fracture treatment in tight formations such as shale triggers the cemented natural fractures, and creates stress induced un-propped secondary fracture network. In order to consider this issue in the reservoir modeling, Apaydin (2012) developed a model using dual porosity concept. This improved model is applied along with the trilinear flow model to represents the natural fracture network in the reservoir. The analytical dual porosity model developed by Apaydin, 2012 and the commercial reservoir simulator (CMG, IMEX, 2012) is used to achieve objectives of this chapter. Moreover, a comparison between the analytical model and CMG for various design parameters is provided. In addition, the dual porosity model, developed by Apaydin (2012), is improved to simulate constant bottom-hole pressure scenarios, and the new approach proposed in this thesis is compared and verified with CMG.

Mathematics of the dual porosity model proposed by Apaydin (2012) for naturally and hydraulically fractured is provided first. The objectives of this chapter are accomplished considering the following categories:

1. Constant natural fracture permeability concept
2. Pressure dependent natural fracture permeability concept
3. Pressure dependent natural and hydraulic fracture conductivity concept

Sensitivity analysis for the certain reservoir and well parameters are conducted and the results are also discussed in this chapter. Finally, geomechanical effects for natural fractures and hydraulic fractures are examined with the commercial reservoir simulator.

4.1 Analytical Dual Porosity Model For Unconventional Reservoirs With Incorporating The Pressure Dependent Natural Fracture Permeability

Apaydin (2012) proposed a dual porosity model which incorporates the matrix slip flow and the pressure dependent fracture permeability. Later, Cho (2012) simplified Apaydin's (2012) model considering only pressure dependent natural fracture permeability. In this thesis, pressure dependent natural fracture permeability is considered. Some of the key parameters are modified / redefined and the results are verified with a numerical commercial reservoir simulator (CMG, IMEX, 2012). It must be noted that the original method is not able to handle pressure dependent natural fracture permeability for the constant bottom-hole pressure production scenario. However, with the new approach proposed in this thesis, the constant bottom hole pressure condition can be modeled with pressure dependent natural fracture permeability feature.

Apaydin's (2012) dual porosity model considers spherical matrix geometry. Ultimate goal of his approach is to derive and implement a new transfer function into the trilinear flow model. As stated earlier, the trilinear model can handle naturally fractured zone between two adjacent hydraulic fractures. Basically, the new transfer function proposed by Apaydin (2012) is used with the trilinear model to represent the fluid flow in naturally and hydraulically fractured unconventional reservoir. A simplified schematic of the trilinear model with the spherical matrix blocks is given in Figure 4.1.

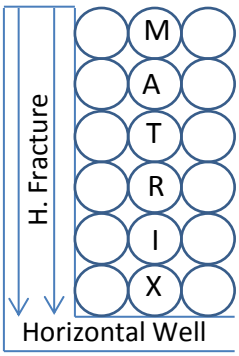

Figure 4.1 Simplified schematic of the trilinear model with spherical matrix blocks (Modified after Apaydin, 2012)

4.1.1 Assumptions for the Dual Porosity Model

Assumptions for the dual porosity model are stated as follows:

1. Isothermal, single gas phase flow with transient dual porosity idealization

The dual porosity model assumes isothermal, transient, and single gas phase flow in the matrix system.

2. Pseudo-pressure approach

Al-Hussainy et al. (1966) pseudo-pressure approach is used to linearize gas diffusivity equations.

3. Isotropic permeability tensor

The model assumes isotropic permeability tensor

4. Perfectly elastic, linear and reversible rock deformation

The model assumes that the rock deformation is perfectly elastic, linear and reversible. Also, stress distribution is uniform at the matrix-fracture boundary.

4.1.2 Formulation of the Dual Porosity Model

The dual porosity model is developed in Laplace domain (Apaydin, 2012) in order to incorporate with the trilinear model which is also in Laplace domain. For consistency with the trilinear model, the model derivation also uses dimensionless

variables. It should be noted that the purpose here to derive an analytical transfer function that considers pressure dependent natural fracture permeability. As stated in the literature review chapter, there are two main techniques available in the literature for pressure dependent permeability concept. These techniques are the permeability tensor, and the modified pseudo-pressure. Apaydin (2012) model follows the modified pseudo pressure approach for the pressure dependent natural fracture permeability solution. Essential derivation steps and definitions of key parameters are provided in this section with starting the modified pseudo-pressure given in Eqn. 4.1.

$$m_{\xi}(p) = 2\int_{p*}^{P} \beta_{\xi} \frac{p' dp'}{\mu z}; \quad \xi = \text{matrix or fracture} \qquad \text{(Eqn. 4.1)}$$

Here β term modifies the original pseudo-pressure equation. The idea is to present all the pressure dependent variables in pseudo-pressure definition. Since only the natural fracture permeability change is taken into consideration in the dual porosity model, matrix and fracture pseudo-pressure definitions differ from each other. The details of pressure dependent fracture permeability concept is given later in this chapter. Eqn. 4.2 represents the β term definition for matrix and natural fracture.

$$\beta_{matrix} = 1 ,$$
$$\beta_{natural\ fracture} = e^{-d_f \Delta p_f} , \qquad \text{(Eqn. 4.2)}$$

where,

d_f – Characteristic parameter of rock, psi^{-1}

Δp_f – Pressure changes in the system, psi .

The model (Apaydin, 2012) solves the matrix and fracture flow equations individually, and later these individual solutions (for matrix and natural fracture flow) are coupled to obtain a transfer function which models fluid flow from the matrix to the natural fractures. Although the model developed for radial flow, the transfer function

obtained can be applied in the trilinear model. Starting from the matrix flow equation, all of the pertinent equations are provided below with following the same approaches as Apaydin (2012) and Cho (2012). Additionally, necessary modifications are highlighted in this section.

Apaydin (2012) applied the mass balance for the flow of real gas in the matrix block which has the radius of r. The diffusivity equation obtained from the mass balance is given in Eqn. 4.3.

$$-\frac{1}{r^2}\frac{\partial}{\partial r}\left(r^2\rho_g v_m\right) = \frac{\partial}{\partial t}\left(\rho_g \phi_m\right), \quad \text{(Eqn. 4.3)}$$

where,

ρ_g– Gas density, lbm/ft^3

v_m – Darcy velocity in the matrix block defined by Eqn. 4.4.

$$v_m = -\frac{k_m}{\mu_g}\frac{\partial p}{\partial r}, \quad \text{(Eqn. 4.4)}$$

where,

k_m – Matrix permeability, md

μ_g – Gas viscosity, cp

p – Pressure, psi

r – Matrix block radius, ft.

$$\rho_g = \frac{M_g p}{Z_g RT}, \quad \text{(Eqn. 4.5)}$$

where,

Z_g– Compressibility factor of gas

M_g – Pseudo molecular mass of gas, lbm/mol

R – Universal gas constant, 10.73 psi-ft^3/lbm-mol-R

T– Temperature, R.

Apaydin (2012) defined dimensionless matrix diffusivity term as given in Eqn. 4.6 and also assumed constant diffusivity term

$$\eta_m = \frac{k_m}{(\phi_m c_{tm} \mu_g)_i}. \qquad \text{(Eqn. 4.6)}$$

Substituting Eqns.4.4 and 4.5 into Eqn.4.3, Eqn. 4.7 is obtained

$$\frac{1}{r^2}\frac{\partial}{\partial r}\left(r^2 \frac{k_m}{\mu_g}\frac{p_m}{z}\frac{\partial \Delta p_m}{\partial t}\right) = (\phi_m c_{tm}\frac{p_m}{z})\frac{\partial \Delta p_m}{\partial t}. \qquad \text{(Eqn. 4.7)}$$

Substituting the matrix pseudo-pressure equation (Eqn. 4.1) and Eqn. 4.6 into Eqn. 4.7, Eqn. 4.8 is derived

$$\frac{1}{r^2}\frac{\partial}{\partial r}\left(r^2 \frac{\partial \Delta m_m}{\partial r}\right) = \frac{1}{\eta_m}\frac{\partial \Delta m_m}{\partial t}. \qquad \text{(Eqn. 4.8)}$$

The initial and boundary conditions for Eqn. 4.8 are given by Eqn. 4.9

The initial condition: $\Delta m_m(r, t = 0) = 0$

The inner boundary condition: $\Delta m_m(r = 0, t) = finite$

The outer boundary condition: $\Delta m_m(r = r_m, t) = \Delta m_f(R_m, t) - \Delta m_b(R_m, t).$

(Eqn. 4.9)

The outer boundary condition of matrix block depends on pseudo-pressure difference between the matrix block and the natural fracture. This pseudo-pressure

difference causes a problem. Although the pressure continuity is considered at the boundary of matrix block and natural fracture, resulting from the definition of pseudo-pressure (Eqn. 4.2), matrix and fracture pseudo-pressures will be different for the same pressure. In order to solve this issue, Δm_b term is defined (Apaydin, 2012). The definition of the Δm_b is given by Eqn. 4.10

$$\Delta m_b(R_m, t) = 2 \int_{pf}^{Pi} \left(\beta_f - \beta_m\right) \frac{p' dp'}{\mu z} . \qquad \text{(Eqn. 4.10)}$$

As it will be discussed later in this chapter this definition creates non-linearity in the differential equation, thus an iterative approach is used to calculate pressure dependent terms such as Δm_b. Apaydin (2012) and Cho (2012) also defined Eqn. 4.11 and dimensionless variables which are given in Eqns. 4.12 and 4.13

$$u_{mD}(r, t) = r_D m_m(r, t) , \qquad \text{(Eqn. 4.11)}$$

$$r_D = \frac{r}{L} , \qquad \text{(Eqn. 4.12)}$$

$$R_D = \frac{R}{L} , \qquad \text{(Eqn. 4.13)}$$

$$\eta_{mD} = \frac{\eta_{fi}}{\eta_{mi}} = \frac{(\phi_m c_{tm} \mu_g)_i k_f}{(\phi_f c_{tf} \mu_g)_i k_m} . \qquad \text{(Eqn. 4.14)}$$

Substituting Eqns. 4.11, 4.12, 4.13 and 4.14 into Eqn. 4.8, Eqn. 4.15 is obtained

$$\frac{\partial^2 u_{m_D}}{\partial {r_D}^2} = \eta_{mDi} \frac{\partial u_{mD}}{\partial t_D} . \qquad \text{(Eqn. 4.15)}$$

The initial condition: $u_{mD}(r_D, R_{mD}, t_D = 0) = 0$

The inner boundary condition: $u_{mD}(r_D = 0, R_{mD}, t_D) = 0$

The outer boundary condition: $u_{mD}(r = r_{mD}, t_D) = m_{fD}(R_m, t_D) - m_{bD}(R_m, t_D)$.

(Eqn. 4.16)

In order to solve Eqn.15 with the given boundary conditions in Eqn. 4.16, Laplace transform is used (Apaydin and Cho, 2012) and Eqns. 4.17, 4.18 and 4.19 are obtained.

$$\frac{\partial^2 u_{\overline{m}_D}}{\partial {r_D}^2} - s\,\eta_{mDi}\bar{u}_{mD} = 0\,, \qquad \text{(Eqn. 4.17)}$$

$$\bar{u}_{mD}(r_D = 0, R_{mD}, s) = 0\,, \qquad \text{(Eqn. 4.18)}$$

$$\bar{u}_{mD}(r = r_{mD}, R_{mD}, s) = \bar{m}_{fD}(R_{mD}, s) - \bar{m}_{bD}(R_m D, s)\,. \qquad \text{(Eqn. 4.19)}$$

Solution for the Eqn. 4.17 with respect to boundary conditions is given in Eqn. 4.20

$$\bar{u}_{mD}(r_D, R_{mD}, s) = \frac{\sinh(\sqrt{s\eta_{mDi}}r_D)}{\sinh(\sqrt{s\eta_{mDi}}r_D)}\left[\bar{m}_{fD}(R_m, s) - \bar{m}_{bD}(R_m, s)\right]. \qquad \text{(Eqn. 4.20)}$$

Apaydin (2012) and Cho (2012) further defined the Eqn. 4.21 as follows:

$$\alpha = 1 - \frac{\bar{m}_{bD}(R_{mD},s)}{\bar{m}_{fD}(R_{mD},s)}\,. \qquad \text{(Eqn. 4.21)}$$

In this thesis, we considered α definition as given in Eqn. 4.22

$$\alpha = \frac{\bar{m}_{mD}(R_{mD},s)}{\bar{m}_{fD}(R_{mD},s)}\,. \qquad \text{(Eqn. 4.22)}$$

Substituting Eqn. 4.22 into Eqn. 4.20 and also using the definition given in Eqn. 4.11, Eqn.4.23 is obtained

$$\bar{m}_{mD}(r_D, R_{mD}, s) = \alpha \frac{r_{mD}\sinh(\sqrt{s/\eta_{mDi}}r_D)}{r_D\sinh(\sqrt{s/\eta_{mDi}}r_{mD})}. \quad \text{(Eqn. 4.23)}$$

Solution of the ODE for matrix flow is given with Eqn. 4.23. This solution will be used later to derive a new transfer function.

Flow in the natural fracture is defined by Eqn. 4.24 in radial coordinates

$$-\frac{1}{R}\frac{\partial}{\partial R}\left(R\rho_g v_g\right) + F(R,t) = \frac{\partial}{\partial t}(\rho_g \phi_f). \quad \text{(Eqn. 4.24)}$$

Apaydin and Cho (2012) indicated that they followed the de Swaan O (1976) assumption to define the source term. The assumption is that the matrix flux is distributed in ½ of the surrounding fracture. Therefore,

$$\frac{1}{2}V_f \approx A_m \frac{h_f}{2} = 4\pi r_m^2 \frac{h_f}{2}, \quad \text{(Eqn. 4.25)}$$

$$F = \left[\frac{\rho_g q_m}{\left({}^{V_f}/_{2}\right)}\right] = -\frac{4\pi}{\left({}^{V_f}/_{2}\right)}\left[r^2 \rho_g \frac{k_m}{\mu_g}\frac{\partial p_m}{\partial r}\right]. \quad \text{(Eqn. 4.26)}$$

They also defined a transmisivity term which is given in Eqn. 4.27

$$\tilde{\lambda} = \frac{k_m L^2}{k_{fi} h_f r_m}. \quad \text{(Eqn. 4.27)}$$

Substituting Eqns. 4.26 and 4.27 into Eqn. 4.24 and using the dimensionless variables, Eqn. 4.24 can be represented by Eqn. 4.28

$$\frac{1}{R_D}\frac{\partial}{\partial R_D}\left(R_D\frac{\partial \bar{m}_{fD}}{\partial R_D}\right) - 2\tilde{\lambda}\left(\frac{\partial \bar{m}_{mD}}{\partial r_D}\right) - s\bar{m}_{fD} = 0\,. \qquad \text{(Eqn. 4.28)}$$

The derivative in the second term of left hand side can be obtained from Eqn. 4.23.

$$\left(\frac{\partial \bar{m}_{mD}}{\partial r_D}\right)\Big|_{rD=1.RmD,s} = -\frac{1}{r_{mD}}\left[1 - \sqrt{s\eta_{mDi}}r_{mD}\ coth\left(\sqrt{s\eta_{mDi}}r_{mD}\right)\right]\alpha\,. \qquad \text{(Eqn. 4.29)}$$

Substituting Eqn. 4.29 into Eqn. 4.28, Eqn. 4.30 is obtained

$$\frac{1}{R_D}\frac{\partial}{\partial R_D}\left(R_D\frac{\partial \bar{m}_{fD}}{\partial R_D}\right) + 2\frac{\tilde{\lambda}}{r_{mD}}\left[1 - \sqrt{s\eta_{mDi}}r_{mD}\ coth\left(\sqrt{s\eta_{mDi}}r_{mD}\right)\right]\alpha - s\bar{m}_{fD} = 0.$$

(Eqn. 4.30)

Apaydin (2012) defined transfer function as follows:

$$f(R_{mD}, s) = 1 - 2\frac{\tilde{\lambda}}{r_{mD}s}\left[1 - \sqrt{s\eta_{mDi}}r_{mD}\ coth\left(\sqrt{s\eta_{mDi}}r_{mD}\right)\right]\alpha\,. \qquad \text{(Eqn. 4.31)}$$

Apaydin (2012) further defined

$$\lambda = \sigma L^2\left[\frac{k_m V_m}{k_{fi}\left({}^{V_f}/_{2}\right)}\right] = \sigma L^2\left[\frac{k_m(4/3)\pi r_m^3}{k_{fi}4\pi r_m^2\left({}^{h_f}/_{2}\right)}\right] = \sigma L^2\left(\frac{2k_m r_m}{3k_{fi}h_f}\right). \qquad \text{(Eqn. 4.32)}$$

Here σ term is an important aspect of dual porosity models which is called shape factor. Apaydin (2012) used n=3 orthogonal fracture sets for the spherical matrix block shape, and defined the shape factor as given in Eqn. 4.33

$$\sigma = \frac{(n+2)}{n\left({}^{V_m}/_{A_m}\right)^2} = \frac{15}{r_m^2}\,. \qquad \text{(Eqn. 4.33)}$$

The storativity ratio is also defined by Eqn. 4.34

$$\omega = \frac{\phi_m c_{tm} V_m}{\phi_f c_{tf} \left(V_m/_2\right)} = \frac{2\phi_m c_{tm} r_m}{3\phi_f c_{tf} h_f} . \quad \text{(Eqn. 4.34)}$$

Substituting transmisivity and storativity equations given in Eqns. 4.32 and 4.34 into dimensionless diffusivity equation, Eqn. 4.35 is obtained

$$\eta_{mDi} = \frac{\eta_{fi} r_m^2}{\eta_{mi} L^2} = \frac{(\phi_m c_{tm} \mu_g)_i k_f r_m^2}{(\phi_f c_{tf} \mu_g)_i k_m L^2} = 15 \frac{\omega}{\lambda} . \quad \text{(Eqn. 4.35)}$$

Finally, the transfer function which has stress dependent natural fracture permeability feature is given by Eqn. 4.36

$$f(R_{mD}, s) = 1 - \frac{\lambda}{5s}\left[1 - \sqrt{\frac{15\omega s}{\lambda}}\, s\, coth\left(\sqrt{\frac{15\omega s}{\lambda}}\right)\right] \alpha . \quad \text{(Eqn. 4.36)}$$

This transfer function is used with the trilinear model in order to represent gas flow in the multiply fractured horizontal well in naturally fractured unconventional reservoir. Definitions of the transmisivity and storativity with the new transfer function are the key elements of Apaydin (2012) model. The alpha term in the transfer equation is a function of pressure, because the definition of natural fracture and matrix pseudo-pressure is different from each other and creates inequality at the matrix-fracture boundary. The original method proposed by Apaydin (2012) and Cho (2012) considers only constant bottom hole pressure production scenario, and examines the pressure dependent natural fracture permeability effects on pressure drop profile. However, it is important to see those effects on production performance. For this purpose, in this thesis we proposed an alternative approach for constant bottom hole pressure scenario. The important point is to find the reference pressure to calculate the alpha term in the transfer function. Apaydin

(2012) and Cho (2012) use the well-bore pressure as a reference to calculate the alpha, while we consider the average reservoir pressure as a reference pressure. Average reservoir pressure calculation for the trilinear model is the new modification proposed in this study. We followed a numerical approach to calculate the average reservoir pressure, details of the numerical discretization is given in the appendix. Basically our method calculates the average reservoir pressure for each time step, and calculated average reservoir pressure is used to update alpha term in the transfer function. We also followed the same approach as Apaydin (2012) and Cho (2012) to update the alpha for the current time step. This approach is an iterative method with an initial guess, and it is observed that the convergence is quite stable through the end of simulation. We further tested our approach with a commercial reservoir simulator and results showed a good agreement. The following section represents the results obtained from the analytical model and commercial reservoir simulator.

4.2 IMPLEMENTATION OF THE DUAL POROSITY MODEL COUPLED WITH THE TRILINEAR MODEL

In this section, a synthetic data set for an unconventional multiply fractured reservoir with natural fractures is evaluated with the Apaydin (2012) dual porosity model. In order to verify results from the modified analytical model, a commercial reservoir simulator is also employed for the same data set. First, existence of natural fracture effect on production performance is analyzed by comparing with a homogeneous reservoir case. For this case the results obtained from analytical dual porosity model is verified with the commercial reservoir simulator (CMG, IMEX, 2012). In addition, a sensitivity study is performed for naturally fractured unconventional reservoir. Secondly, pressure dependent natural fracture permeability effect on production performance is evaluated both with the modified analytical model and the commercial reservoir simulator (CMG, IMEX, 2012).

Finally, sensitivity analysis is conducted to identify under which circumstances the pressure dependent naturally fracture permeability must be taken into account, and the results are discussed in detail.

4.2.1 Comparison of Homogeneous Unconventional Reservoir Model and Naturally Fractured Unconventional Reservoir Model for a Synthetic Case Study

Hydraulic fractures are the main channels for the flow of hydrocarbon in unconventional reservoirs. However, having only hydraulic fractures in the system still limits the production performance. Researchers claim that to have such a high initial production performance observed from unconventional shale gas resources, there must be a secondary fracture network to conduit the flow. In this section a synthetic reservoir production performance is evaluated with homogeneous reservoir condition (no natural fractures), and naturally fractured reservoir in order to observe the effects of natural fracture network on production performance. A program is developed in MATLAB to calculate gas production with the analytical model. Another simulation model is also created with CMG (IMEX, 2012) to examine the natural fracture effects on production performance. The synthetic data set is given in Table 4.1. The model considered in the CMG is given in Figure 4.2.

Table 4.1: Input parameters for naturally fractured reservoir case

Parameter	Value(s)	Unit
The model dimensions	3,900 (length), 660 (width), 330 (height)	ft
Initial reservoir pressure	3500	psi
BHP	500	psi
Production time	30	year
Reservoir temperature	200	^{o}F
Gas viscosity	0.0184	cp
Initial gas saturation	1	fraction
Total compressibility	$5x10^{-4}$	psi^{-1}
Matrix permeability	0.0006	md
Matrix porosity	0.06	fraction
Natural fracture permeability	100	md
Natural fracture thickness	$5x10^{-4}$	ft
Number of natural fractures	10	#
Fracture half length	330	ft
Fracture stage spacing	300	ft
Fracture height	330	ft
Number of hydraulic fracture stages	14	#
Number of well	1	number

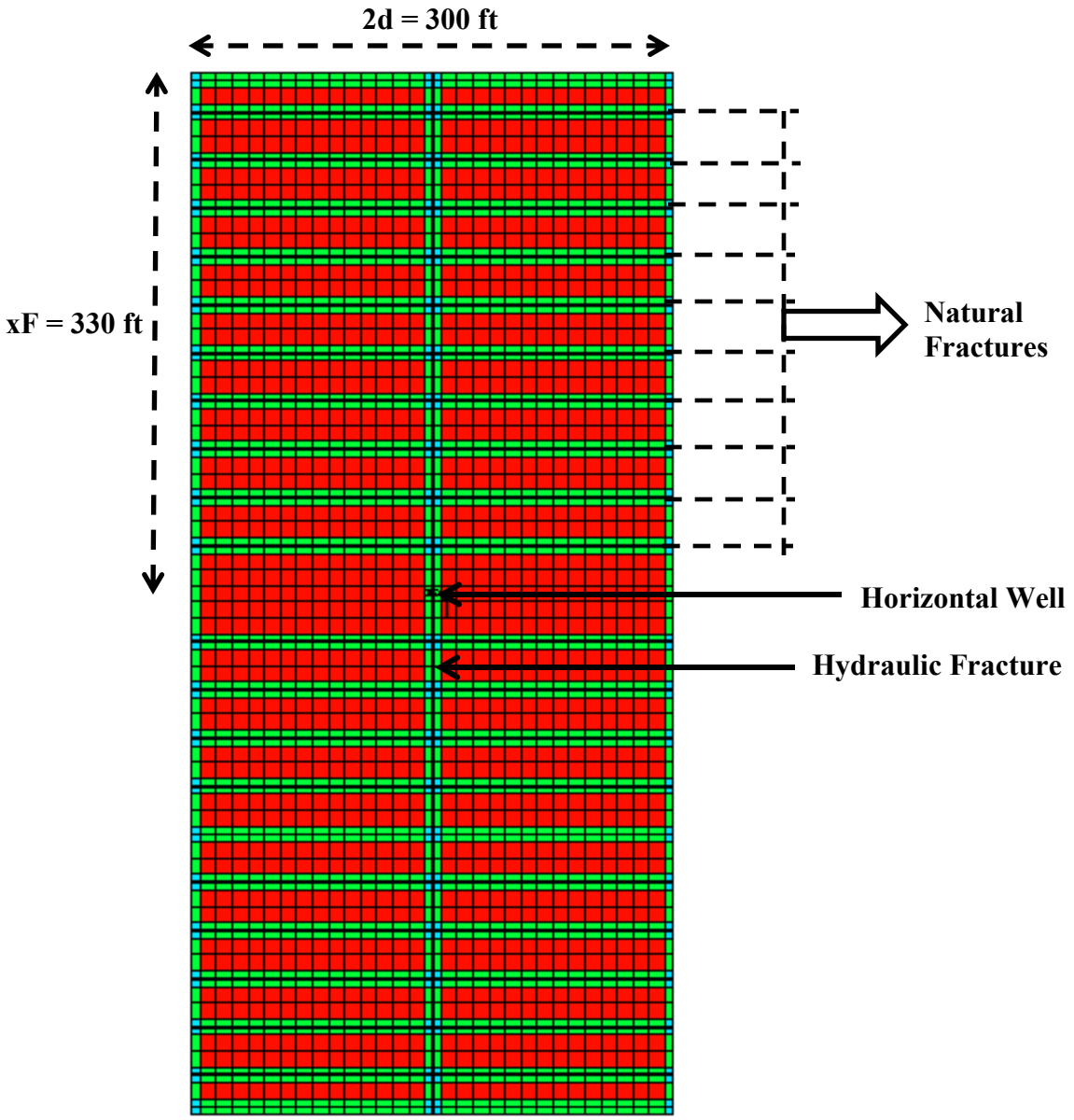

Figure 4.2 2-D CMG Model for naturally and hydraulically fractured reservoir

The purpose is to compare the analytical solution with the commercial reservoir simulator (CMG, IMEX, 2012), and also compare the homogeneous and naturally fractured cases production performances for a long-term scenario. The results obtained from the analytical model and the numerical reservoir simulator is given in Figures 4.3 and 4.4.

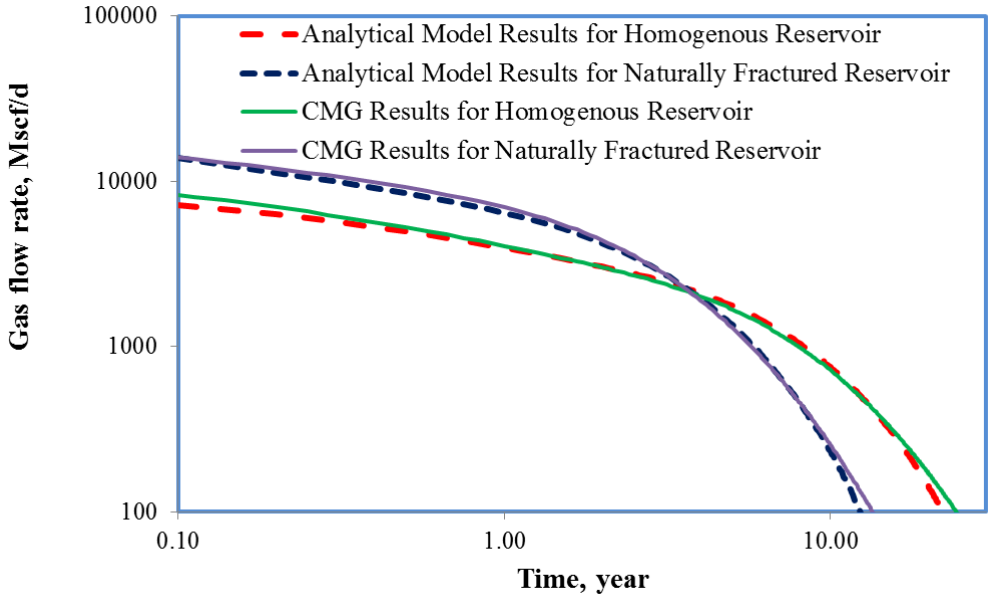

Figure 4.3 Comparison of gas flow rate performances obtained from the Analytical Model and CMG by considering homogeneous and naturally fractured unconventional reservoir

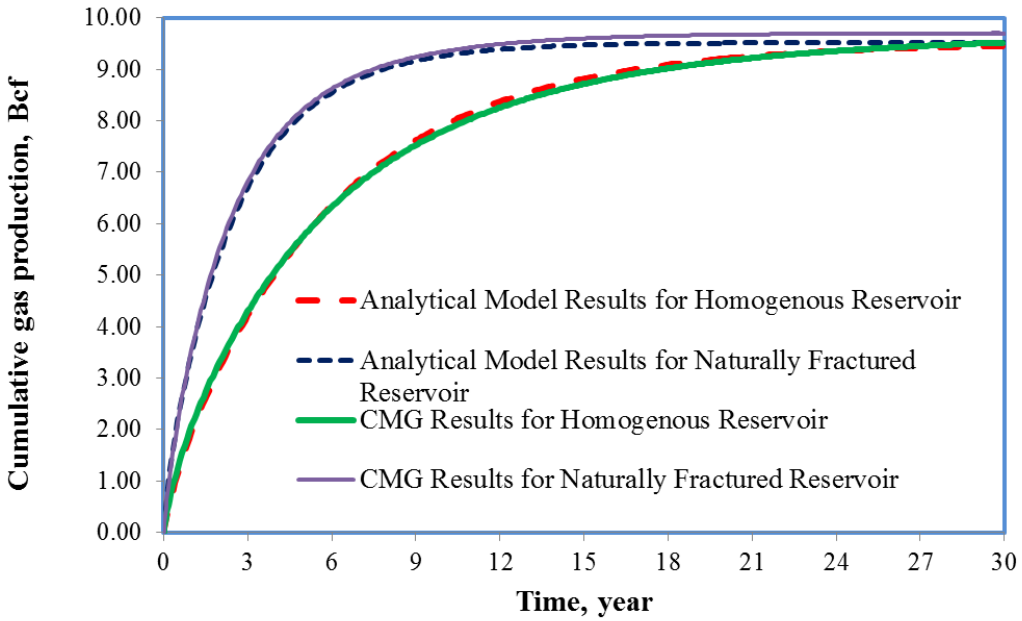

Figure 4.4 Comparison of cumulative gas production performances obtained from the Analytical Model and CMG by considering homogeneous and naturally fractured unconventional reservoir

As can be seen in Figures 4.3 and 4.4, production performances for homogeneous and naturally fractured reservoirs are remarkably different from each other. Initial gas flow rate is almost two times higher in the naturally fractured reservoir case. However, high gas flow rate is no longer exists in naturally fractured reservoir case after 3.5 years of production, because 75% of cumulative gas production in 30 years is produced within the first 3.5 years. As it is expected, homogeneous reservoir case produces with lower flow rates, but eventually reaches the same absolute cumulative gas production limits in 30 years. Resulting from the nature of the analytical model, natural fractures enhance the permeability of system. This effect clearly seen in the results that the production reaches the absolute production limits in 10 years. Pressure distributions of naturally fractured reservoir for one, five, ten, and thirty years of production are provided in Figures 4.5, 4.6,

4.7, and 4.8, respectively. It is shown that after 10 years of production, reservoir pressure is almost depleted in the naturally fractured reservoir.

The results obtained from the analytical model and the commercial reservoir simulator give identical responses both for naturally fractured and homogeneous reservoir cases. This fact verifies the accuracy of the analytical solution which is computationally faster and relatively simple to employ. Also, analytical dual porosity model implemented with the trilinear model can capture the fundamental physics of the problem and gives the results with minimum computational efforts. Commercial reservoir simulators model this problem (naturally fractured unconventional reservoir) using more computational expense and effort, since creating the input file for such a simulation study is quite time consuming.

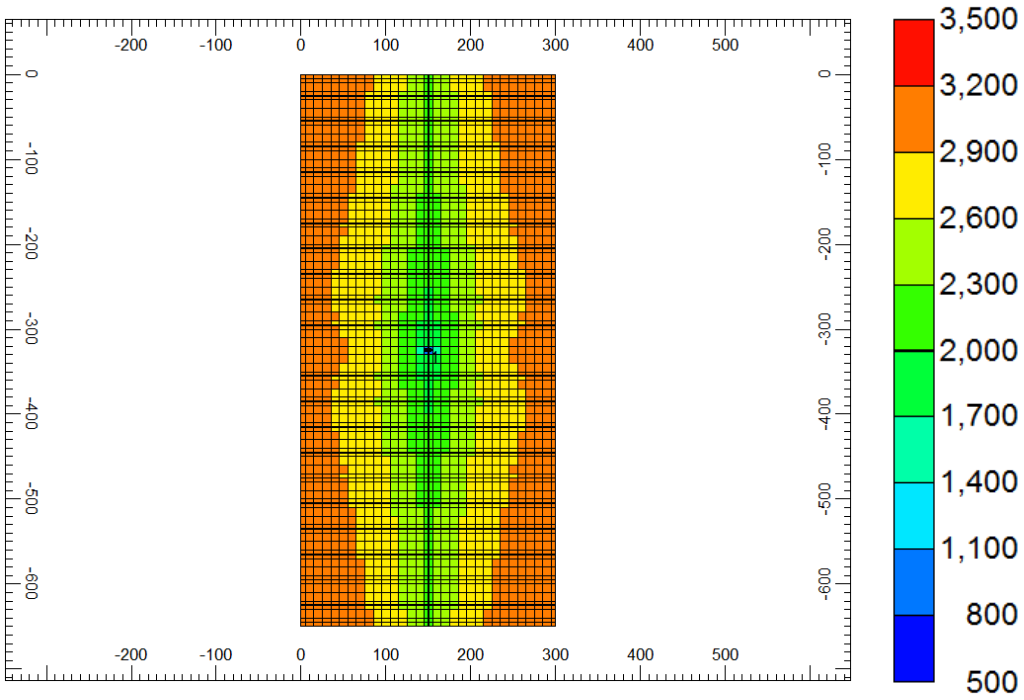

Figure 4.5: Naturally and hydraulically fractured reservoir pressure distribution after 1 year of production

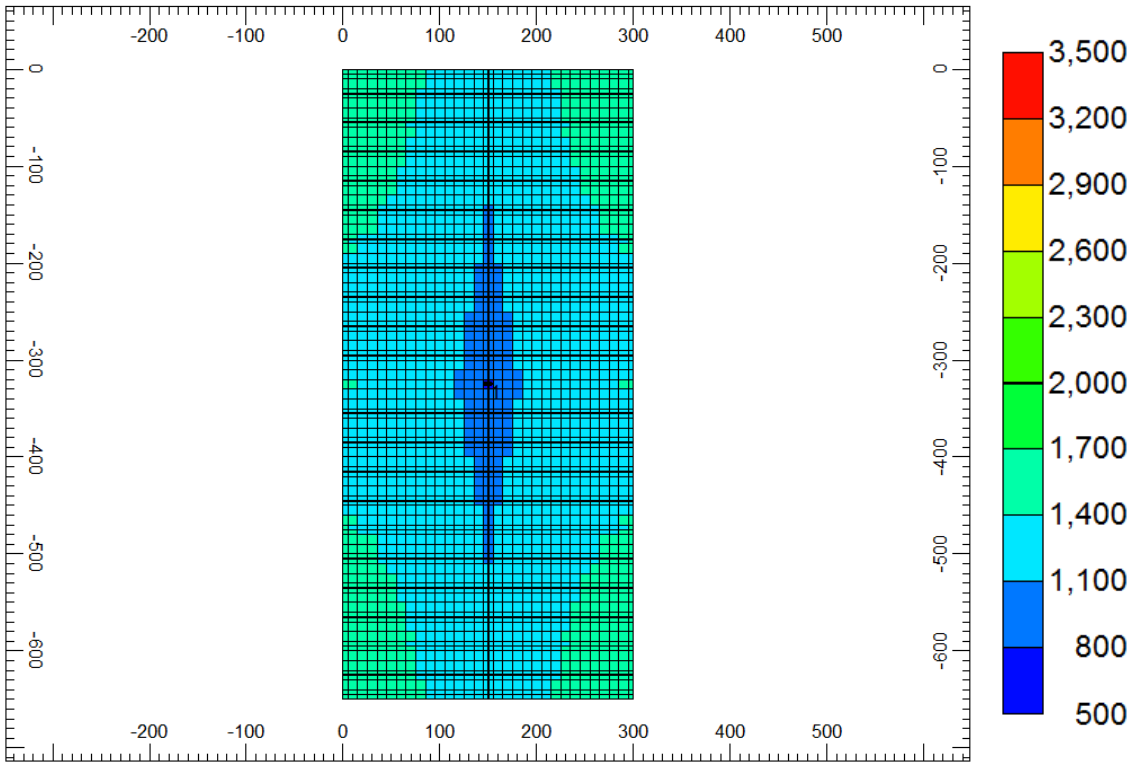

Figure 4.6: Naturally and hydraulically fractured reservoir pressure distribution after 5 years of production

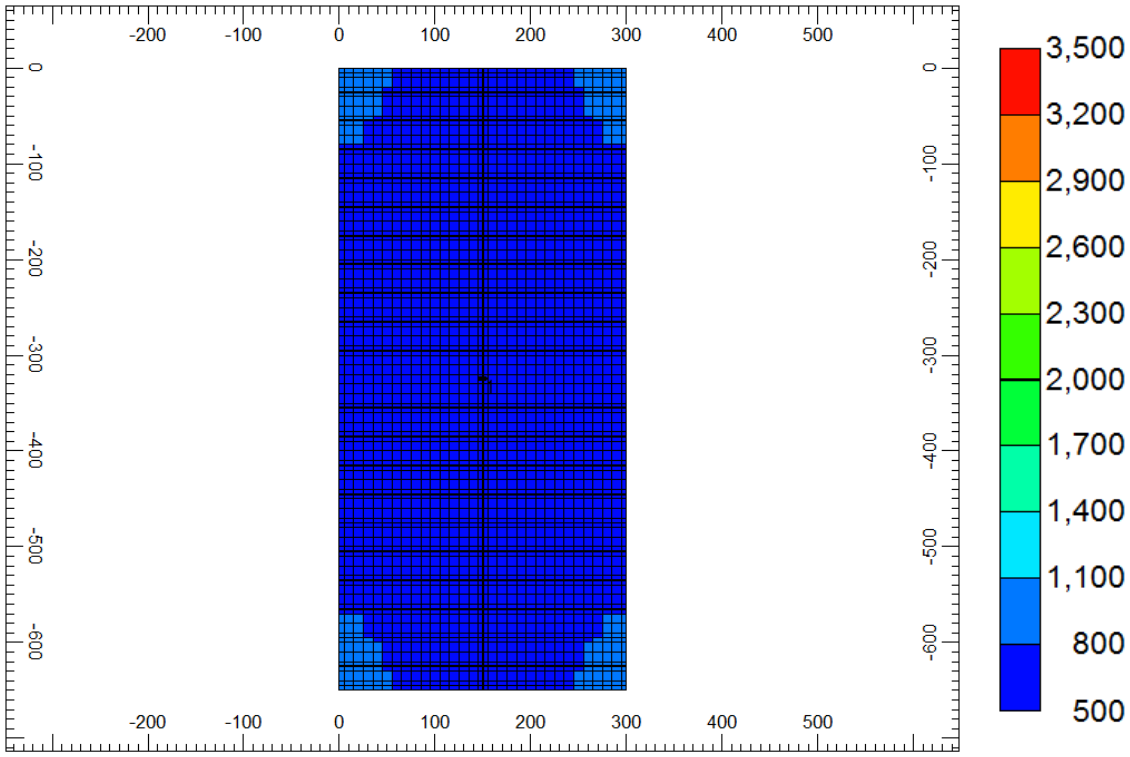

Figure 4.7: Naturally and hydraulically fractured reservoir pressure distribution after 10 years of production

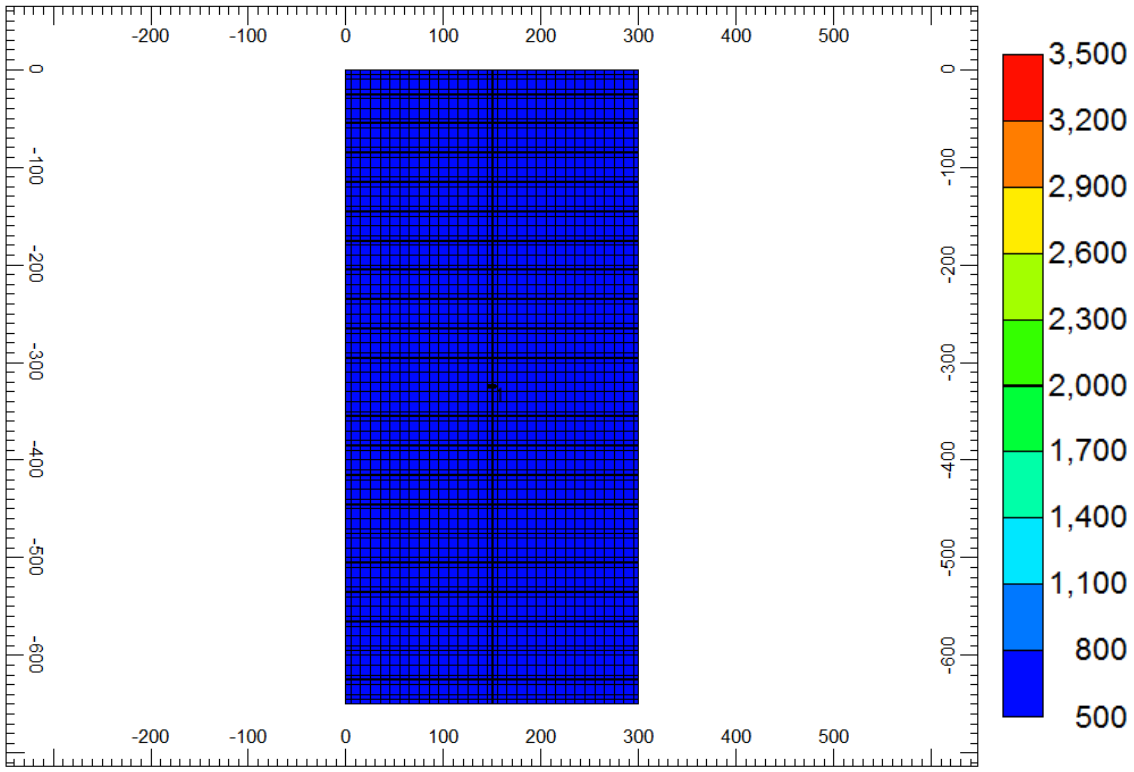

Figure 4.8: Naturally and hydraulically fractured reservoir pressure distribution after 30 years of production

4.2.2 Sensitivity Analysis for a Naturally Fractured Unconventional Reservoir

Sensitivity study for the homogeneous unconventional reservoir and completion parameters are performed and presented in Chapter 3. In this section, sensitivity analysis is performed only for the dual porosity parameters such as matrix and fracture permeability and natural fracture density in the reservoir pay zone using the analytical dual porosity model. Since naturally fractured unconventional reservoirs initially produce with higher flow rates, after 10 years daily production rates cannot reach the economical limits according to reservoir pressure distribution. The Base Case parameters and sensitivity parameters are given in Tables 4.1 and 4.2, respectively.

Table 4.2: Sensitivity parameters used in naturally fractured reservoir study

Parameter	Minimum	Mean	Maximum	Unit
Matrix permeability	0.0002	0.0006	0.0008	md
Fracture permeability	10	100	1000	md
Number of natural fractures	5	10	20	#

4.2.2.1 Matrix Permeability Sensitivity Analysis

Three different matrix permeabilities are examined and the sensitivity results are provided in Figures 4.10 and 4.11. It is observed that the matrix permeability is not the main controlling parameter for production performances of the naturally fractured unconventional reservoirs. The lowest matrix permeability, 0.0002 md, can still supply sufficient fluid flow to natural fractures. Gas production performances of three different matrix permeabilities give an identical response as can be seen in Figures 4.10 and 4.11.

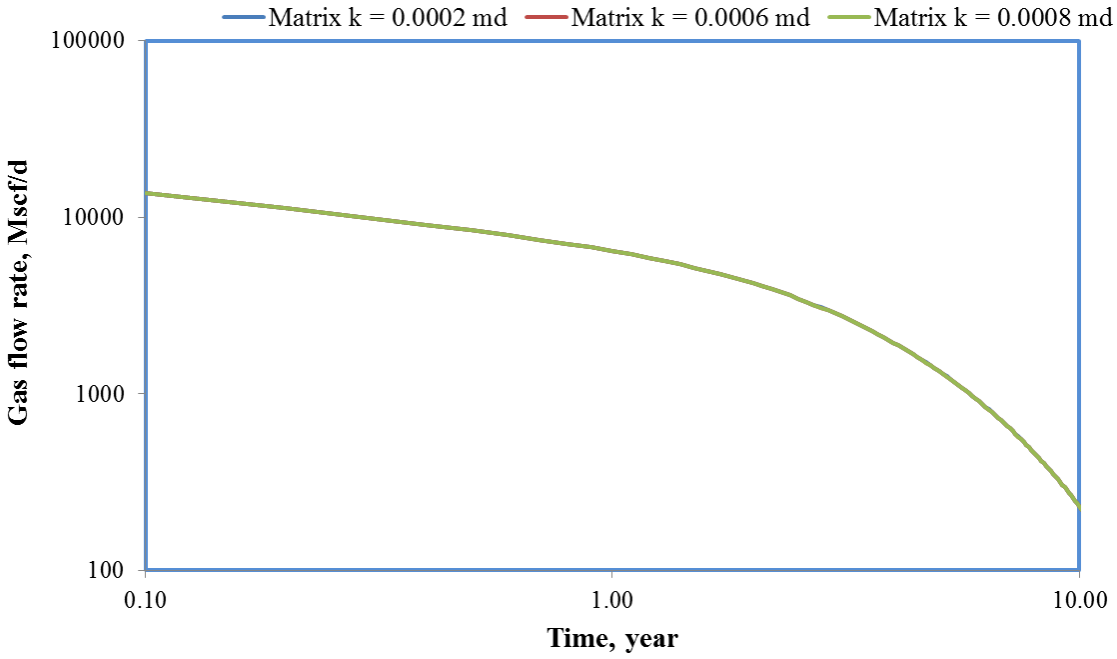

Figure 4.9 Gas flow rate performances for different matrix permeabilities

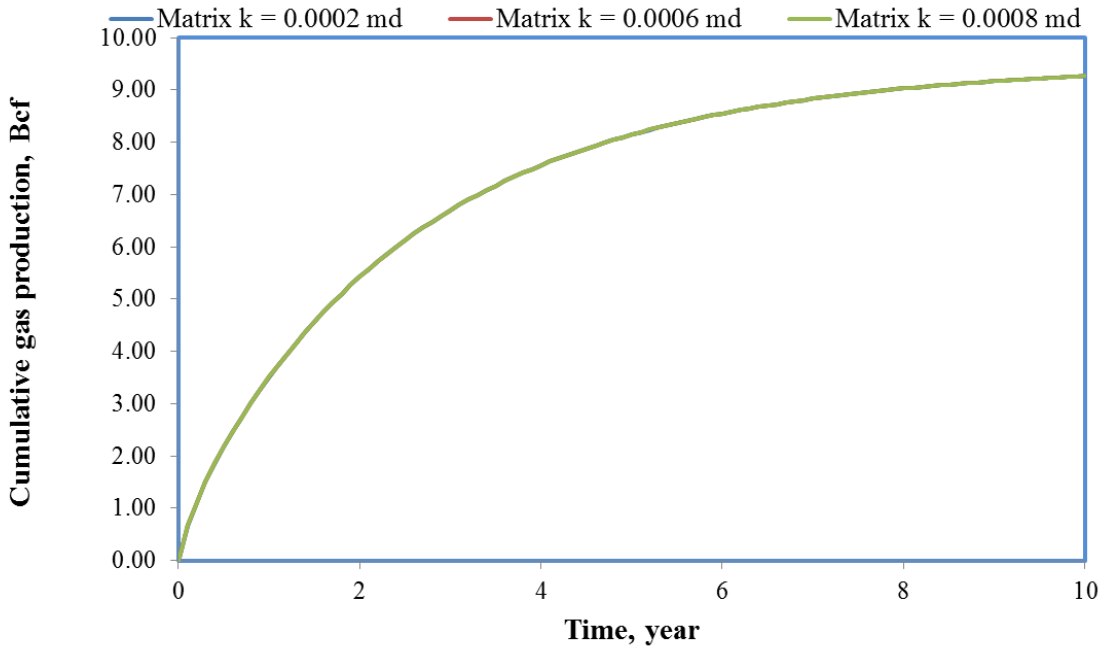

Figure 4.10 Cumulative gas production performances for different matrix permeabilities

4.2.2.2 Natural Fracture Permeability Sensitivity Analysis

Natural fractures are the main conduit for fluid flow from reservoir matrix to hydraulic fractures, so it is essential to perform a sensitivity analysis to identify the critical parameters influencing the production performance. Since the natural fractures are un-propped, their properties such as permeability are beyond an engineer's control. In this sensitivity analysis three different natural fracture permeabilities are examined. Analytical dual porosity model manifests that the natural fracture permeability ranks the most important parameter affecting the production from naturally fractured unconventional reservoir. It must be noted that the production profile with a natural fracture permeability of 10 md shows different behavior than the other two cases. This fact can be explained with the model's assumption; as Ozkan et al. (2011) stated that the

dual porosity model is accurate when the permeability difference between matrix and fractures is significant.

Daily production rates are remarkably differing from each other for the cases with 100 md and 1000 md natural fracture permeability. Natural fracture permeability of 100 md and 1000 md cases reach the same absolute production limits after 10 years, but initially the case with 1000 md natural fracture permeability produces higher flow rates than the case with 100 md natural fracture permeability. Daily and cumulative production performances are provided in Figures 4.11 and 4.12 for different natural fracture permeabilities.

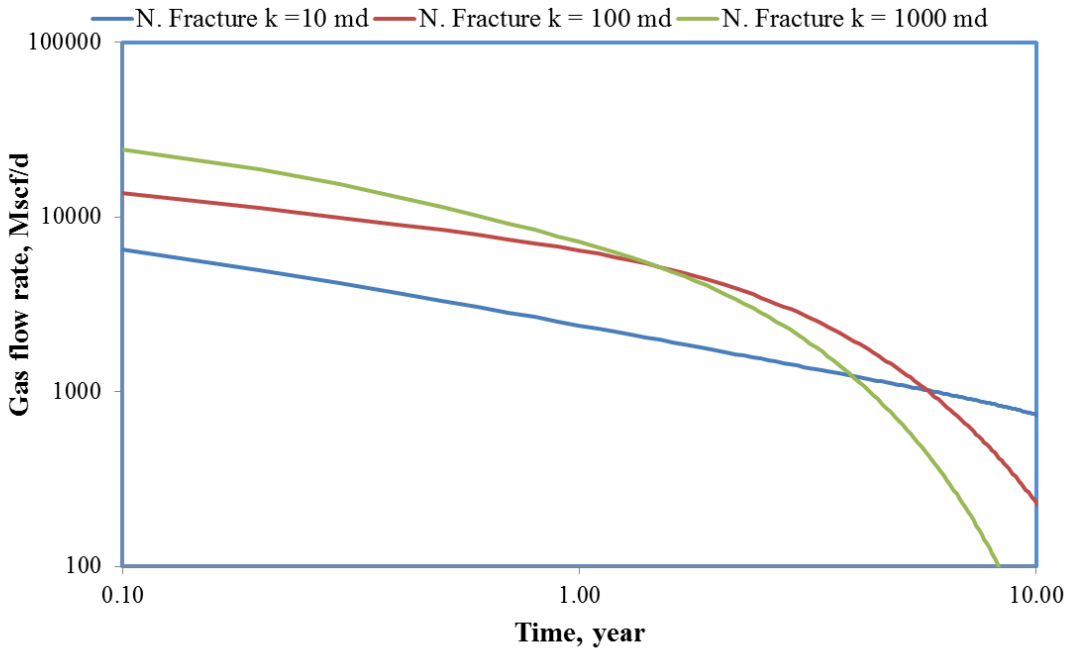

Figure 4.11 Gas flow rate performances for different natural fracture permeabilities

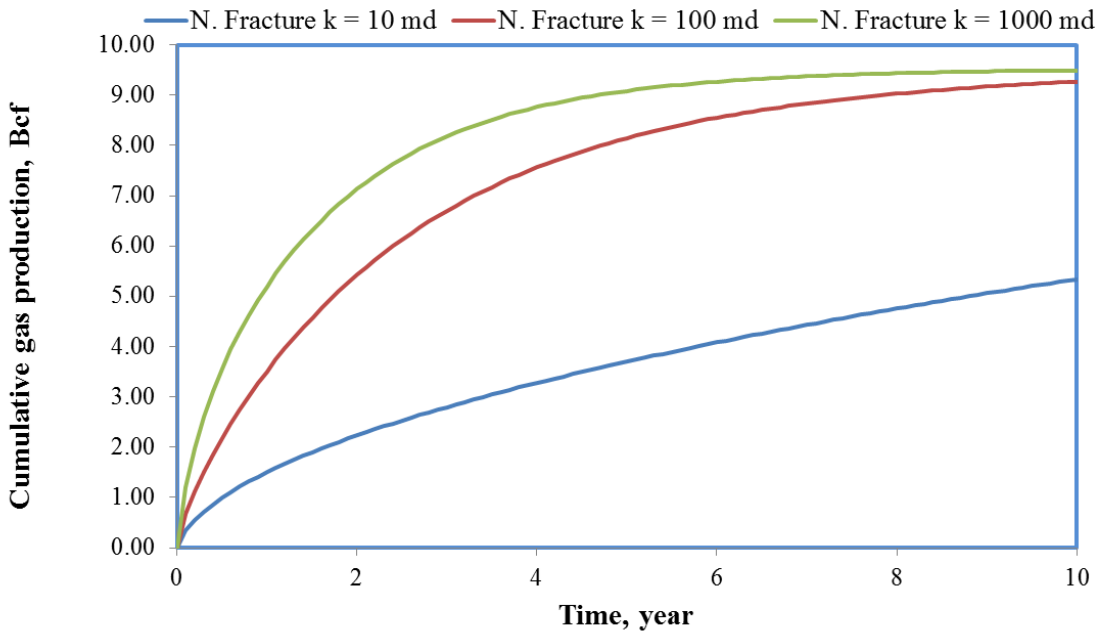

Figure 4.12 Cumulative gas production performances for different natural fracture permeabilities

4.2.2.3 Natural Fracture Density Sensitivity Analysis

Natural fracture density in the pay zone is also an important parameter enhancing the production performance of naturally fractured reservoirs. Natural fracture density refers to the number of existing natural fractures in a particular pay zone. Increasing density of the natural fractures results in more conduits for reservoir fluid flow. Natural fracture networks are very complex structures. Therefore, it is impossible to determine and model them exactly. In order to represent them in an analytical model, some idealization and assumptions must be made. For this purpose, an arbitrary number of natural fractures are determined, and various scenarios are evaluated. In this study, three different natural fracture densities is used, and the results show that natural fracture density is critical for production performance evaluation of unconventional reservoirs. Gas flow rate and cumulative production are given in Figures 4.13 and 4.14. It is

concluded that having a high number of natural fractures in the system, enhances the effective permeability of the system. Therefore, cases with relatively high natural fracture density reach the absolute maximum production limits sooner. This effect can be clearly seen in Figure 4.14, when the cases with 10 and 20 natural fractures deplete in 10 years, the case with 5 natural fractures could not reach the absolute maximum production limits for the same reservoir size,

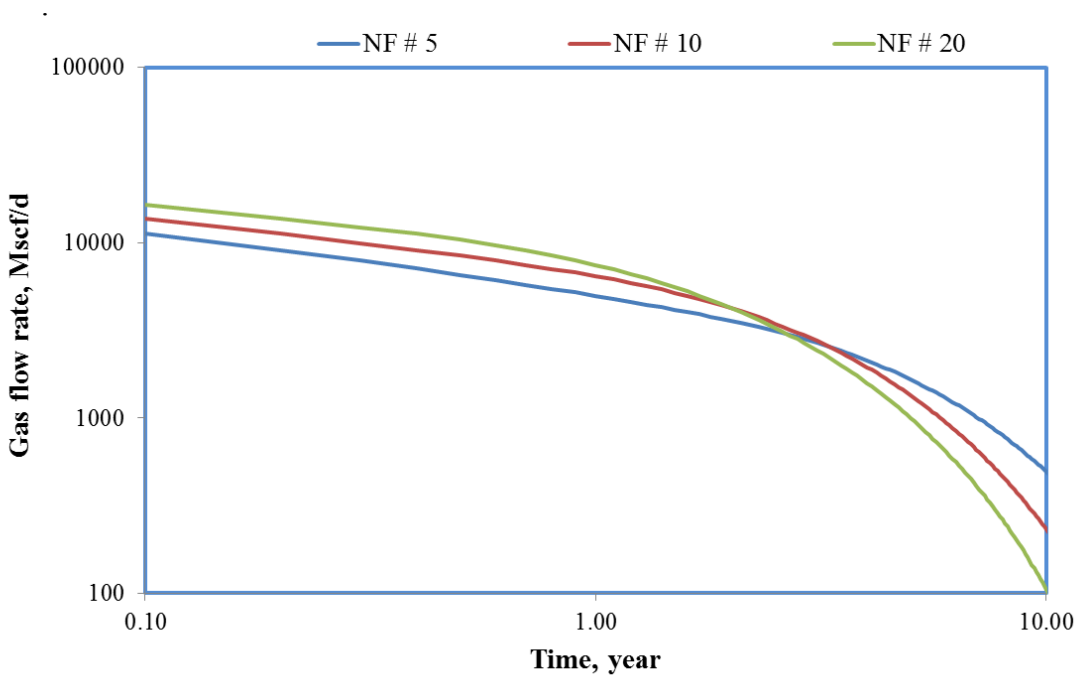

Figure 4.13 Gas flow rate performances for different natural fracture densities

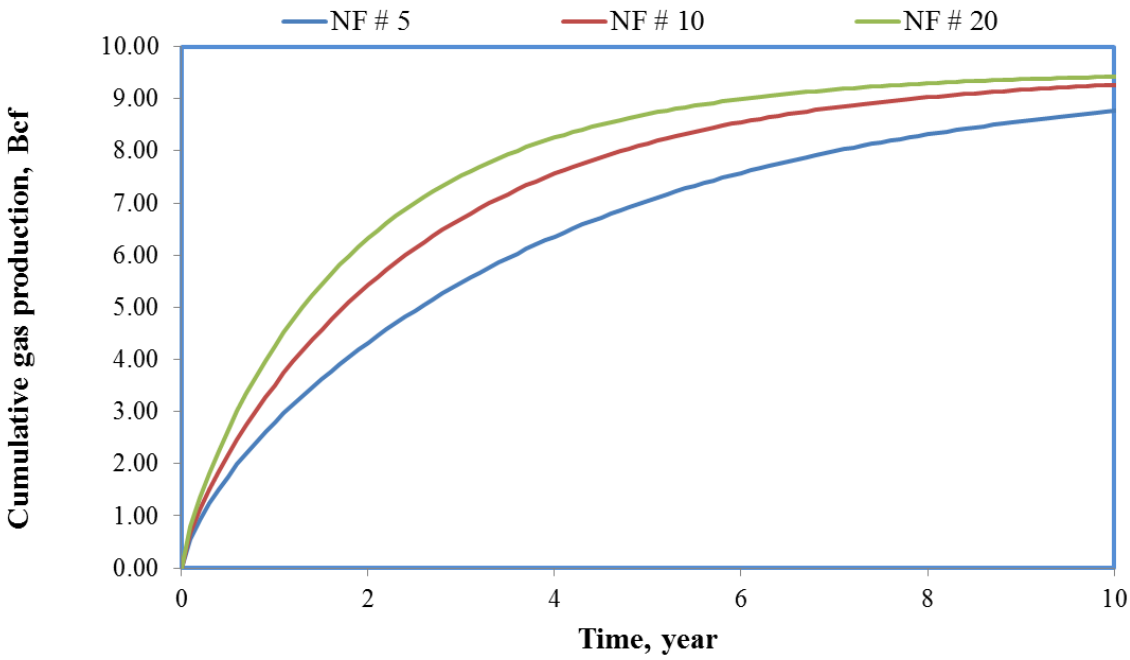

Figure 4.14 Cumulative gas production performances for different natural fracture densities

4.3 Comparison of the Analytical Model and the Commercial Reservoir Simulator Results for the Pressure Dependent Natural Fracture Permeability

Reservoir rock properties such as permeability, behave dynamic rather than static with continuing production and changing stress conditions in unconventional reservoirs. In order to take this fact into account, Apaydin (2012) considered pressure dependent natural fracture permeability concept in his dual porosity flow model. The importance of natural fractures on production performance is evaluated in the previous section, so it is necessary to study the dynamic behavior of natural fracture properties and also their impact on production performance. This section describes the pressure dependent permeability concept, and the pressure dependent natural fracture effects on production performance. For this purpose the analytical model (Apaydin, 2012) and the commercial

reservoir simulator (CMG, IMEX, 2012) are employed for a synthetic data set to observe pressure dependent natural fracture permeability impact on production performance.

4.3.1 Pressure Dependent Natural Fracture Permeability Concept

Natural fractures in unconventional reservoirs, unlike hydraulic fractures, do not have any propant to retain their permeability under the increasing stress conditions. By continuing production from the reservoir, pressure in the natural fractures will decrease. This fact increases the net effective stress applying on the natural fractures. Relationship between the pore pressure and net effective stress can be represented by Terzaghi's poro elastic equation:

$$\sigma = S - P_p \ , \qquad \text{(Eqn. 4.37)}$$

where,

σ – Net effective stress applying on medium, psi

S – Total stress applying on medium, psi

P_p – Pore pressure, psi.

As can be seen in Eqn. 4.37, decreasing pore pressure results in higher effective stress applied on the natural fractures. This phenomenon also causes changes in rock properties such as permeability. There are several correlations available in the literature to represent permeability changes with changing pore pressure. The correlation proposed by Raghavan and Chin (2004) is used in this thesis, and it is also compatible with modified pseudo-pressure equation given in Eqn. 4.1.

Raghavan and Chin (2004) proposed a correlation for permeability reduction with decreasing pore pressure. Although this correlation is recommended for the matrix permeability, it can be used for natural fractures if it is confirmed by experimental data. For this purpose Cho et al. (2013) conducted a permeability measurement experiments

with shale specimens under various stress conditions, and concluded that the Raghavan and Chin (2004) correlation, given in Eqn. 4.38, is valid for fracture permeability changes with changing pore pressure.

$$k_f = k_{fi} e^{-d_f \Delta p_f} , \qquad \text{(Eqn. 4.38)}$$

where,

k_f – Natural fracture permeability, md

k_{fi} – Initial natural fracture permeability, md

d_f – Characteristic parameter of rock, psi^{-1}

Δp_f – Pressure changes in the system, psi.

Cho et al. (2013) also provide the d_f coefficient for shale rock samples. We used their experimental results and coefficients in our pressure dependent natural fracture permeability calculations in this study. In order to represent changes in natural fracture permeability in the commercial reservoir simulator (CMG, IMEX, 2012) we implemented a natural fracture conductivity table. Their experimental results are considered as medium shale, but we also defined soft and hard shale conditions. Normalized conductivity table, which is given in Figure 4.2, used in the commercial reservoir simulator (CMG, IMEX, 2012).

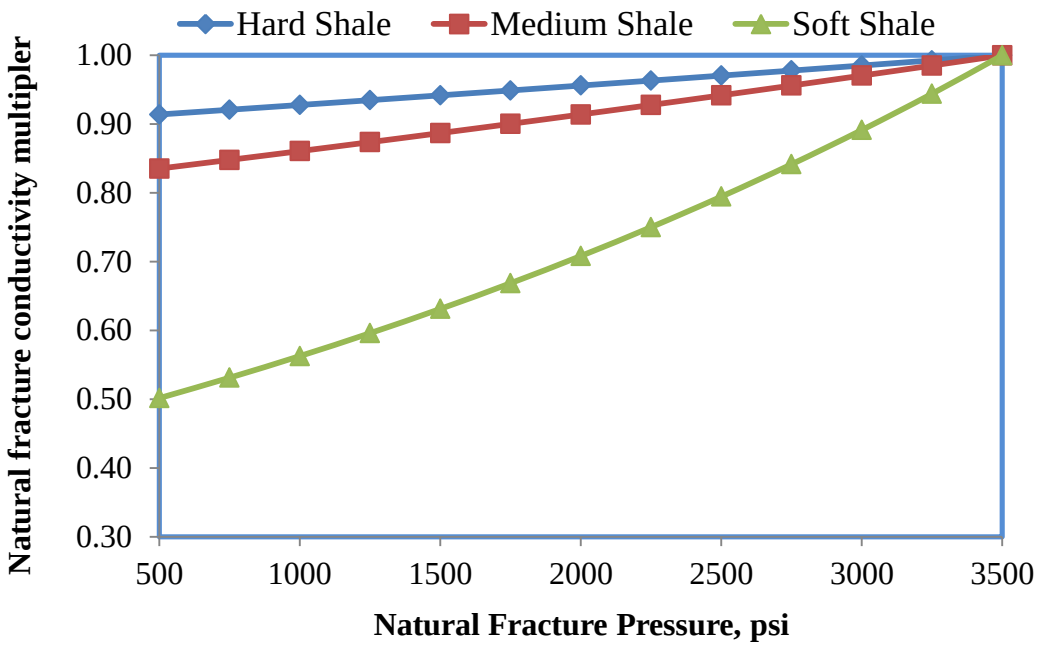

Figure 4.15 Normalized natural fracture conductivity multiplier for CMG (IMEX, 2012)

The effect of pressure dependent natural fracture conductivity on production is also examined with the modified analytical solution, and the results are given in the following section.

4.3.2 Verification of the Modified Analytical Model and the Commercial Reservoir Simulator for Pressure Dependent Natural Fracture Permeability

This section investigates the effect of pressure dependent natural fracture permeability on production performance of unconventional hydraulically fractured wells. Details of the analytical model and pressure dependent permeability concept were provided in the previous sections of this chapter. In order to perform simulations for this section, the modified analytical dual porosity model and the commercial reservoir simulator (CMG, IMEX, 2012) is used with the synthetic data provided in Table 4.1. Raghavan and Chin (2004) correlation is employed for the pressure dependent natural fracture permeability. Permeability changes with decreasing pore pressures are provided in Figure 4.16. Medium shale is considered for the Base Case.

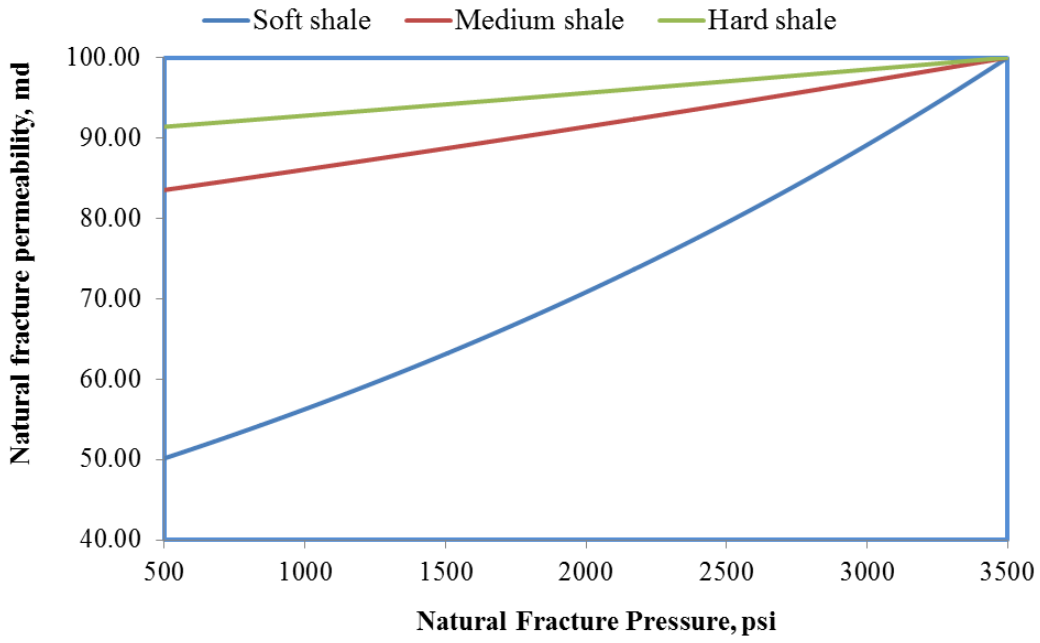

Figure 4.16 Natural fracture permeability changes with depleting reservoir pressure for different shale types

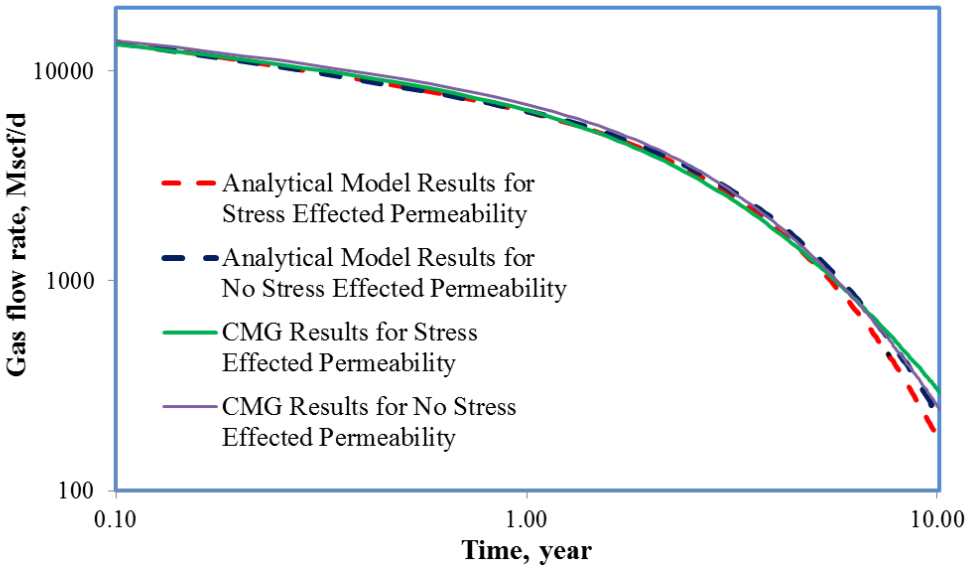

Figure 4.17 Comparison of the gas flow rate performances of the Modified Analytical Model and CMG for pressure dependent natural fracture permeability and constant natural fracture permeability

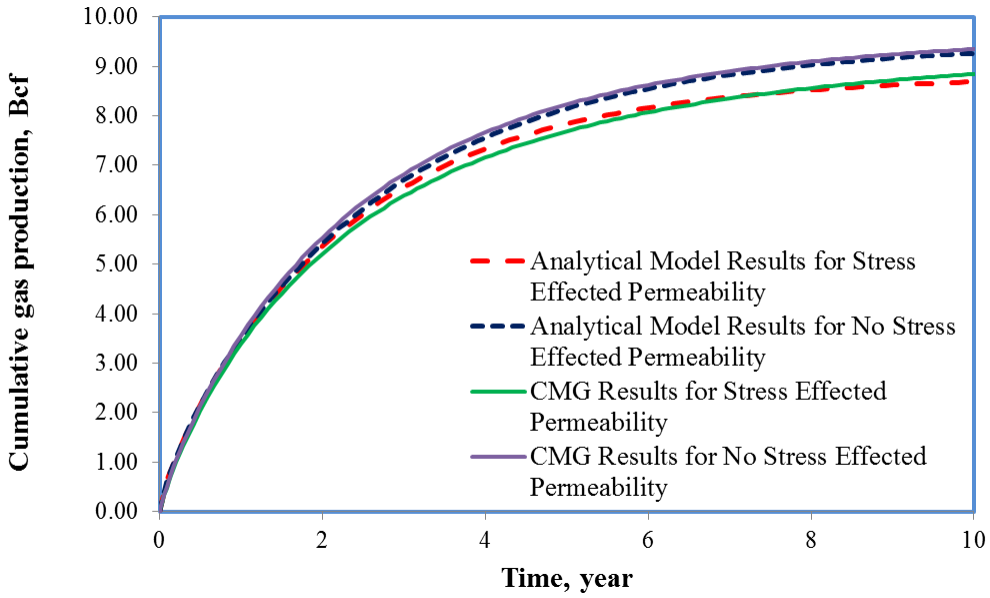

Figure 4.18 Comparison of the cumulative gas production performances of the Modified Analytical Model and CMG for pressure dependent natural fracture permeability and constant natural fracture permeability

A good match between the modified analytical model and the commercial simulator is obtained for both daily and cumulative production performances. Figures 4.17 and 4.18 show this agreement for the constant natural fracture permeability and pressure dependent natural fracture permeability cases. Cumulative production difference between the constant and the pressure dependent natural fracture permeability is around 6% after 10 years of production. The effect of pressure dependent natural fracture permeability becomes apparent after 2.5 years of production. In order to identify that in which conditions the pressure dependent natural fracture permeability becomes critical, different scenarios are defined and evaluated using the modified analytical model in the next section.

4.3.3 Identifying the Importance of Pressure Dependent Natural Fracture Permeability

Sensitivity analysis for design parameters and reservoir properties are already studied in this thesis. This section attempts to shed light on the reservoir conditions in which pressure dependent natural fracture permeability causes significant production loss. For this purpose, various matrix and fracture permeabilities, different shale plays, as well as a range of bottom-hole pressures are investigated using the naturally fractured analytical trilinear reservoir model. The Base Case inputs are given in Table 4.1, and also Table 4.3 presents the range of variables considered for the sensitivity study. The effect of pressure dependent permeability on production is evaluated individually for each specific parameter. In order to identify the effect of pressure dependent permeability, production performances are examined with the constant and the pressure dependent natural fracture conditions. It must be noted that the mean values given in Table 4.3 are already assessed and the results are provided in Figures 4.17 and 4.18.

Table 4.3: Sensitivity parameters used in pressure dependent natural fracture permeability study

Parameter	Minimum	Mean	Maximum	Unit
N. Fracture permeability	10	100	1000	md
Matrix permeability	0.00006	0.0006	0.006	md
Shale type	Soft	Medium	Hard	---
Bottom hole pressure	200	400	600	psi

4.3.3.1 Initial Natural Fracture Permeability - 10 md

Importance of natural fracture permeability was discussed in the previous section. This time the effect of pressure dependent natural fracture permeability on production is investigated for different initial fracture permeabilities. First, initial natural fracture permeability is considered as 10 md. It must be noted that the production forecast is considered for 30 years, since the 10 years of production is not a sufficient production period for such a low permeability reservoir. However, 30 years of production forecast, as can be seen in Figures 4.19 and 4.20, manifest that there is an insignificant difference between the pressure dependent natural fracture and the constant natural fracture permeability cases. This fact can be explained by the extremely low permeability, because reservoir pressure does not deplete too fast to close the natural fractures and reduce production performance.

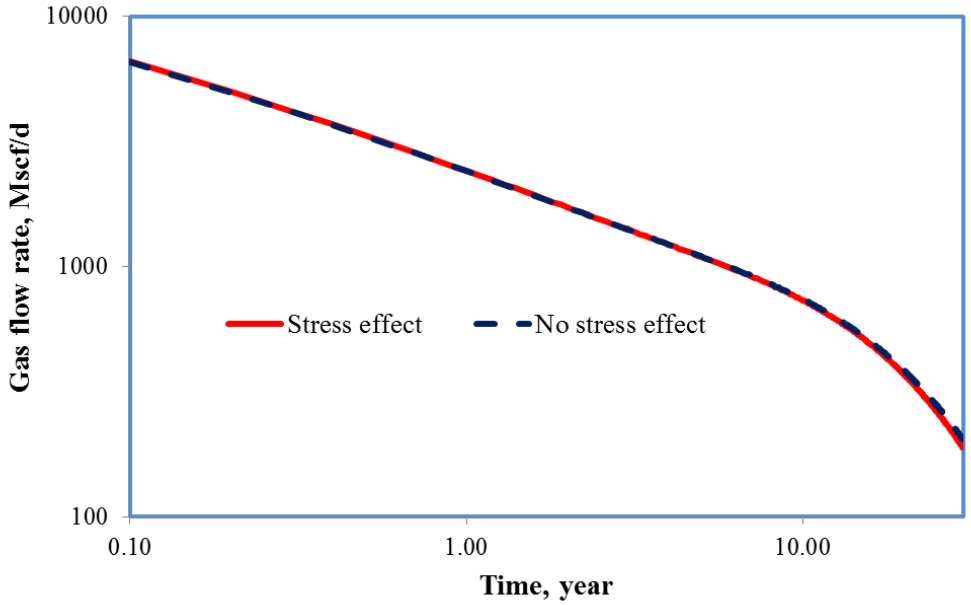

Figure 4.19 Gas flow rate using natural fracture permeability of 10 md by considering with and without stress effect

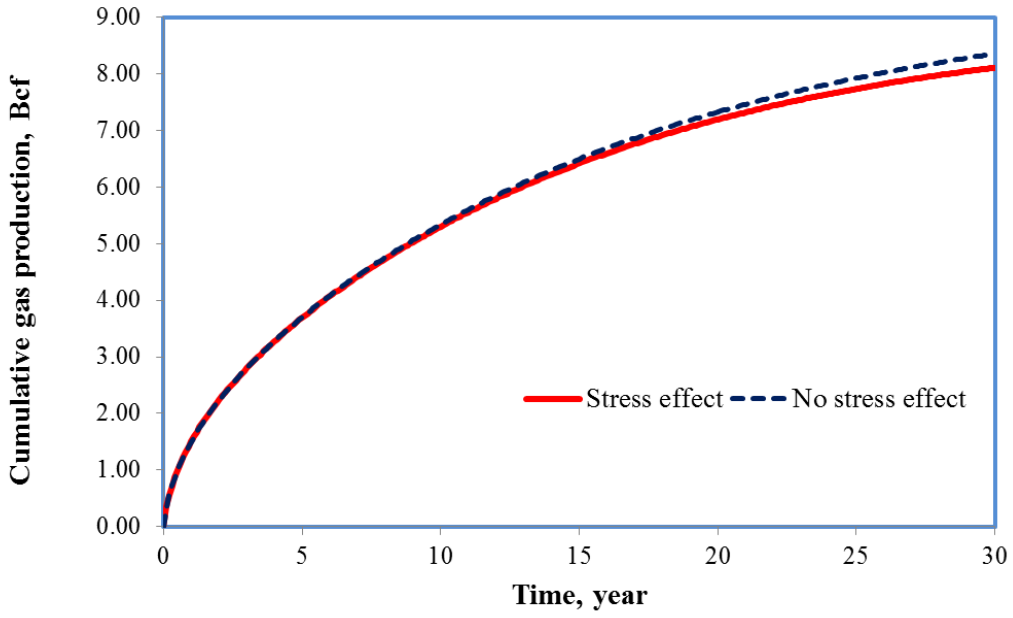

Figure 4.20 Cumulative gas production using natural fracture permeability of 10 md by considering with and without stress effect

4.3.3.2 Initial Natural Fracture Permeability - 1000 md

Increasing natural fracture permeability to 1000 md significantly increases the gas production rate performance, and also the absolute maximum production limit is reached in 10 years. As can be seen in Figures 4.21 and 4.22, the effect of pressure dependent natural fracture permeability becomes apparent after 1 year of production compared with the Base Case in which it takes 3 years. The cumulative production differences between constant natural fracture permeability and pressure dependent natural fracture permeability cases is around 6% at the end of 10 years of production. This result shows that initial fracture permeability is the key parameter that controls the impact of pressure dependent natural fracture permeability on production performance of unconventional reservoirs.

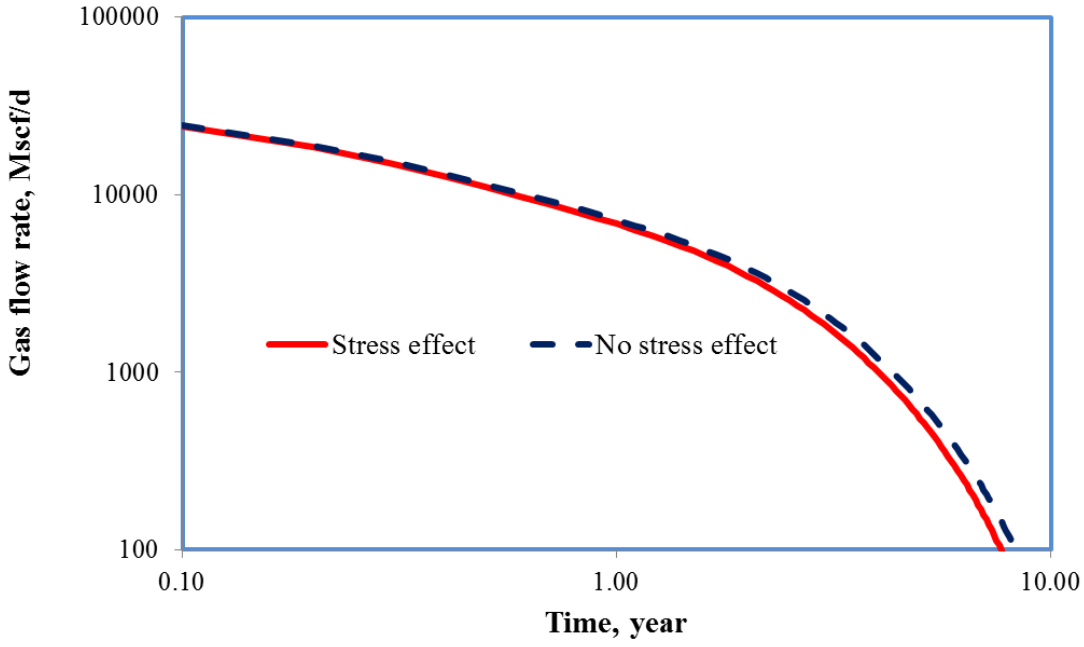

Figure 4.21 Gas flow rate using natural fracture permeability of 1000 md by considering with and without stress effect

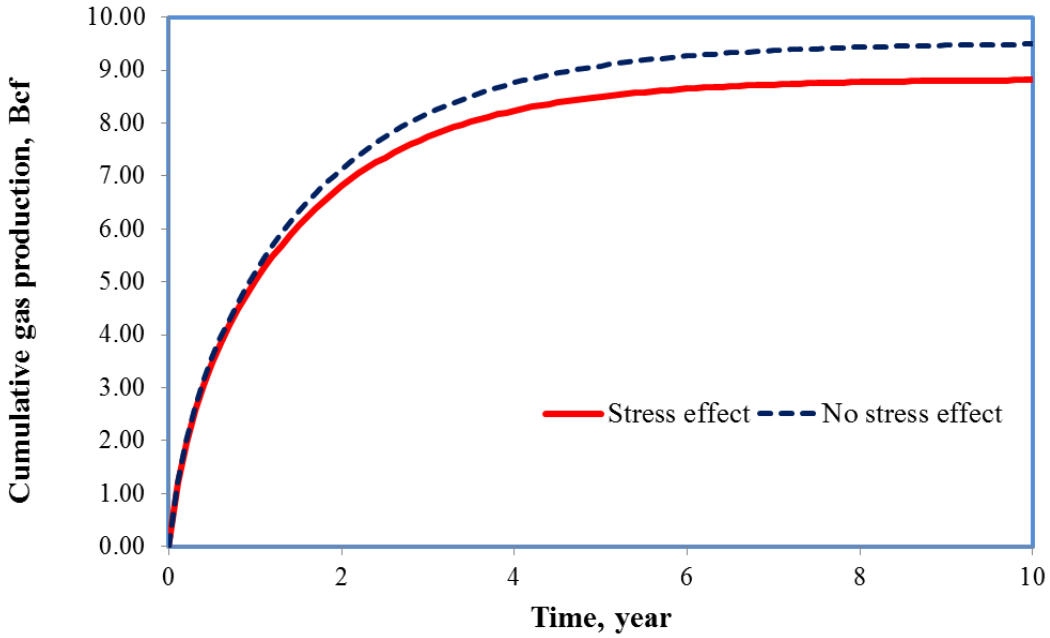

Figure 4.22 Cumulative gas production using natural fracture permeability of 1000 md by considering with and without stress effect

4.3.3.3 Matrix Permeability - 0.00006 md

Matrix permeability is an important property of the naturally fractured unconventional reservoirs. In this section the matrix permeability is considered to be 0.00006 md, while the fracture permeability is 100 md. It is observed that the effect of pressure dependent natural fracture permeability becomes apparent after 3 years of production (Figures 4.23 and 4.24). The cumulative production differences between the constant natural fracture permeability and pressure dependent natural fracture permeability cases is 6% in 10 years of production. Results of the Base Case (Figures 4.17 and 4.18), which has 10 times higher matrix permeability, manifests the same behavior with matrix permeability of 0.00006 md. This fact shows that the matrix

permeability does not significantly affect the importance of pressure dependent natural fracture permeability on production.

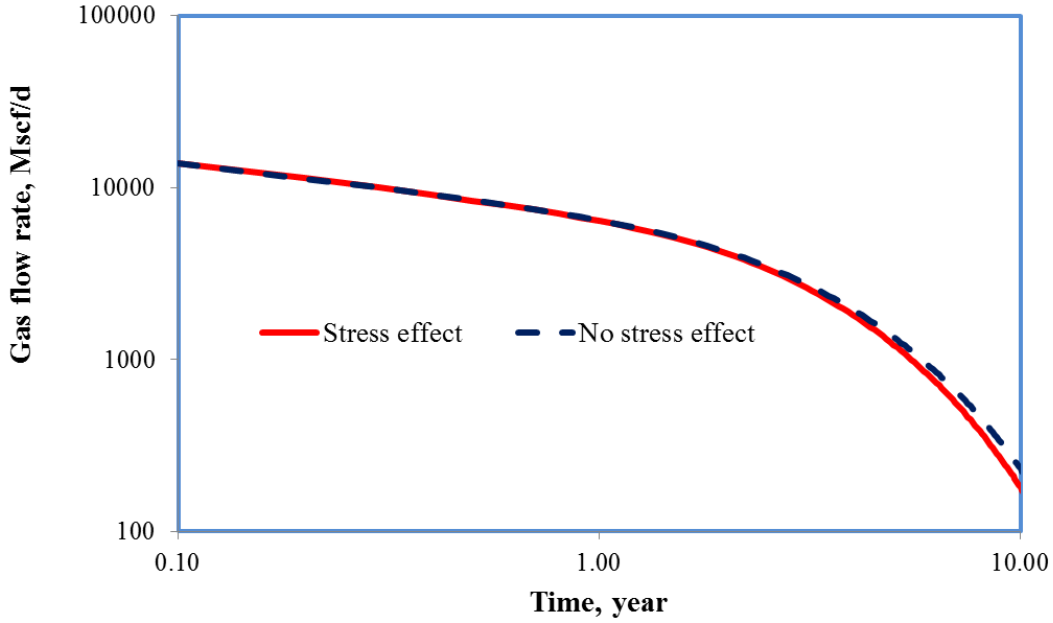

Figure 4.23 Gas flow rate using matrix permeability of 0.00006 md by considering with and without stress effect

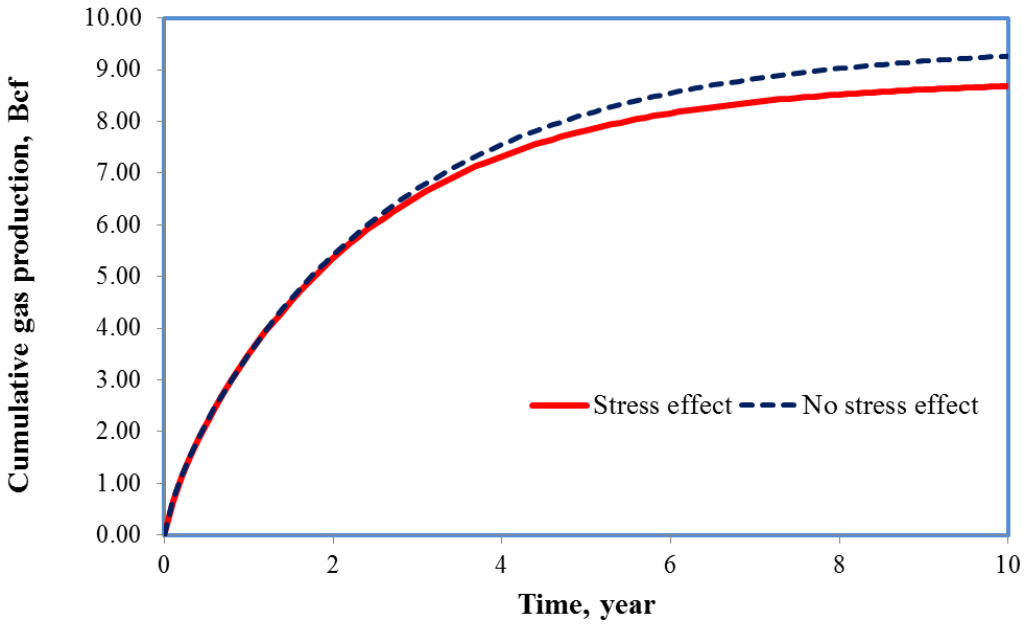

Figure 4.24 Cumulative gas production using natural fracture permeability of 0.00006 md by considering with and without stress effect

4.3.3.4 Matrix Permeability - 0.006 md

It is observed that increasing the matrix permeability to 0.006 md slightly affects the production performance behavior of the pressure dependent natural fracture permeability case. Results for the matrix permeability of 0.006 md are provided in Figures 4.25 and 4.26. Similarly, the effects of pressure dependent natural fracture effects becomes apparent after 3 years, and difference in cumulative production the cumulative production between the constant natural fracture permeability and the pressure dependent natural fracture permeability scenario is around 6%. This result proves our earlier statement in the 0.00006 md matrix permeability case discussion section, and once again it is concluded that the matrix permeability is not the key element that controls the effect of pressure dependent natural fracture permeability on production performance. This conclusion is also in agreement with the model nature which indicates

that natural fractures are the main conduits for flow in the reservoir. Obviously, their parameters are more critical to be investigated than the matrix permeability.

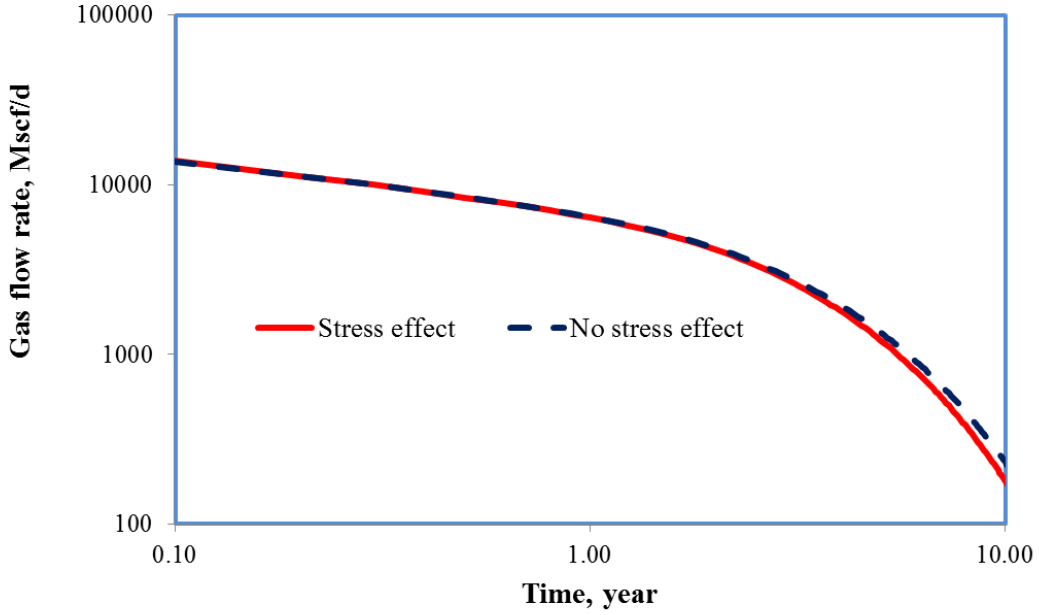

Figure 4.25 Gas flow rate using matrix permeability of 0.006 md by considering with and without stress effect

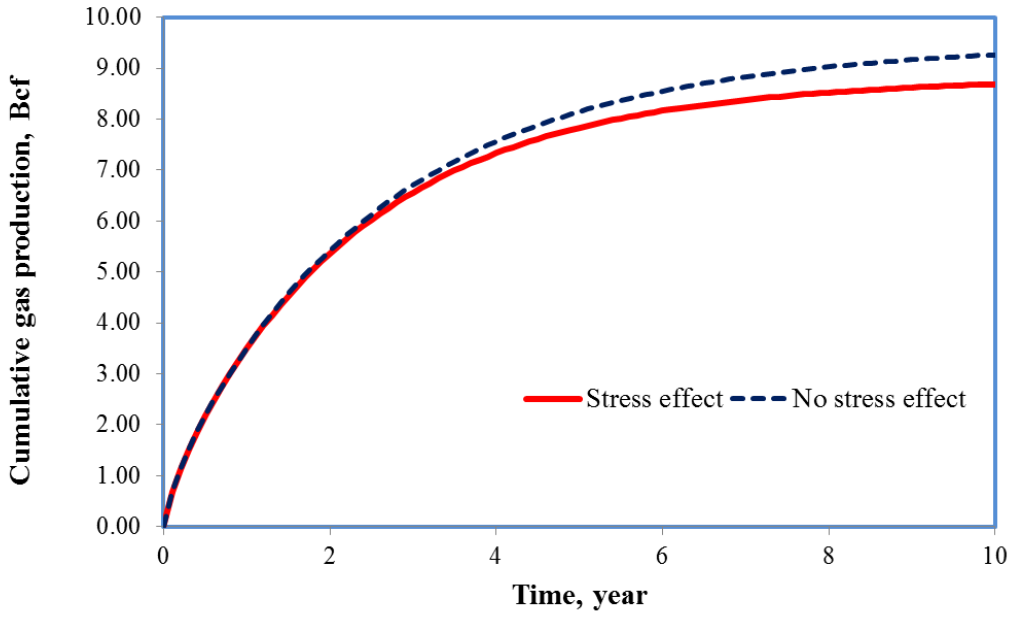

Figure 4.26 Cumulative gas production using natural fracture permeability of 0.006 md by considering with and without stress effect

4.3.3.5 Bottom Hole Pressure 200 psi & 800 psi

Bottom-hole pressure (BHP) of a horizontal well is an important engineering parameter since it affects all other pressure dependent parameters. Bottom-hole pressure conditions of 200 psi and 800 psi are investigated in this section to analyze the effects of pressure dependent natural fracture permeability on production. As can be seen in Figures 4.27 and 4.28, the effect of pressure dependent natural fracture becomes apparent after 3 years of production for 200 psi BHP, and the cumulative production differences between the constant and dynamic natural fracture permeability cases is 6% which is similar to 600 psi BHP case. BHP condition of 800 psi is also considered and the results, which are given in Figures 4.29 and 4.30, keep the same trend with the other two BHP conditions (200 psi and 600 psi). The cumulative production varies around 5% from the constant to pressure dependent natural fracture permeability in 10 years with 800 psi BHP. It can be

concluded that the bottom hole pressure has a minor effect on pressure dependent natural fracture permeability, thus on production performance.

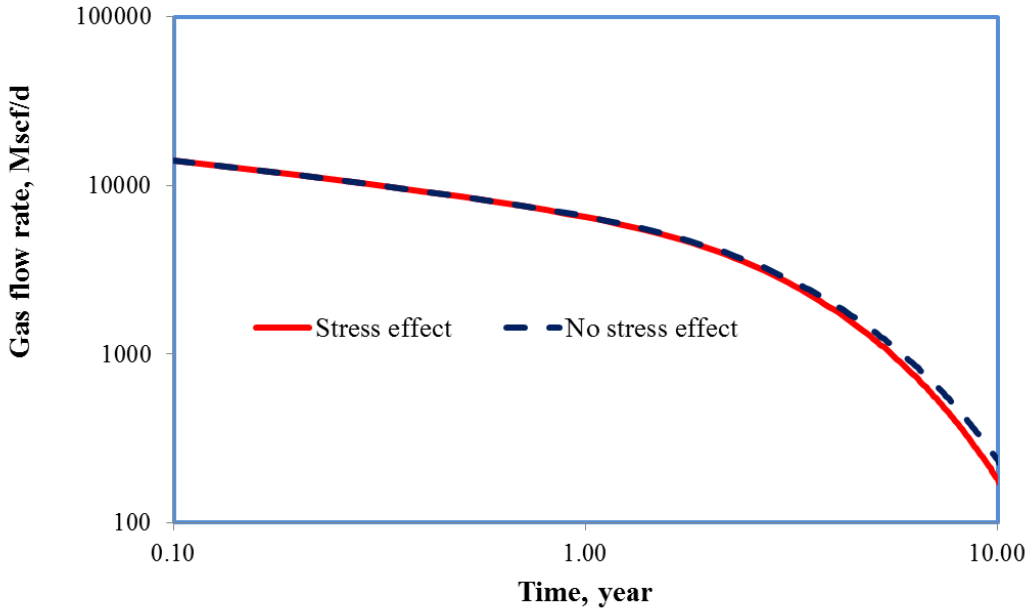

Figure 4.27 Gas flow rate using BHP of 200 psi by considering with and without stress effect

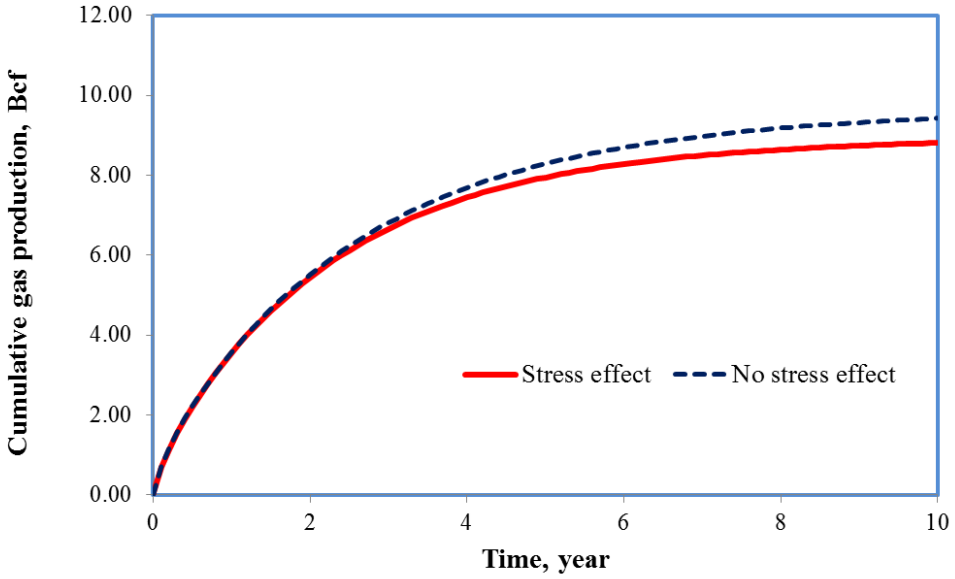

Figure 4.28 Cumulative gas production using BHP of 200 psi by considering with and without stress effect

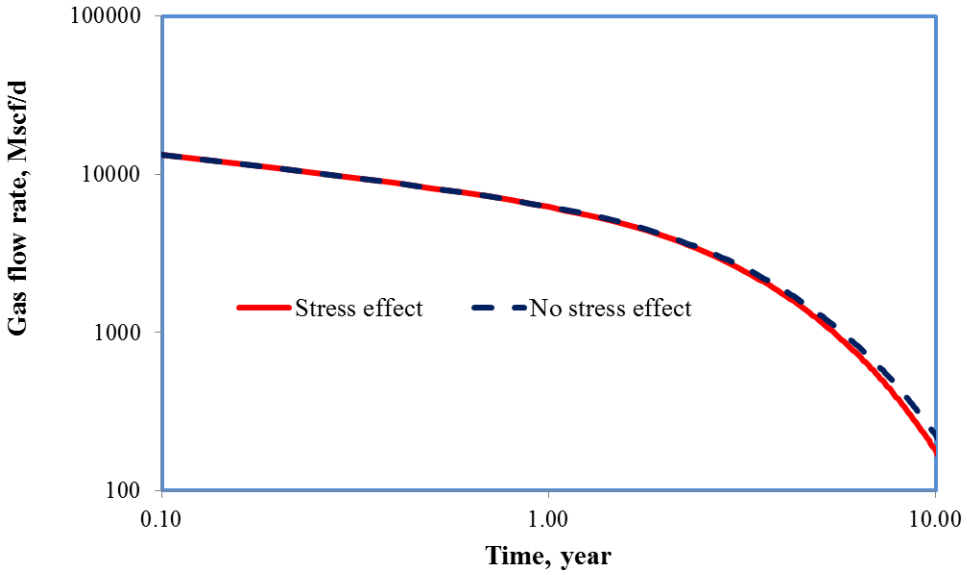

Figure 4.29 Gas flow rate using BHP of 800 psi by considering with and without stress effect

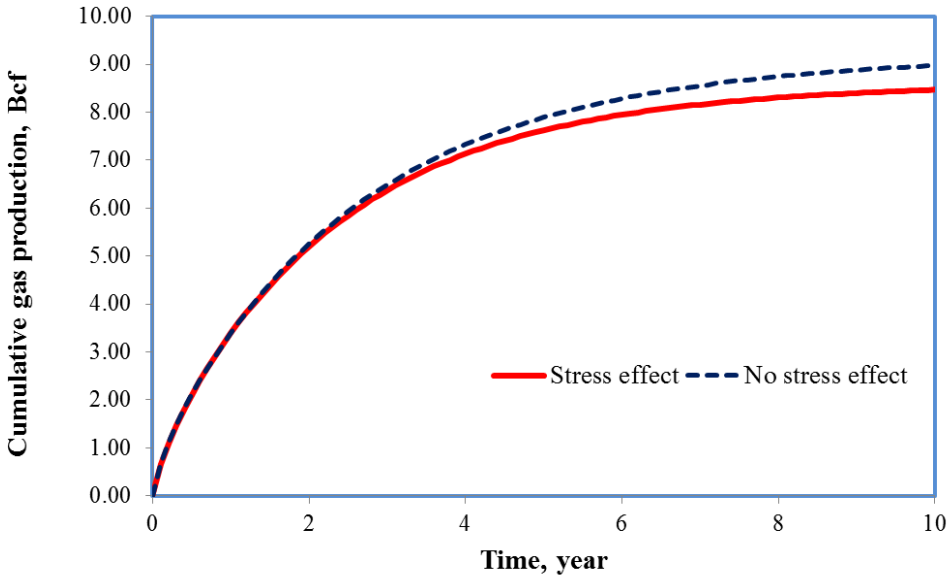

Figure 4.30 Cumulative gas production using BHP of 800 psi by considering with and without stress effect

4.3.3.6 Different Shale Plays

Changes of natural fracture permeability with increasing stress vary for different shale types. As stated previously in the pressure dependent permeability section of this chapter, laboratory experiments are necessary for pressure dependent permeability calculation. In this section, experimental data documented by Cho et al. (2013) is used to define the rock mechanical properties in the Raghavan and Chin (2004) correlation. Cho et al. (2013) provided characteristics of the shale core they conducted experiments on. In this study we considered their experimental data as medium shale. Beside this, two other rock characteristics are chosen to represent medium and hard shale conditions. Natural fracture permeability versus pore pressure for different shale plays are provided in the Figure 4.16. It is observed that the hard shale's natural fracture permeability reduced by 10% when the bottom hole pressure (500 psi) is reached, and the soft shale case it is around 50%. It is also critical to couple this effect with reservoir fluid flow. The modified

analytical flow model is employed and the cumulative production differences for different shale types are provided in Figure 4.31. As can be seen in Figure 4.31, the soft shale case produces slightly less than the hard shale and medium shale cases. It is concluded that in order to have a reliable result, experimental data are necessary for different shale plays.

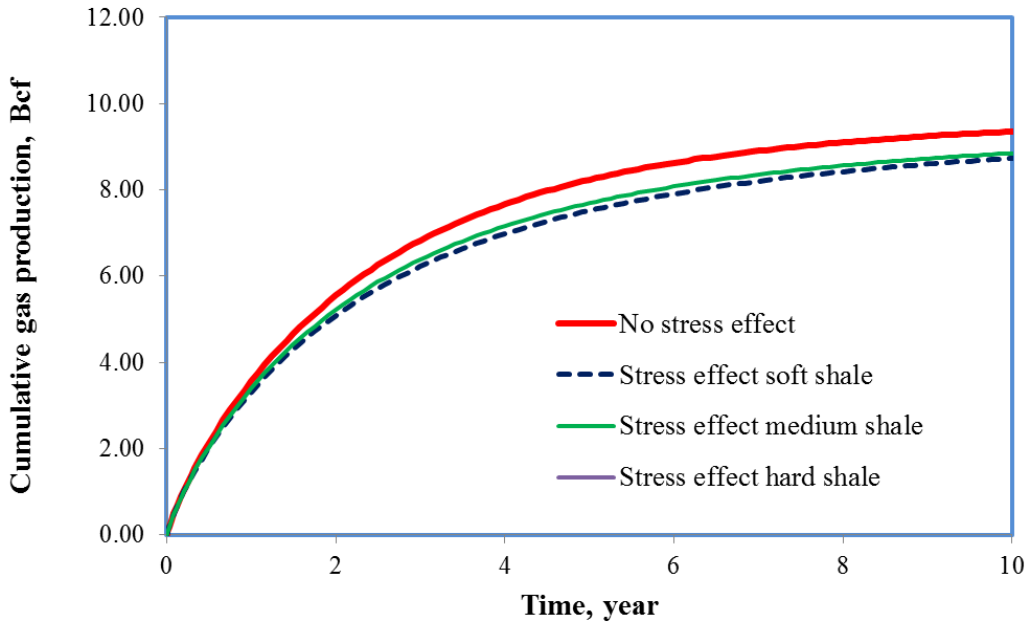

Figure 4.31 Cumulative gas production using different shale types by considering with and without stress effect

4.4 Natural & Hydraulic Fracture Conductivity Loss Effects on Production Performance of Unconventional Reservoirs

This section investigates the effect of geomechanics on combined hydraulic and natural fractures conductivities, and ultimate production performance of unconventional reservoirs. Previous section studied the pressure dependent natural fracture permeability effects on production. Since the analytical model is unable to capture hydraulic fracture conductivity changes, results are obtained using the commercial reservoir simulator

(CMG, IMEX, 2012). Although hydraulic fractures, unlike natural fractures, are propped prior to production, their conductivities may decrease with increasing applied net stress. This conductivity lost may reduce the production performances in long term, so this fact also needs to be coupled with the reservoir flow. As stated in the literature review, experiments are conducted for both propped and un-propped fracture conditions, and their conductivities are measured under various stress conditions. However, many of these experimental researches consider either propped or un-propped fracture conditions. Since the aim is to analyze both individual and combined effect on production performance, it is necessary to have a data set from the same experimental study for propped and un-propped fractures. For this purpose, experimental results reported by Suarez-Rivera et al. 2013 are employed in our reservoir model. Geomechanics effects on production performances are evaluated for various cases using the commercial reservoir simulator (CMG, IMEX, 2012).

4.4.1 Experimental Data for Propped and Un-propped Fracture Conductivity under Increasing Closure Stress Conditions

In order to accomplish this section, experimental study conducted by Suarez-Rivera et al. (2013) is used. Propped fracture conductivities represent the hydraulic fractures, while the un-propped fracture conductivities are representing the natural fractures. Conductivity losses of natural fractures under increasing closure stress are to the order of magnitude higher than conductivity losses of propped fractures, since propants prevents closure of hydraulic fracture to some degree. The raw data given by Suarez-Rivera et al. (2013) is normalized for hydraulic and natural fracture conductivities that measured at 500 psi closure stress, given in Figure 4.32, and used to examine the pressure dependent natural and hydraulic fracture conductivity effects on production performance. Once the conductivity data is normalized for a reference pressure, which is

500 psi here, it needs to be converted to conductivity multiplier to be used in the reservoir simulator. Pressure dependent conductivity multiplier used in the commercial reservoir simulator is given in Figure 4.33. Comparison between hydraulic and natural fracture conductivity loss effects on production is accomplished using these experimental data. The conductivity multiplier data provided in Figure 4.33 is used in CMG (IMEX, 2012) commercial reservoir simulator in order to couple reservoir fluid flow with geomechanical considerations.

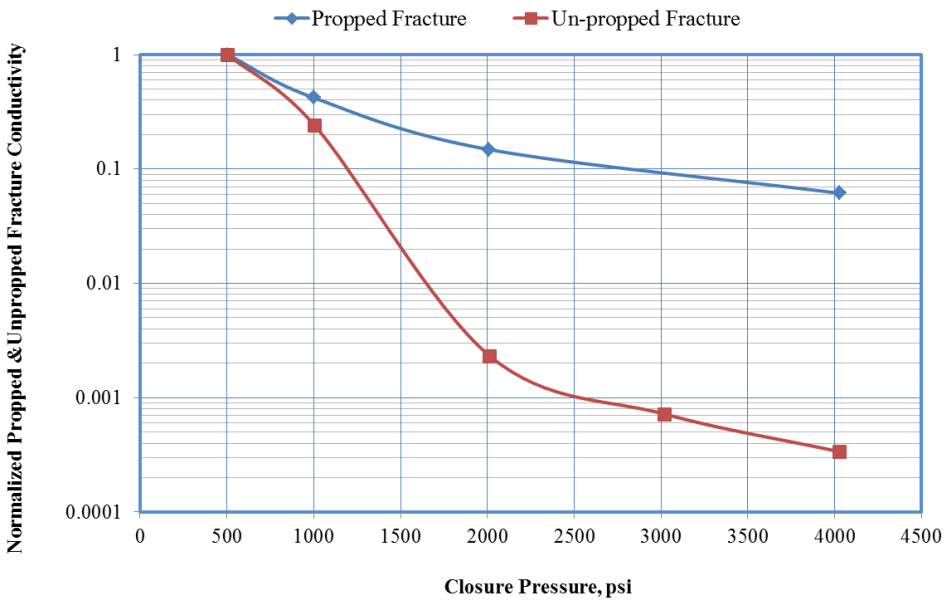

Figure 4.32 Normalized propped and un-propped fracture conductivity

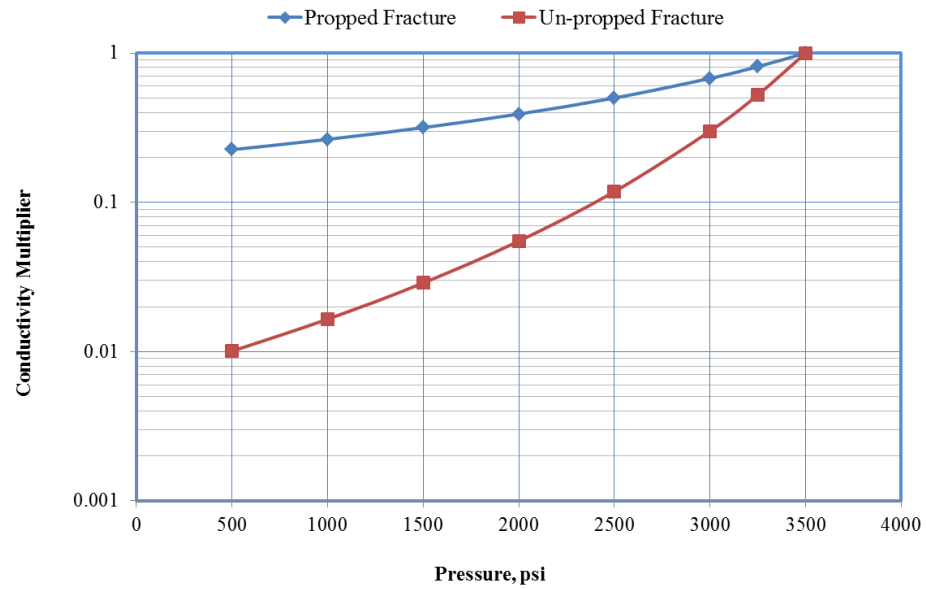

Figure 4.33 Conductivity multiplier used in CMG (IMEX, 2012)

4.4.2 Implementation of Coupled Reservoir Flow with Geomechanical Effects

Experimental results show that both natural and hydraulic fracture conductivities can be reduced by the order of magnitude by increasing net stress. In order to investigate the impact of conductivity reduction on the production performance, a synthetic multiply fractured unconventional reservoir model is generated and used in this study. In addition to the Base Case, a sensitivity analysis is also performed for certain reservoir characteristics. Table 4.4 includes the synthetic reservoir parameters considered as the Base Case, and Table 4.5 shows the sensitivity parameters used in this section.

Table 4.4: Input parameters for implementation of coupled reservoir flow with geomechanics effects

Parameter	Value(s)	Unit
The model dimensions	3,900 (length), 330 (width), 330 (height)	ft
Initial reservoir pressure	3500	psi
BHP	500	psi
Production time	15	year
Reservoir temperature	200	^{o}F
Gas viscosity	0.0184	cp
Initial gas saturation	1	fraction
Total compressibility	$5x10^{-4}$	psi^{-1}
Matrix permeability	0.0006	md
Matrix porosity	0.06	fraction
Initial natural fracture conductivity	0.05	md-ft
Initial hydraulic fracture conductivity	6	md-ft
Number of natural fractures	10	#
Fracture half length	330	ft
Fracture stage spacing	300	ft
Fracture height	330	ft
Number of hydraulic fracture stages	14	#
Number of well	1	#

Table 4.5: Sensitivity parameters used in coupled reservoir flow with geomechanical effects

Parameter	Minimum	Mean	Maximum	Unit
Matrix permeability	0.0002	0.0006	0.0008	md
Initial natural fracture conductivity	0.005	0.05	0.5	md-ft
Initial hydraulic fracture conductivity	2	6	10	md-ft

Production performances of the Base Case are provided in Figures 4.34 and 4.35, and the cumulative production differences between the constant conductivity case and the other conditions are given in Table 4.6. It must be noted that the difference column in Table 4.6 refers to the percentage difference in cumulative production after 15 years between the constant conductivity (without geomechanics) condition and with geomechanical effects. It is observed that the impact of natural fracture conductivity loss, which causes 10% less production than the case without any geomechanics, is more than the hydraulic fracture conductivity loss which causes 7% less cumulative production. It is also observed that if the geomechanical considerations are taken into account for both natural and hydraulic fractures, production is less (14%) than the sum of the individual effects of hydraulic and natural fractures (17%). However, the case where geomechanical effects apply to both natural and hydraulic fractures has the most influence on the cumulative production performance. This condition is explained by the conductivity versus closure pressure behavior of the natural and the hydraulic fractures. Figure 4.32 indicates that the natural fracture conductivity loss is larger than the hydraulic fractures for the same stress conditions; because of this, natural fracture conductivity loss has more effect specifically for the shale sample used in Suarez-Rivera et al. (2013) experiments.

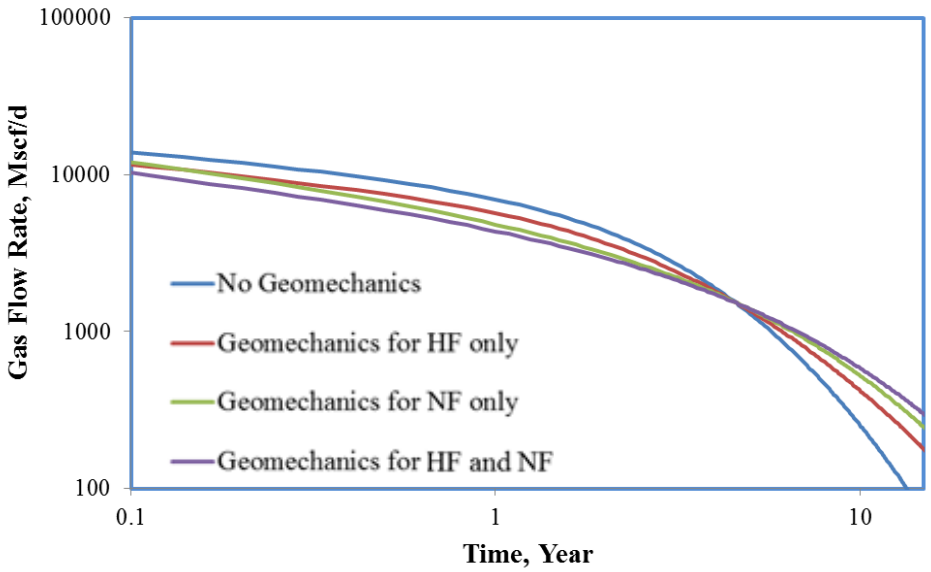

Figure 4.34 Gas flow rate performance for the Base Case by considering no geomechanics, geomechanics only for hydraulic fractures, geomechanics only for natural fractures, and geomechanics for both hydraulic and natural fractures

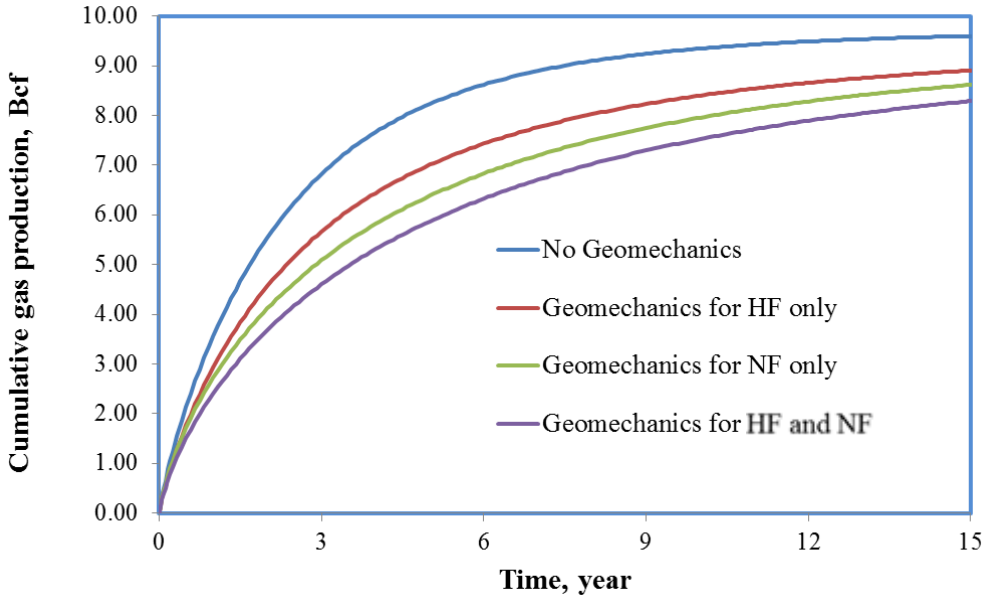

Figure 4.35 Cumulative gas production for the Base Case by considering no geomechanics, geomechanics only for hydraulic fractures, geomechanics only for natural fractures, and geomechanics for both hydraulic and natural fractures

Table 4.6: Cumulative gas production performances for the Base Case with and without geomechanical considerations

Condition	Cum. Prod. for 15 years, BCF	Difference
No Geomechanics	9.60	------
Geomechanics for HF only	8.91	0.07
Geomechanics for NF only	8.62	0.10
Geomechanics for both	8.29	0.14

Reservoir pressure distribution for the Base Case is also provided for different production times in Figures 4.36, 4.37, 4.38 and 4.39. Figure 4.36 represents the pressure distribution after 1 year for the cases with and without geomechanics considerations, and it is observed that the pressure in the most outer parts does not deplete in the case with

geomechanics effects applied for both hydraulic and natural fractures. However, in the case without geomechanics pressure distribution is almost evenly in the drainage area.

Figure 4.37 shows the pressure distribution after 5 years of production. It is observed that hydraulic fracture closure (Figure 4.37, b) becomes apparent and reduces the drainage efficiency in 5 years of production. The same phenomenon is also observed for the case with geomechanics on natural fractures.

Figure 4.38 represent the pressure distribution after 10 years of production. The case without any geomechanics almost depleted in that period. However, the cases with geomechanics effects taken into account still have the high pressure zones, due to closure of fractures. As stated earlier, the drainage efficiency is reduced with continuing production and geomechanics effects become apparent in pressure distribution.

Figure 4.39 shows the pressure distribution in the reservoir after 15 years of production. The case without any geomechanics is depleted in that period. However, the cases with geomechanical considerations does not deplete because of fracture closures with continuing production, but their cumulative production profile, which is given in Figure 4.35, almost reach the plateau, and daily production rates of these cases are very low, most probably not economically feasible. That means because of the fracture closure production is not continuing even though reservoir pressure is still considerably high. In order to produce the remaining gas in the reservoir re-fracturing operation can be perform to increase the fracture conductivities close to their initial values. Hence, remaining gas in the reservoir can be produced accordingly.

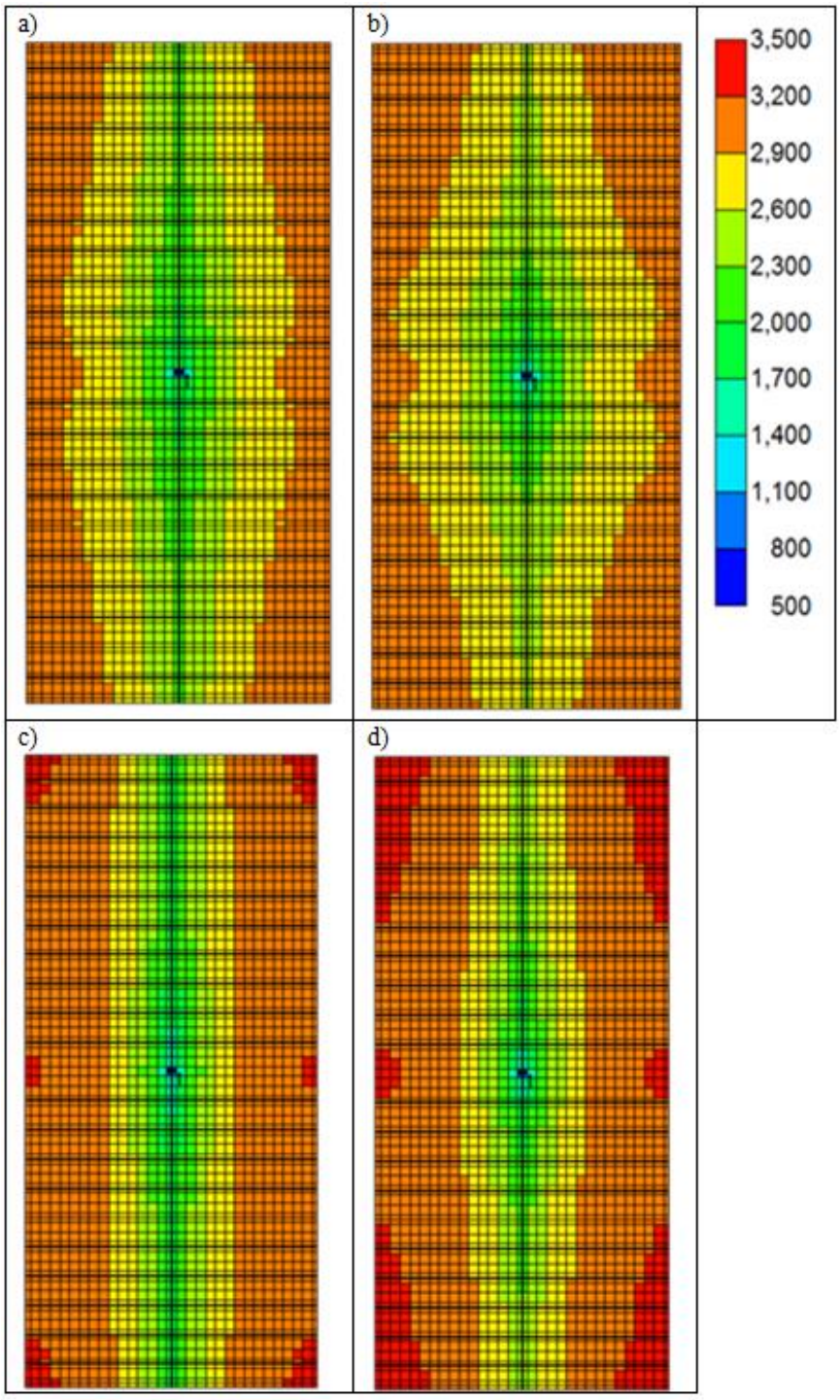

Figure 4.36 Reservoir Pressure Distributions after 1 year of production
a) No Geomechanics b) Geomechanics for HF only c) Geomechanics for NF only d) Geomechanics for both HF and NF

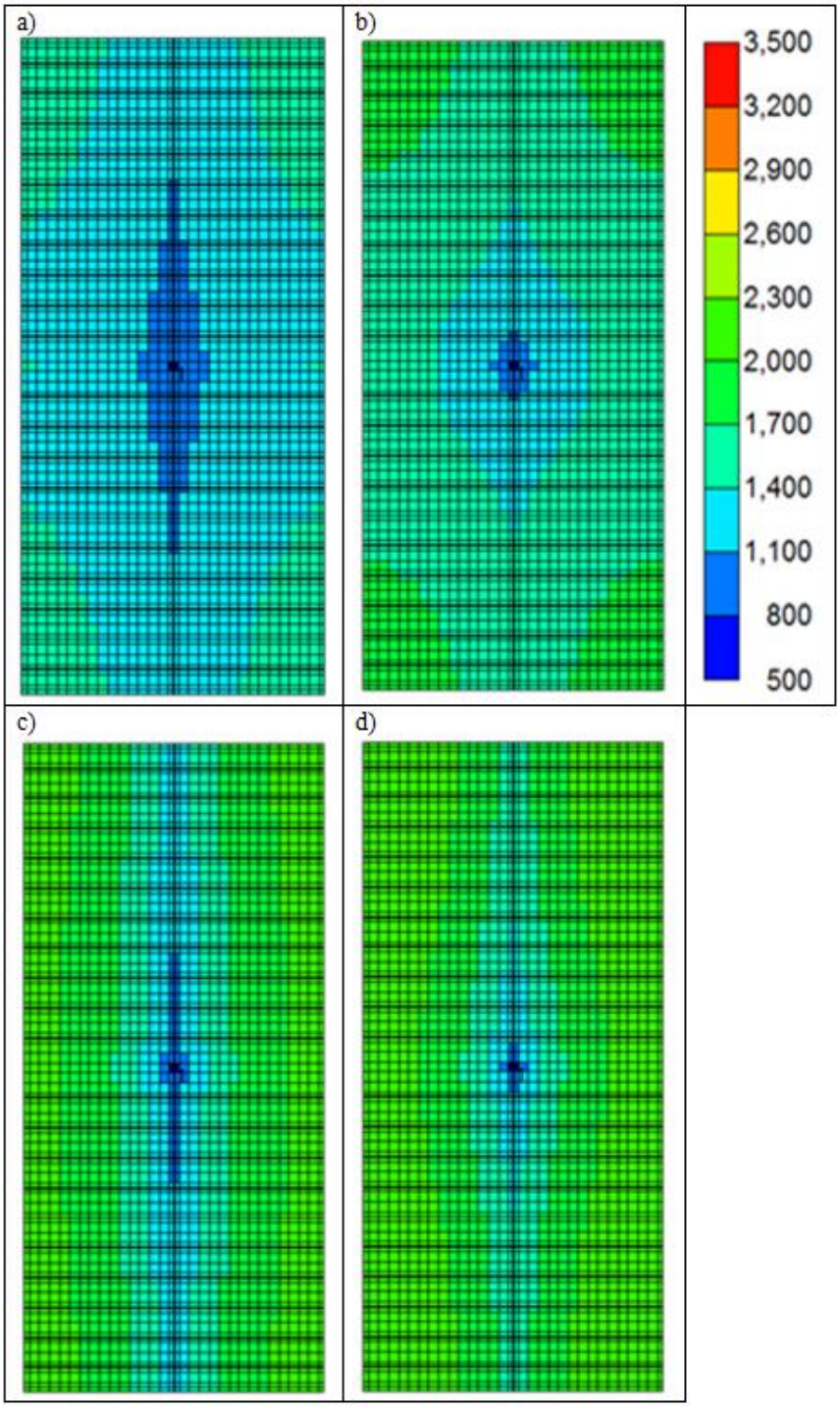

Figure 4.37 Reservoir Pressure Distributions after 5 years of production
a) No Geomechanics b) Geomechanics for HF only c) Geomechanics for NF only d) Geomechanics for both HF and NF

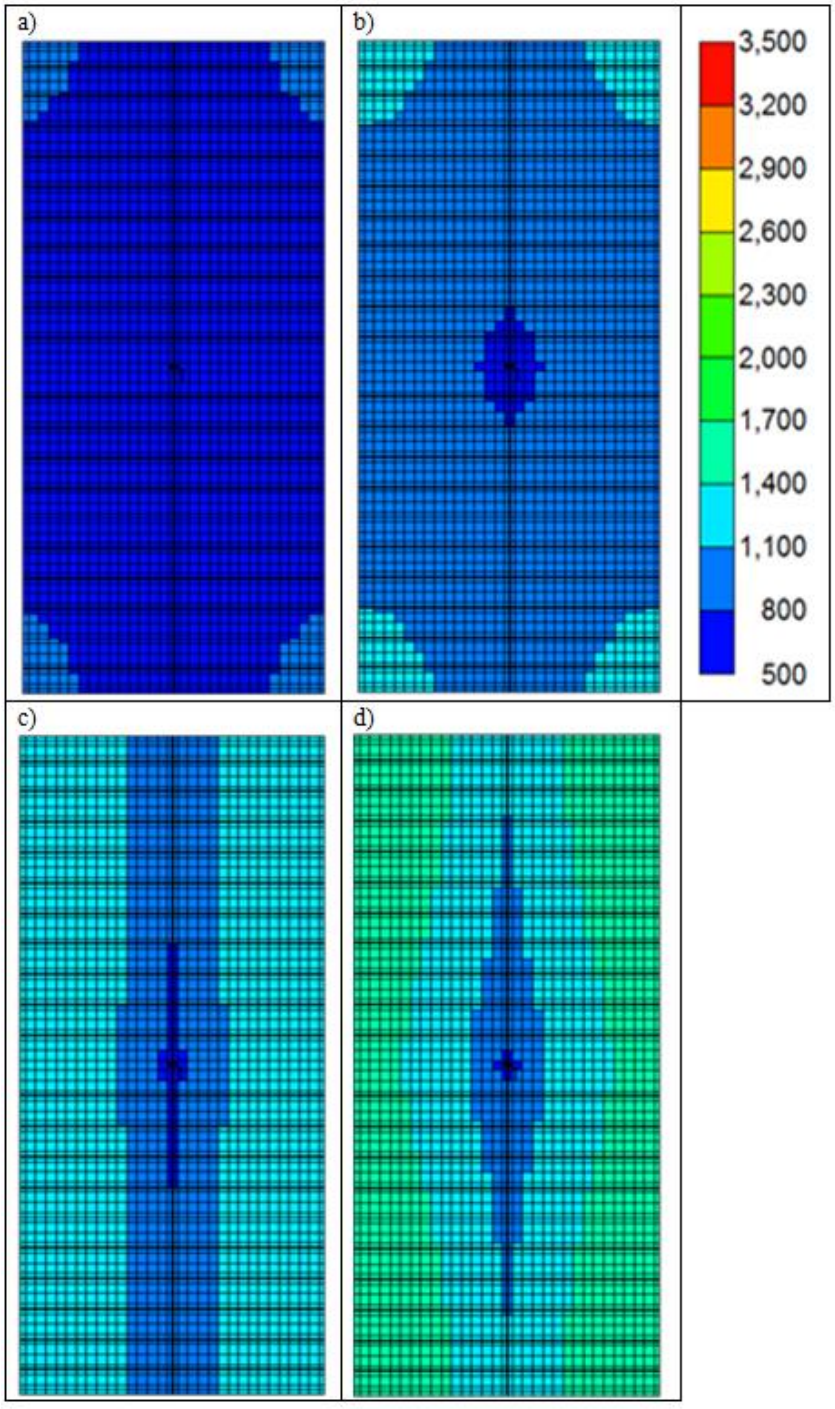

Figure 4.38 Reservoir Pressure Distributions after 10 years of production
a) No Geomechanics b) Geomechanics for HF only c) Geomechanics for NF only d) Geomechanics for both HF and NF

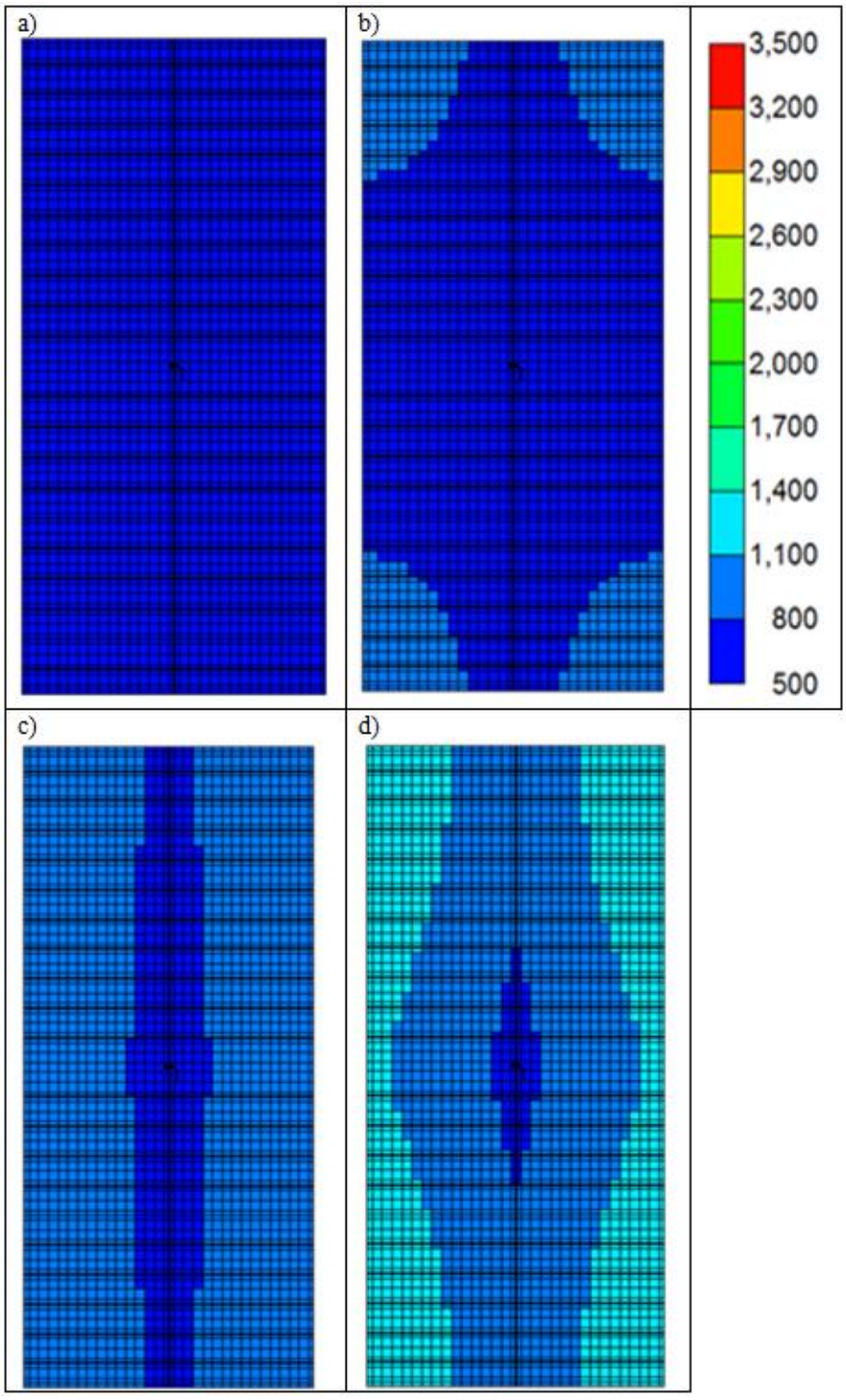

Figure 4.39 Reservoir Pressure Distributions after 15 years of production
a) No Geomechanics b) Geomechanics for HF only c) Geomechanics for NF only d) Geomechanics for both HF and NF

4.4.2.1 Matrix Permeability – 0.0002 md

Three different matrix permeabilities are considered in this study. The lowest matrix permeability considered is 0.0002 md, and the results for this case are provided in Figures 4.40, 4.41, and Table 4.7. Decreasing matrix permeability does not change the effect of pressure dependent hydraulic fracture conductivity. However, it is observed that decreasing matrix permeability to some extent increases the effects of pressure dependent natural fracture conductivity. For the Base Case which has 0.0006 md matrix permeability, pressure dependent natural fracture conductivity causes 10% less production than the case without geomechanics, while the matrix permeability of 0.0002 md causes around 25% less cumulative production. This shows the importance of natural fracture existence especially for the very low matrix permeability formation discussed here.

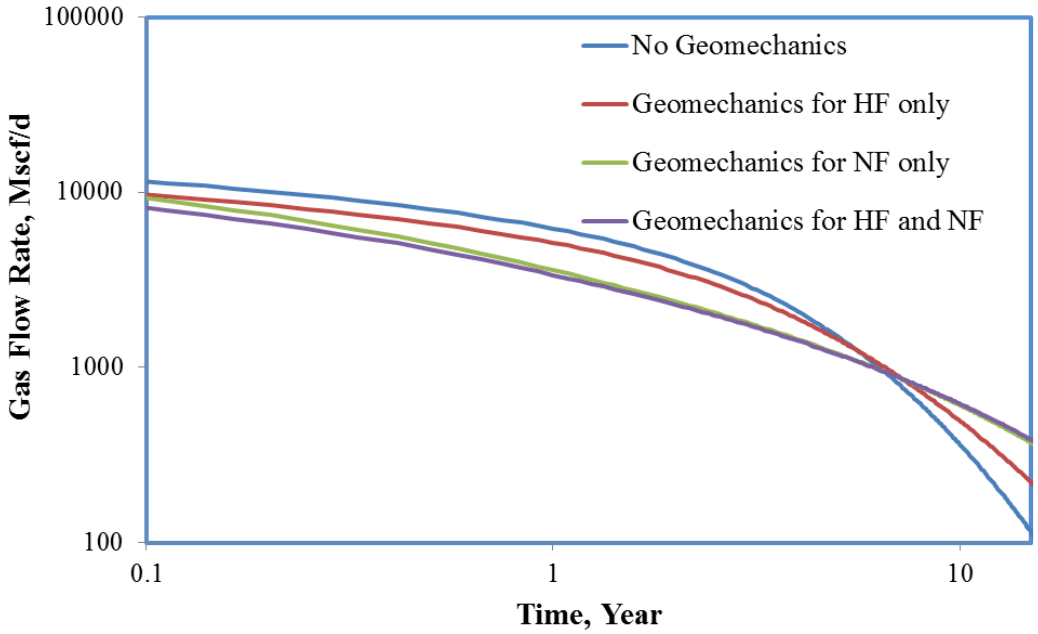

Figure 4.40 Gas flow rate performance using matrix permeability of 0.0002 md by considering no geomechanics, geomechanics only for hydraulic fractures, geomechanics only for natural Fractures, and geomechanics for both hydraulic and natural fractures

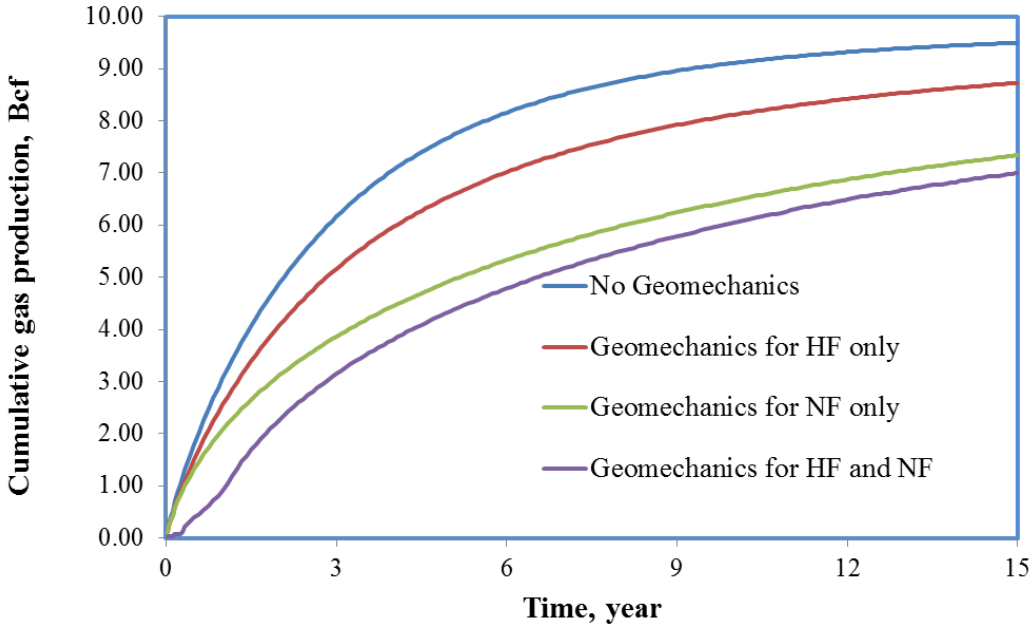

Figure 4.41 Cumulative gas production using matrix permeability of 0.0002 md by considering no geomechanics, geomechanics only for hydraulic fractures, geomechanics only for natural fractures, and geomechanics for both hydraulic and natural fractures

Table 4.7: Cumulative gas production for the matrix permeability 0.0002 md with and without geomechanical considerations

Condition	Cum. Prod. for 15 years, BCF	Difference
No Geomechanics	9.49	------
Geomechanics for HF only	8.72	0.08
Geomechanics for NF only	7.34	0.23
Geomechanics for both	7.09	0.25

4.4.2.2 Matrix Permeability – 0.0008 md

The highest matrix permeability considered in this study is 0.0008 md, and the results for this case are provided in Figures 4.42, 4.43 and Table 4.8. Increasing matrix permeability does not change the effect of pressure dependent hydraulic fracture

conductivity effects on cumulative production performances for 15 years. Increasing matrix permeability to some extent reduces the effects of pressure dependent natural fracture conductivity on production performances. As given in Table 4.8 below, the case with natural fracture conductivity loss produces 8% less than the case without any geomechanics. It is already discussed that for the matrix permeability 0.0002 md and 0.0006 md pressure dependent natural fracture conductivity cases cause 25% and 10% less cumulative productions, respectively for pressure dependent natural fracture conductivity conditions. Combined effect of natural and hydraulic fracture conductivity loss is around 11%, which is less than the sum of individual effects of natural and hydraulic fracture conductivity losses.

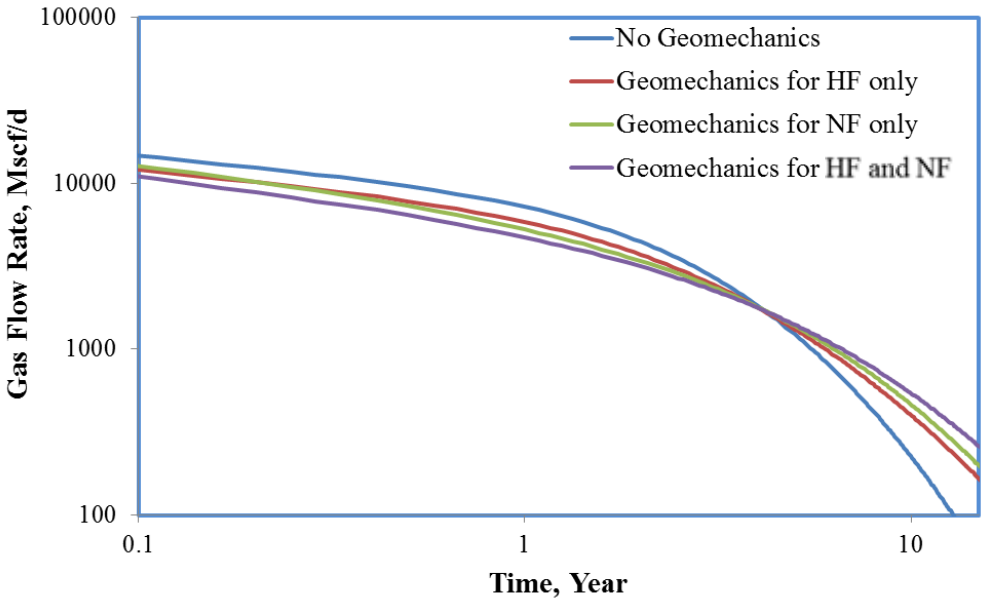

Figure 4.42 Gas flow rate performance using matrix permeability of 0.0008 md by considering no geomechanics, geomechanics only for hydraulic fractures, geomechanics only for natural fractures, and geomechanics for both hydraulic and natural fractures

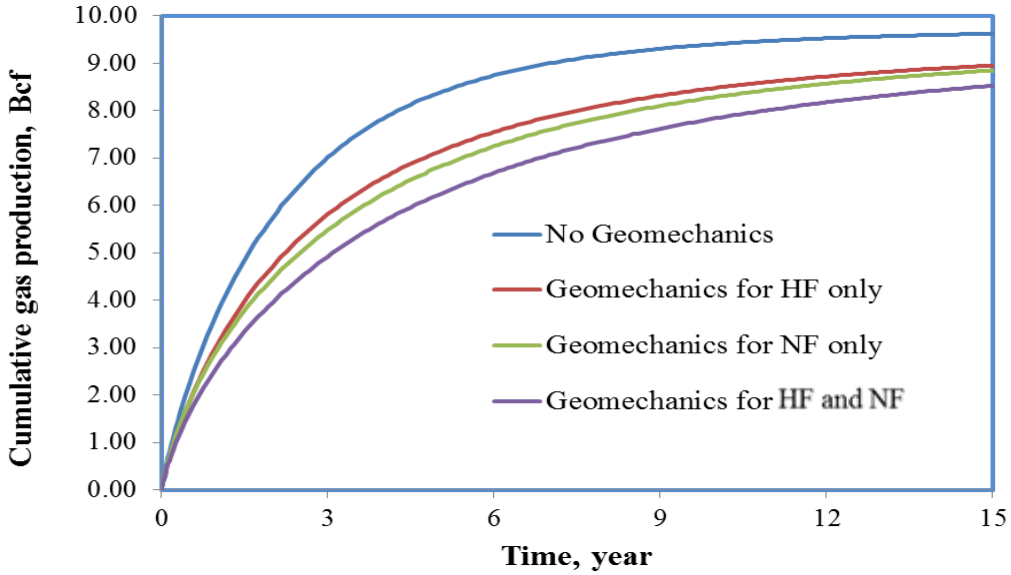

Figure 4.43 Cumulative gas production using matrix permeability of 0.0008 md by considering no geomechanics, geomechanics only for hydraulic fractures, geomechanics only for natural fractures, and geomechanics for both hydraulic and natural fractures

Table 4.8: Cumulative gas production for the matrix permeability 0.0008 md with and without geomechanical considerations

Condition	Cum. Prod. for 15 years, BCF	Difference
No Geomechanics	9.62	------
Geomechanics for HF only	8.95	0.07
Geomechanics for NF only	8.85	0.08
Geomechanics for both	8.53	0.11

4.4.2.3 Initial Natural Fracture Conductivity – 0.005 md-ft

Three different initial natural fracture conductivities are considered in this section. The same conductivity multiplier plot, given in Figure 4.33, is applied for three different initial natural fracture conductivity cases. First, initial natural fracture permeability

considered as 0.005 md –ft. For a fair comparison, each case evaluated for 15 years of production, and is observed that 0.005 md-ft initial natural fracture case cannot reaches the absolute maximum production limits even by 15 years (Figure 4.45), and this fact can also be observed in gas flow rate plot given in Figure 4.44. This fact also masks the effect of pressure dependent natural fractures on cumulative production performances. As given in the Table 4.9, individual effects of pressure dependent natural fracture conductivity results in 7% less cumulative production in 15 years. However, the initial natural fracture conductivity of 0.05 md-ft causes 10% less production in 15 years. This condition verifies that very low initial natural fracture conductivity postpones the geomechanical effects become apparent, since the reservoir pressure does not deplete so fast in 15 years to affect the cumulative production performance.

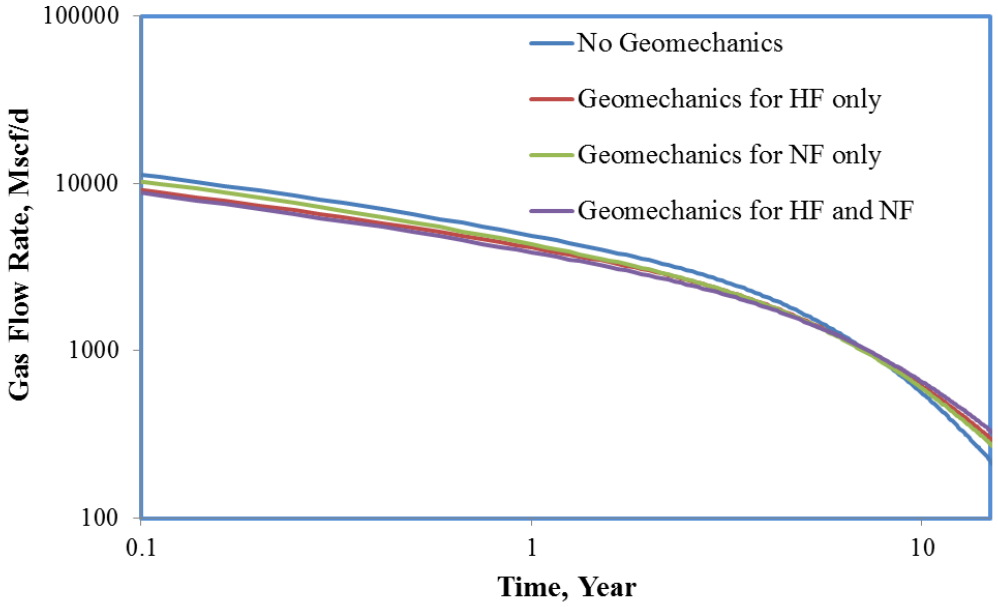

Figure 4.44 Gas flow rate performance using initial natural fracture conductivity of 0.005 md-ft by considering no geomechanics, geomechanics only for hydraulic fractures, geomechanics only for natural fractures, and geomechanics for both hydraulic and natural fractures

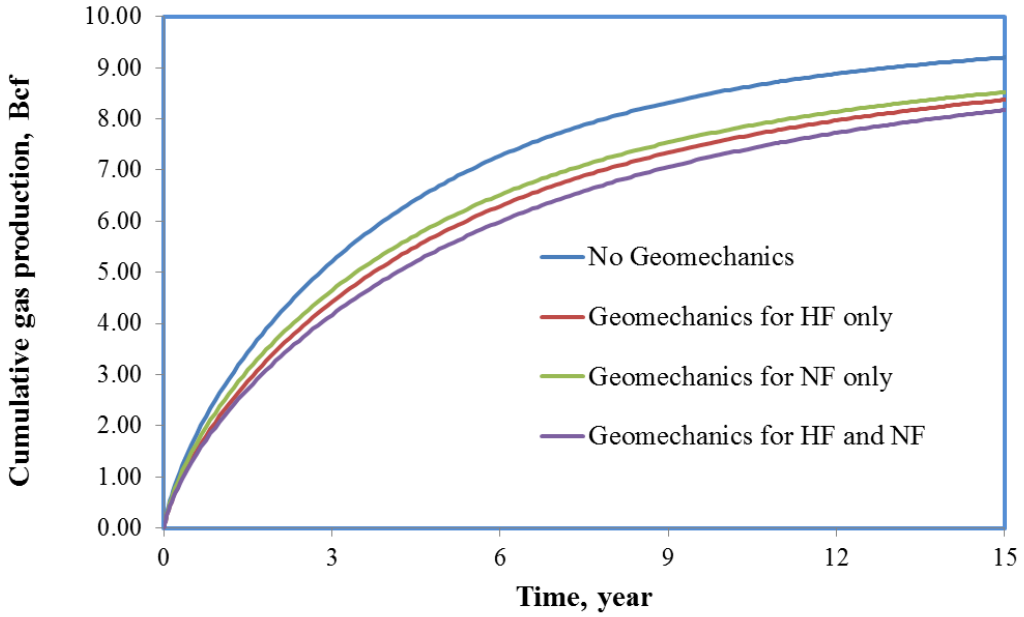

Figure 4.45 Cumulative gas production using initial natural fracture conductivity of 0.005 md-ft by considering no geomechanics, geomechanics only for hydraulic fractures, geomechanics only for natural fractures, and geomechanics for both hydraulic and natural fractures

Table 4.9: Cumulative gas production for the natural fracture conductivity of 0.005 md-ft with and without geomechanical considerations

Condition	Cum. Prod. for 15 years, BCF	Difference
No Geomechanics	9.20	------
Geomechanics for HF only	8.37	0.09
Geomechanics for NF only	8.52	0.07
Geomechanics for both	8.17	0.11

4.4.2.4 Initial Natural Fracture Conductivity – 0. 5 md-ft

Initial natural fracture conductivity is considered to be 0.5 md-ft, and the simulation results are provided in Figure 4.46 and Table 4.10. As it was expected, increasing initial natural fracture conductivity reduces the geomechanical effects on

production performance. Comparing Table 4.10 and the results for the Base Case (Table 4.6) indicates that if the natural fracture conductivity remains high, then the geomechanical effects will not cause significant long term production loss.

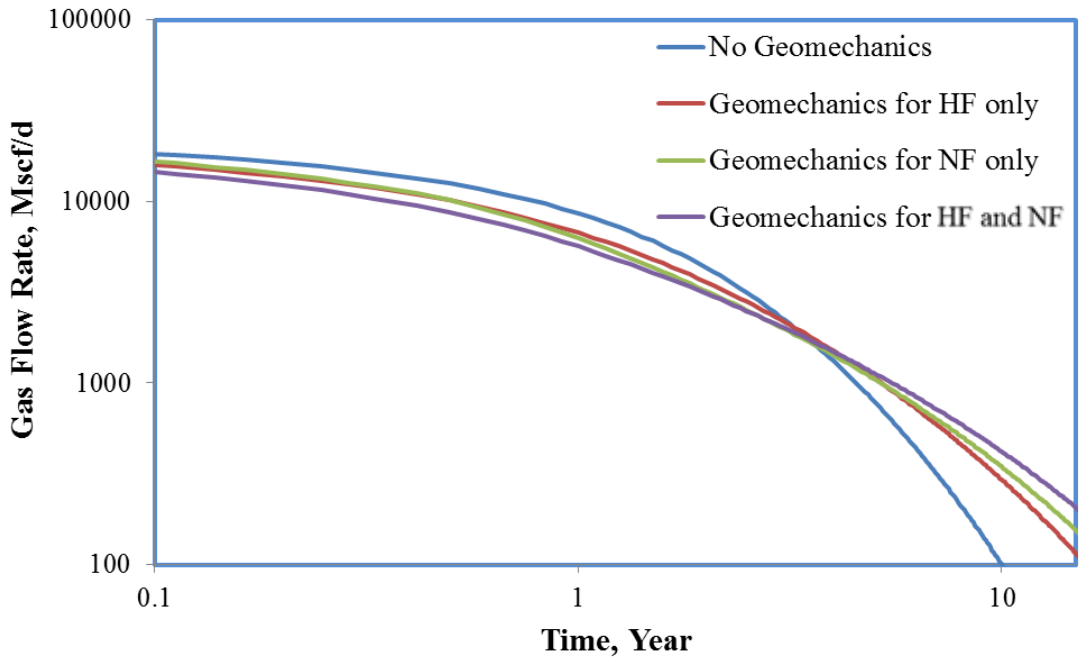

Figure 4.46 Gas flow rate performance using initial natural fracture conductivity of 0.5 md-ft by considering no geomechanics, geomechanics only for hydraulic fractures, geomechanics only for natural fractures, and geomechanics for both hydraulic and natural fractures

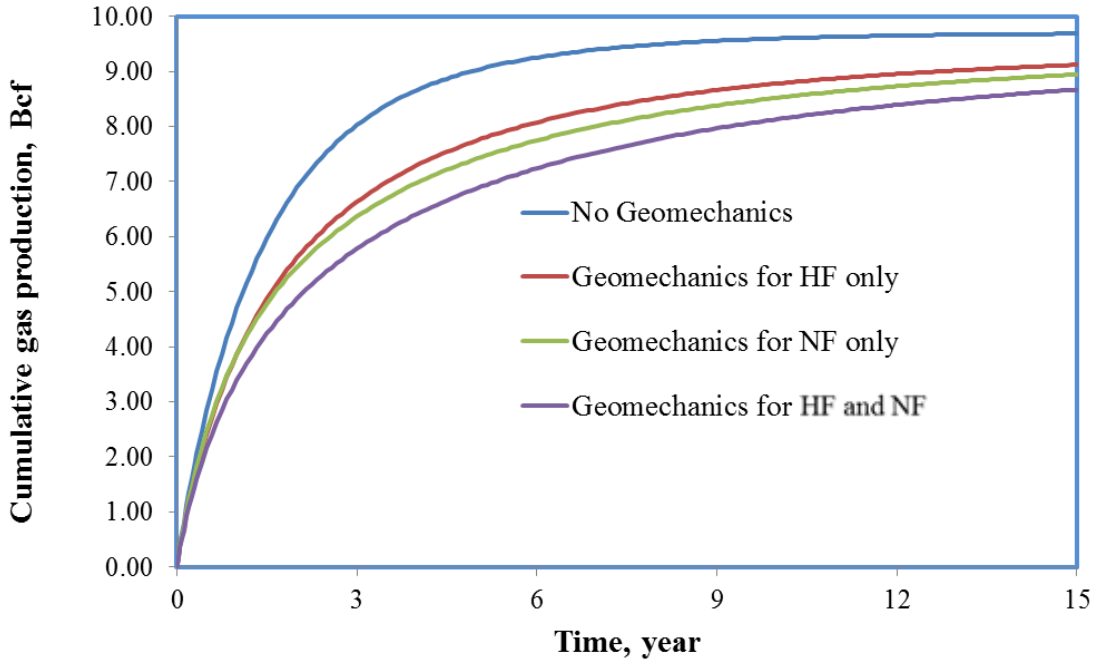

Figure 4.47 Cumulative gas production using initial natural fracture conductivity of 0.5 md-ft by considering no geomechanics, geomechanics only for hydraulic fractures, geomechanics only for natural fractures, and geomechanics for both hydraulic and natural fractures

Table 4.10: Cumulative gas production for the natural fracture conductivity of 0.5 md-ft with and without geomechanical considerations

Condition	Cum. Prod. for 15 years, BCF	Difference
No Geomechanics	9.68	------
Geomechanics for HF only	9.12	0.06
Geomechanics for NF only	8.94	0.08
Geomechanics for both	8.67	0.10

4.4.2.5 Initial Hydraulic Fracture Conductivity – 2 md-ft

The effect of hydraulic fracture conductivity on production performances of unconventional reservoirs is discussed in Chapter 3. It is also critical to investigate

various hydraulic fracture conductivities considering the geomechanical effects. For this purpose, three different initial hydraulic fracture conductivities are considered and the results for the Base Case with 6 md-ft initial hydraulic fracture conductivity are given in Figures 4.34, 4.35 and Table 4.6. The lowest hydraulic fracture conductivity is 2 md-ft, and the results for that case provided in Figures 4.47, 4.48, and Table 4.11. It is observed that by decreasing the initial hydraulic fracture conductivity, geomechanical effects show greater impact on production performance. This can be clearly seen by comparing Table 4.11 (2 md-ft) and Table 4.12 (10 md-ft). Although decreasing initial hydraulic fracture conductivity does not affect the individual importance of natural fracture conductivity loss, the combined effect of natural and hydraulic fracture closure rises by decreasing initial hydraulic fracture conductivity.

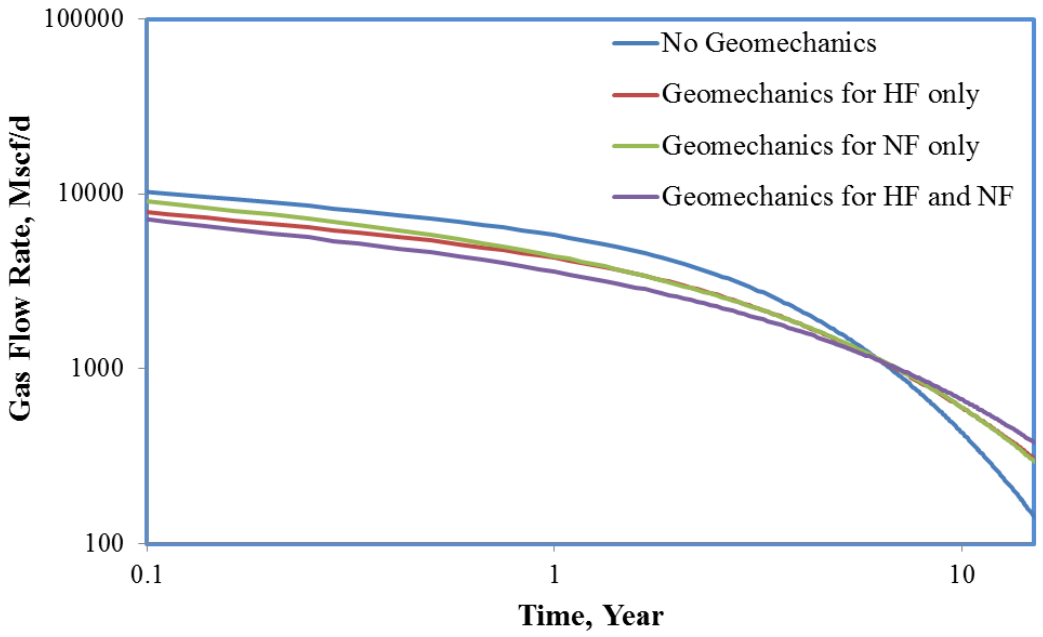

Figure 4.48 Gas flow rate performance using initial hydraulic fracture conductivity of 2 md-ft by considering no geomechanics, geomechanics only for hydraulic fractures, geomechanics only for natural fractures, and geomechanics for both hydraulic and natural fractures

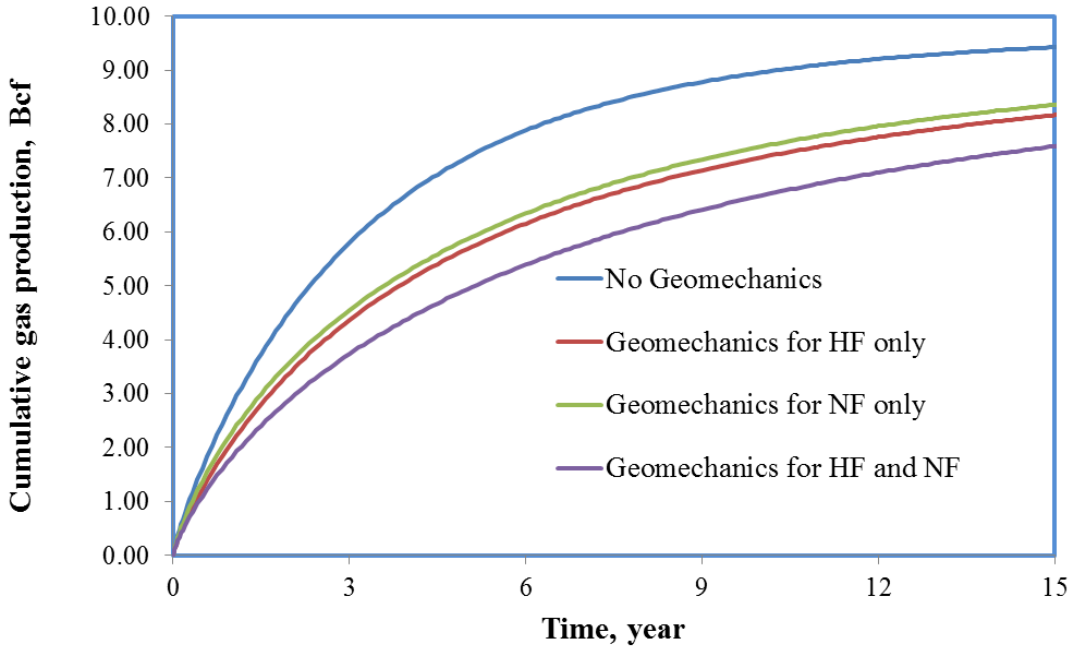

Figure 4.49 Cumulative gas production using initial hydraulic fracture conductivity of 2 md-ft by considering no geomechanics, geomechanics only for hydraulic fractures, geomechanics only for natural fractures, and geomechanics for both hydraulic and natural fractures

Table 4.11: Cumulative gas production for the initial hydraulic fracture conductivity of 2 md-ft with and without geomechanical considerations

Condition	Cum. Prod. for 15 years, BCF	Difference
No Geomechanics	9.43	------
Geomechanics for HF only	8.17	0.13
Geomechanics for NF only	8.36	0.11
Geomechanics for both	7.59	0.19

4.4.2.6 Initial Hydraulic Fracture Conductivity – 10 md-ft

Initial hydraulic fracture is considered as 10 md-ft, and the results are provided in Figures 4.49 and 4.50 and Table 4.12. It is observed that increasing the initial hydraulic

fracture conductivity does not change the effect of pressure dependent natural fracture conductivity on production. Comparing with the Base Case results, increasing initial hydraulic fracture conductivity reduces the effects of pressure dependent hydraulic fracture conductivity on cumulative production. Finally, the combined effect of pressure dependent natural and hydraulic fracture conductivities is negligible when the initial hydraulic fracture conductivity increases from 6 md-ft to 10 md-ft.

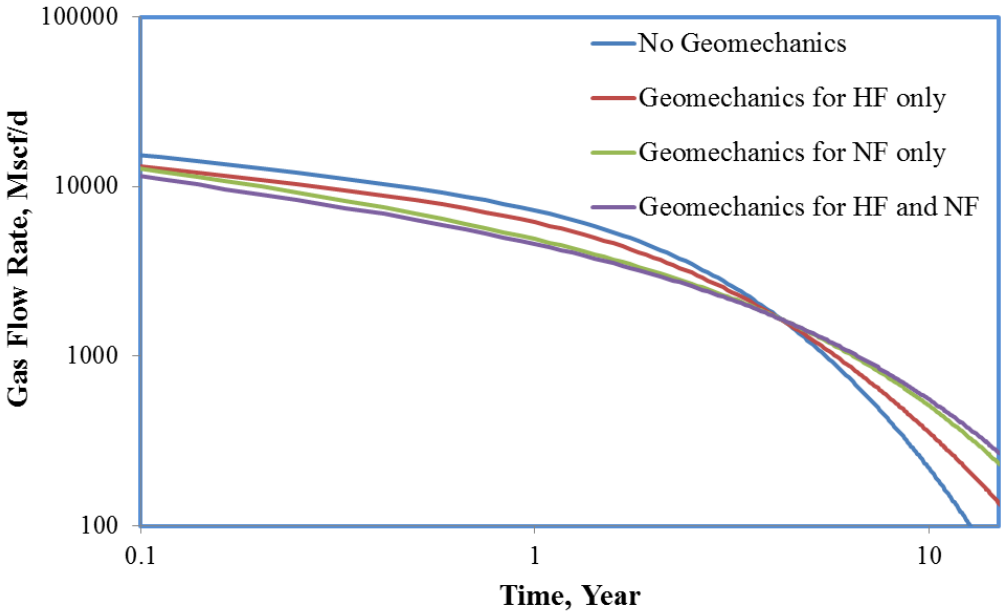

Figure 4.50 Gas flow rate performance using initial hydraulic fracture conductivity of 10 md-ft by considering no geomechanics, geomechanics only for hydraulic fractures, geomechanics only for natural fractures, and geomechanics for both hydraulic and natural fractures

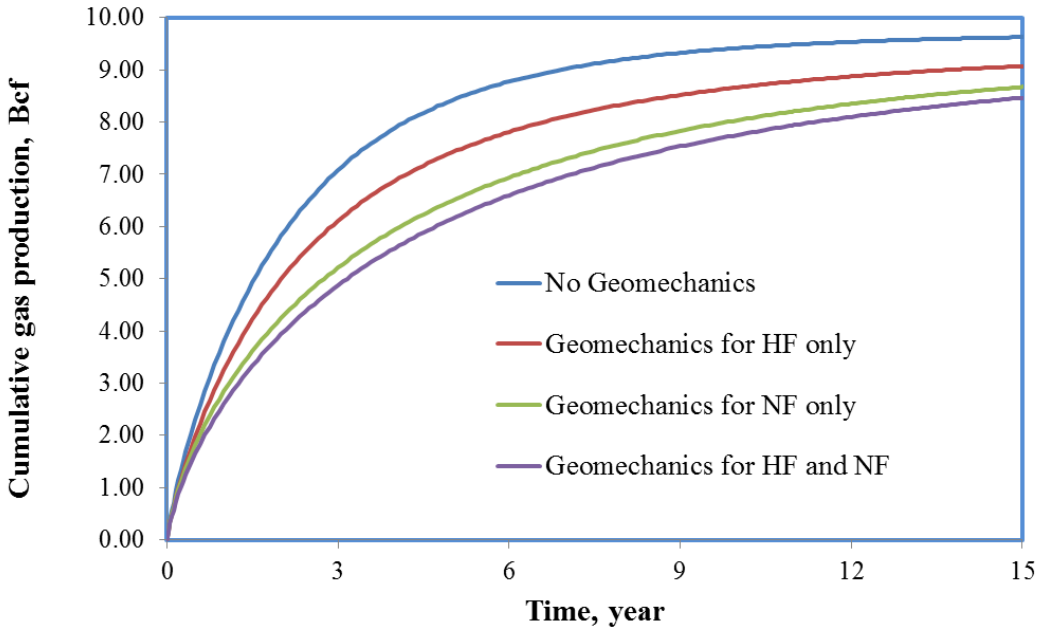

Figure 4.51 Cumulative gas production using initial hydraulic fracture conductivity of 10 md-ft by considering no geomechanics, geomechanics only for hydraulic fractures, geomechanics only for natural fractures, and geomechanics for both hydraulic and natural fractures

Table 4.12: Cumulative gas production for initial hydraulic fracture conductivity of 10 md-ft with and without geomechanical considerations

Condition	Cum. Prod. for 15 years, BCF	Difference
No Geomechanics	9.62	------
Geomechanics for HF only	0.07	0.06
Geomechanics for NF only	8.67	0.10
Geomechanics for both	8.46	0.12

Chapter 5: Summary, Conclusions, and Recommendations

This chapter summarizes this thesis and presents the conclusions. Finally, recommendations are stated for future studies.

5.1 SUMMARY

This thesis has been accomplished in two main phases. First, reservoir modeling in homogeneous unconventional reservoirs is investigated both numerically and analytically. For this purpose two analytical models from the available literature, one with infinite fracture conductivity assumption proposed by Patzek et al. (2013), while the other model with finite conductivity assumption developed by Ozkan et al. (2009), are employed. In addition, a commercial reservoir simulator (CMG, IMEX, 2012) is used to compare the results obtained by the analytical models. It is observed that the results obtained from the analytical models showed a perfect agreement with commercial reservoir simulator for various completion scenarios. It is also concluded that analytical models are capable to capture main physics with minimum computational efforts and input data.

For the first phase of this study, a sensitivity analysis is also performed for certain reservoir and completion parameters for a synthetic unconventional reservoir. Production performance of hydraulically fractured wells is highly affected by completion design parameters such as hydraulic fracture spacing and fracture half-length. Unconventional reservoir parameters have high uncertainty, so not only the design parameters, but also the uncertainty parameters such as permeability, porosity and formation thickness are considered as well. The advantages of analytical models become apparent with this uncertainty analysis since different conditions can be evaluated quickly compare to the

commercial reservoir simulators. Conclusions reached by sensitivity analysis are stated in conclusions section of this chapter.

The second phase of this study focused on naturally fractured unconventional reservoir models and their production behaviors. In addition, geomechanical effects are coupled with reservoir flow. In order to carry out this study, both analytical and numerical solutions are employed. Analytical dual porosity model developed by Apaydin (2012) is used to model natural fractures in unconventional models, and CMG is used to compare the results obtained by the analytical model. It is verified that the analytical model can accurately simulate naturally fractured unconventional reservoir model accurately. Production behavior differences between homogeneous and naturally fractured reservoirs are given in conclusions section of this chapter.

In order to couple reservoir flow with geomechanical effects, Apaydin (2012) dual porosity model is employed. However, the original model proposed by Apaydin (2012) and Cho (2012) cannot simulate constant bottom-hole pressure production scenarios. In this study we improved their model by proposing a new technique to simulate constant bottom hole pressure scenario, and coupled reservoir flow with geomechanical considerations. We further verified our approach with the CMG simulator. It must be noted that the analytical model takes geomechanical effects into account only for natural fractures.

As stated previously, the analytical dual porosity model couples only natural fracture geomechanics with reservoir flow. In order to couple both natural and hydraulic fractures geomechanics with reservoir flow, the commercial reservoir simulator is used (CMG, IMEX, 2012). The results obtained from this study are given in conclusions section of this chapter. Throughout the simulation studies within this thesis,

geomechanical effects on unconventional reservoir production performances were seen to decrease the cumulative production.

5.2 CONCLUSIONS

Conclusions driven by this study are stated in this section. In the following, Chapters 3 and 4 conclusions are stated, respectively.

5.2.1 Homogeneous Unconventional Reservoir Models Conclusions

This section highlights the conclusions driven by homogeneous unconventional reservoir models and the sensitivity analysis results.

- Two analytical unconventional reservoir models are investigated in this study and their responses verified against the commercial reservoir simulator (CMG, IMEX, 2012). It is concluded that both of these analytical models can accurately simulates unconventional reservoirs production performance with minimum computational efforts.
- Sensitivity analysis is performed for 5, 10, and 30 years of production, and it is concluded that each time period is sensitive to different reservoir and design parameters.
- Fracture height and reservoir porosity are two important parameters which control production performance in each time period, because these two parameters control the volume of original gas in place.
- For 5 years of production fracture height, porosity, permeability, stage spacing, fracture conductivity, fracture half-length, and bottom hole pressure are important, respectively.

- For 10 years of production porosity, fracture height, permeability, stage spacing, fracture half length, fracture conductivity, and bottom hole pressure are important, respectively.
- For 30 years of production, all of the design and reservoir parameters except fracture height and porosity loss their impact on production, because reservoir is already depleted.
- It is concluded that operator companies must perform sensitivity studies on completion design parameters and analytical models can accurately and relatively simply simulates different scenarios.

5.2.2 Naturally Fractured Unconventional Reservoir Models Conclusions

This section summarizes the sensitivity analysis performed using the analytical dual porosity model implemented in the trilinear reservoir model. Critical points from this sensitivity analysis are highlighted as follows:

- Modified analytical dual porosity model accurately predicts the hydraulically and naturally fractured unconventional reservoir production performance with little computational effort. Results obtained from the analytical model show a good agreement with the commercial reservoir simulator for a synthetic reservoir case.
- Existence of natural fractures significantly improves the production performance of unconventional reservoirs compared with a homogeneous unconventional reservoir models.
- It is observed that the matrix permeability is not the key parameter that controls the hydraulically and naturally fractured unconventional reservoir production performance.

- It is also concluded that the natural fractures are the main conduits for hydrocarbon flow from reservoir to the hydraulic fracture. Hence, natural fracture properties such as permeability and thickness are the key parameters which are controlling the production performance. Basically, the matrix can supply enough gas flow to the natural fractures, but if the natural fractures are not able to transmit the gas to the hydraulic fractures then production will be limited.
- Another conclusion driven by this study show that increasing natural fracture density in the pay zone improves the production performance.

5.2.3 Pressure Dependent Natural Fracture Permeability Conclusions

This section summarizes the sensitivity analysis performed using the modified analytical dual porosity model coupled with the trilinear reservoir model for pressure dependent natural fracture permeability. Conclusions reached from this sensitivity analysis are expressed as follows:

- Low initial natural fracture permeability (10 md) postpones the effect of pressure dependent natural fracture permeability on production since the reservoir pressure does not deplete fast enough to change natural fracture permeability.
- If the initial natural fracture permeability is high (1000 md), the pressure dependent natural fracture permeability effects become apparent after 1 year and the cumulative production decreases around 6% less in 10 years.
- It is observed that the matrix permeability is not the key parameter that controls the effect of pressure dependent natural fracture permeability on production performance.
- It is also observed that the bottom hole pressure has a minor effect on the pressure dependent natural fracture permeability effects.

- It is concluded that the pressure dependent natural fracture permeability causes slightly less cumulative production for the soft shale compared to medium and hard shale samples.

5.2.4 Coupled Reservoir Flow with Geomechanical Effects Conclusions

This section summarizes the results achieved by the coupled reservoir flow with geomechanics using CMG (IMEX, 2012) commercial reservoir simulator. Important outcomes from this study are highlighted as following:

- For the rock samples used in this study, individual effect of pressure dependent natural fracture conductivity on production performance is greater than the individual effects of pressure dependent hydraulic fracture conductivity. This fact can be explained by the conductivity graph given in Figure 4.32. Conductivity losses of un-propped fractures with increasing closure stress are two log-cycles greater than the propped fracture.
- When the conductivity losses are coupled with the reservoir flow, reduction in cumulative production performance is higher in pressure the dependent natural fracture permeability case. In addition to this, the significant contribution of natural fractures on production in unconventional reservoirs is validated with the results which are a well-established concept in modeling of unconventional reservoirs.
- One of the major motivations of this study was to examine both individual and combined effects of pressure-dependent natural and hydraulic fracture conductivity on production performances. It is concluded that the combined effect of natural and hydraulic fracture conductivity losses is less than the sum of the individual effects.

- For the scenarios considered in this thesis, it is observed that individual effects of natural fracture conductivity loss on productions vary from 10% to 25%. On the other hand, considering only hydraulic fracture conductivity losses cause 5% to 15% less production in 15 years. Combined effect of natural and hydraulic fracture conductivity losses reduce the cumulative production 10% to 25% in 15 years.
- A reasonable range of matrix permeabilities are evaluated in this study and it is concluded that decreasing matrix permeability increases the severity of effects of pressure dependent natural fracture conductivities on the cumulative production. Since natural fractures are the main conduit for the reservoir flow, their characteristics such as conductivity becomes significant for low matrix permeability conditions. This explains that why the matrix permeability reduction increases the severe effect of pressure dependent natural fracture conductivity.
- Different values of initial natural fracture conductivity are also examined in this work, and it is observed that having extremely low initial fracture conductivity postpones the geomechanical effects on production. This study considered 15 years of production, and the reservoir pressure, for the lowest initial natural fracture conductivity case, does not drop enough to cause any obvious geomechanical effect in 15 years.
- Three different initial hydraulic fracture conductivities are simulated considering geomechanical effects. As a result of these simulations, it is observed that by increasing the initial hydraulic fracturing conductivity, severe geomechanical effect vanish. This was technically expected, because even though the same pressure depletion occurs in the reservoir, the remaining hydraulic fracture

conductivity would be larger in the higher initial hydraulic fracture conductivity case.

- For a fair comparison on the effect of hydraulic and natural fracture conductivity losses on production, experiments must be conducted on the same rock specimens for propped and un-propped conditions.
- For the cases with geomechanics effects considered, there is still significant amount of gas present in the reservoir with relatively high-pressure, but the remaining gas cannot be produced due to fracture closures. In order to alleviate this issue, a systematic re-fracturing operation can be performed to have high conductivity flow channels again.

5.3 RECOMMENDATIONS

Recommendations for future work are summarized as follows:

1) Improve analytic and semi-analytical models to capture non-linearity in the diffusion equation caused by desorption, non-Darcy flow, and slippage effect.
2) Incorporate the field data from different shale plays such as Barnett, Marcellus, and Albany shale etc. in analytical models to enhance the accuracy of the results and to provide better understanding of the physics of the flow in unconventional reservoirs.
3) Improve an analytical model in order to capture combined effect of natural and hydraulic fracture closures on the production performances of unconventional reservoirs.
4) Improve an analytical model to characterize the multi porosity and permeability nature of the rock matrix and fracture natural fracture network of unconventional shale reservoirs.

5) Develop a model to incorporate geomechanical behavior of the reservoir during hydraulic fracturing and post treatment production of unconventional reservoirs.
6) Identify the optimum re-fracturing time to overcome the production problems caused by natural and hydraulic fracture closures. Economic considerations also should be considered.
7) Conduct laboratory experiments to understand the conductivity changes of different shale plays with changing stress conditions.
8) Quantify the effect of proppant quality on the conductivity loss of different shale plays.

Appendix: Average Reservoir Pressure Calculation

We present the numerical approach used to calculate average reservoir pressure of the trilinear reservoir model. The reservoir is defined in two zones, inner zone and the hydraulic fracture. Inner zone is modeled and the governing equations are solved in two dimensions, x and y. The hydraulic fracture is extremely narrower than the main inner zone, which is modeled in one dimension; x. Average reservoir pressure is calculated by coupling the governing equations of both zones with a same boundary condition, equal gas flux on the interface of two zones. Calculated average reservoir pressure incorporated with the pressure dependent natural fracture permeability dual porosity model described in Section 4.1.2. Figure A.1 depicts the reservoir model. Numerical discretization for the inner zone (Zone 1) and the hydraulic fracture (Zone 2) are given respectively.

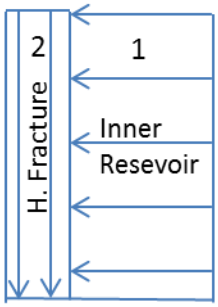

Figure A.1 Reservoir model considered in the average reservoir pressure calculation (Modified after Brown, 2009)

The Inner Reservoir Discretization

Governing flow equation for the inner reservoir (Zone 1) given by Eqn. A.1, and numerical discretization for that equation presented below.

$$\frac{\partial^2 m_I}{\partial x^2} + \frac{\partial m_I}{\partial y^2} = \frac{1}{\eta_I}\frac{\partial m_I}{\partial t}, \qquad \text{(Eqn. A.1)}$$

$$\frac{1}{\eta_I}\frac{m_{I_{i,j}}^{k+1} - m_{I_{i,j}}^{k}}{\Delta t} = \frac{m_{I_{i+1,j}}^{k} - 2\,m_{I_{i,j}}^{k} + m_{I_{i-1,j}}^{k}}{\Delta x^2} + \frac{m_{I_{i,j+1}}^{k} - 2\,m_{I_{i,j}}^{k} + m_{I_{i,j-1}}^{k}}{\Delta y^2}, \quad \text{(Eqn. A.2)}$$

Let us define;

$$\Delta x = \Delta y = h, \quad \text{(Eqn. A.3)}$$

and,

$$\alpha = \frac{\eta_I \Delta t}{h^2}. \quad \text{(Eqn. A.4)}$$

Therefore:

$$m_{I_{i,j}}^{k+1} = (1 - 4\alpha) m_{I_{i,j}}^{k} + \alpha[m_{I_{i+1,j}}^{k} + m_{I_{i-1,j}}^{k} + m_{I_{i,j+1}}^{k} + m_{I_{i,j-1}}^{k}]. \quad \text{(Eqn. A.5)}$$

The stability criterion for this numerical approach is given by Eqn. A.6 by following Kreyszig (2010).

$$(1 - 4\alpha) > 0, \quad \text{(Eqn. A.6)}$$

$$\alpha < \frac{1}{4} \rightarrow \Delta t < \frac{h^2}{4\eta_I}. \quad \text{(Eqn. A.7)}$$

The boundary conditions for the inner reservoir (Zone 1) are given below:

$$\text{y} = 0, \text{j} = 1 \rightarrow \frac{\partial m_I}{\partial y} = 0 \rightarrow m_{I_{i,j}}^{k} = m_{I_{i,j-1}}^{k}, \quad \text{(Eqn. A.8)}$$

$$\text{y} = \text{y}_{\text{external}}, \text{j} = 1 \rightarrow m_{I_{i,j}}^{k} = m_{H_{i,j}}^{k}, \quad \text{(Eqn. A.9)}$$

$$\text{x} = 0 \rightarrow \frac{\partial m_I}{\partial x} = 0 \rightarrow m_{I_{i-1,j}}^{k} = m_{I_{i+1,j}}^{k}, \quad \text{(Eqn. A.10)}$$

$$\text{x} = \text{x}_{\text{external}} \rightarrow \frac{\partial m_I}{\partial x} = 0 \rightarrow m_{I_{i-1,j}}^{k} = m_{I_{i+1,j}}^{k}. \quad \text{(Eqn. A.11)}$$

The Hydraulic Fracture Discretization

Governing flow equation for the hydraulic fracture flow is given by Eqn A.12, and numerical discretization for that equation is presented as follows:

$$\frac{\partial^2 m_H}{\partial x^2} + \frac{2}{C_{FD}} \frac{\partial m_I}{\partial y} = \frac{1}{\eta_F} \frac{\partial m_F}{\partial t} \qquad \text{(Eqn. A.12)}$$

$$\frac{1}{\eta_F} \frac{m_I{}_i^{k+1} - m_I{}_i^k}{\Delta t} = \frac{2}{C_{FD}} \frac{m_I{}_{i,j}^k - 2\, m_I{}_{i,j-1}^k}{\Delta y} + \frac{m_H{}_{i+1}^k - 2\, m_H{}_i^k + m_H{}_{i-1}^k}{\Delta x^2} \qquad \text{(Eqn. A.13)}$$

Therefore:

$$m_H{}_j^{k+1} = m_H{}_j^k (1 - 2\alpha_2) + \alpha_2 [m_H{}_{j+1}^k + m_H{}_{j-1}^k + \frac{2}{C_{FD}} \frac{m_I{}_{i,j}^k - m_I{}_{i,j-1}^k}{\Delta y}] \qquad \text{(Eqn. A.14)}$$

The stability criterion for this numerical approach is given by Eqn. A.15 by following Kreyszig (2010).

$$(1 - 2\alpha_2) > 0 \qquad \text{(Eqn. A.15)}$$

$$\alpha_2 < \frac{1}{2} \rightarrow \Delta t < \frac{h^2}{4\eta_F} \qquad \text{(Eqn. A.16)}$$

The boundary conditions for the hydraulic fracture (Zone 2) are as the following:

$$x = x_{external} \rightarrow \frac{\partial m_H}{\partial x} = 0 \rightarrow m_I{}_{j-1}^k = m_I{}_{j+1}^k \qquad \text{(Eqn. A.17)}$$

$$x = 0 \; ; \; i = 1 \rightarrow \frac{\partial m_H}{\partial x} = \frac{-\pi}{C_{FD}} = C_1 \rightarrow m_H{}_{i+1}^k = m_H{}_{i-1}^k + 2\Delta x C_1 \qquad \text{(Eqn. A.18)}$$

References

Al-Hussainy, R., and Ramey Jr., H. J., 1966. Application of Real Gas Flow Theory to Well Testing and Deliverability Forecasting. *Journal of Petroleum Technology*, *18*(5), 637–642. SPE 1243-PA

Al-Hussainy, R., Ramey Jr., H. J., and Crawford, P. B., 1966. The Flow of Real Gases through Porous Media. *Journal of Petroleum Technology*, *18*(5), 624–636. SPE 1243-A

Al-Kobaisi, M., Ozkan, E., & Kazemi, H., 2006. A Hybrid Numerical / Analytical Model of a Finite-Conductivity Vertical Fracture Intercepted by a Horizontal Well. *SPEREE* **9** (4): 345 - 355. SPE 92040-PA.

Apaydin, O.G., 2012. New Coupling Considerations Between Matrix and Multiscale Natural Fractures in Unconventional Resource Reservoirs, PhD dissertation. Colorado School of Mines, Golden, Colorado.

Aybar, U., Eshkalak, M. O., and Sepehrnoori, K., Patzek. T. W., 2014. Long Term Effect of Natural Fractures Closure on Gas Production from Unconventional Reservoirs. Paper SPE 171010 presented at Eastern Regional Meeting held in Charleston, West Virginia, USA, 21–23 October.

Bagheri, M., & Settari, A., 2008. Modeling of Geomechanics in Naturally Fractured Reservoirs, *SPE Reservoir Evaluation and Engineering*, Vol. 11, 108-118.

Bai, M., Meng, F., Elsworth, D., Abousleiman, Y., and Roegiers, J.C., 1999. Numerical Modelling Of Coupled Flow And Deformation In Fractured Rock Specimens, *International Journal for Numerical and Analytical Methods in Geomechanics, Vol. 23, 141-160*.

Bandis, S. C., Lumsden, A. C., and Barton, N. R., 1983. Fundamentals of rock joint deformation. *International Journal of Rock Mechanics and Mining Sciences & Geomechanics Abstracts*, *20*(6), 249–268.

Barton, N.R., Bandis, S.C., and Bakhtar, K., 1985. Strength, deformation and conductivity coupling of rock joints. *International Journal of Rock Mechanics and Mining Sciences & Geomechanics Abstracts*, *22*(3), 121–140.

Bennett, C. O., Camacho-V., R.G., Reynolds, A.C., and Raghavan, R., 1985. Approximate Solutions for Fractured Wells Producing Layered Reservoirs, *SPEJ* **25** (5(: 729-742. SPE 11599-PA.

Brown, M. L., 2009. Analytical Trilinear Pressure Transient Model for Multiply Fractured Horizontal Wells in Tight Shale Reservors. M.Sc. Thesis. Colorado School of Mines. Golden, Colorado.

Brown, M., Ozkan, E., Raghavan, R., and Kazemi, H. 2009. Practical Solutions for Pressure Transient Responses of Fractured Horizontal Wells in Unconventional Reservoirs, SPE ATCE, New Orleans, LA, 4-7 October, SPE 125043.

Brown, M., Ozkan, E., Raghavan, R., & Kazemi, H. (2011). Practical solutions for pressure-transient responses of fractured horizontal wells in unconventional shale reservoirs. *SPE Reservoir Evaluation & Engineering*, **14**(06), 663-676.

Camacho, R.G., Raghavan, R., and Reynolds, A. C., 1987. Response of Wells Producing Layered Reservoirs : Unequal Fracture Length, *SPEFE* **2** (1): 9 -28, SPE 12844-PA

Carslaw, H. S., and Jaeger, J. C., 1959. Conduction of Heat In Solids. *Oxford: Clarendon Press, 1959, 2nd Ed.*

Celis, V., Silva, R., Ramones, M., Guerra, J., and Da Prat, G., 1994. A New Model for Pressure Transient Analysis in Stress Sensitive Naturally Fractured Reservoirs. *SPE Advanced Technology Series*, *2*(01), 126–135.

Chin, L. Y., Raghavan, R., and Thomas, L. K., 2000. Fully Coupled Analysis of Well Responses in Stress-Sensitive Reservoirs, SPE Res Eval & Eng 3 (5): 435 – 443, SPE 66222.

Cho, Y., 2012. Effects Of Stress-Dependent Natural-Fracture Permeability On Shale-Gas Well Production, MSc Thesis, Colorado School of Mines, Golden, Colorado.

Cho, Y., Ozkan, E., & Apaydin, O. G., 2013. Pressure-Dependent Natural-Fracture Permeability in Shale and Its Effect on Shale-Gas Well Production. *SPE Reservoir Evaluation & Engineering*, 16(02), 216-228.

Cinco-ley, H., and Samaniego-v, and Dominguez, A. N., 1978. Transient Pressure Behavior for a Well with a Finite-Conductivity Vertical Fracture, *SPEJ* **18** (4):253-264, SPE 6014-PA.

Cinco-Ley, H., and Meng, H.-Z., 1988. Pressure Transient Analysis of Wells With Finite Conductivity Vertical Fractures in Double Porosity Reservoirs. *Proceedings of SPE Annual Technical Conference and Exhibition*, SPE 18172.

Cinco-ley, H., and Samaniego-v, F., 1981. Transient Pressure Analysis for Fractured Wells, *JPT* **33** (9) (September), 1749–1766, SPE 7490-PA.

Cipolla, C. L., Lolon, E. P., Erdle, J. C., and Rubin, B., 2010. Reservoir Modeling in Shale-Gas Reservoirs, *SPE Res Eval & Eng* **13** (4): 638-653, SPE 125530-PA.

CMG:"IMEX User's Guide," Computer Modeling Group Ltd., 2012.

De Swaan O. A., 1976. Analytic Solutions for Determining Naturally Fractured Reservoir Properties by Well Testing. *Society of Petroleum Engineers Journal*, **16(03)**, 117–122, SPE 5346-PA

Eshkalak, M. O., Mohaghegh S. D., and Esmaili, S., 2013. Synthetic, Geomechanical Logs for Marcellus Shale. Paper SPE 163690 presented at Digital Energy Conference and Exhibition held in the The Woodlands, Texas, USA, 5-7 March.

Eshkalak, M. O., Aybar, U., and Sepehrnoori, K., 2014. An Integrated Reservoir Model for Unconventional Resources, Coupling Pressure Dependent Phenomena. Paper SPE 171008 presented at Eastern Regional Meeting held in Charleston, West Virginia, USA, 21–23 October.

Franquet, M., Ibrahim, M., Wattenbarger, R., and Maggard, J., 2004, June. Effect of Pressure-Dependent Permeability in Tight Gas Reservoirs, Transient Radial Flow. *Proceedings of Canadian International Petroleum Conference*, 1–10. doi:10.2118/2004-089

Fredd, C. N., McConnell, S. B., Boney, C. L., and England, K. W. 2001. Experimental Study of Fracture Conductivity for Water-Fracturing and Conventional Fracturing Applications. *SPE Journal*, **6**(03), 288–298. SPE-74138-PA. doi:10.2118/74138-PA

Gringarten, A. C., Ramey, H.J., and Raghavan, R., 1975. Applied Pressure Analysis for Fractured Wells. *JPT* **27** (7): 887–892. SPE 5496-PA

Gringarten, A. C., Ramey, H. J., and Raghavan, R., 1974. Unsteady-State Pressure Distributions Created by a Well With a Single Infinite-Conductivity Vertical Fracture. *SPEJ* **14** (4): 347-360. SPE 4051-PA.

Gutierrez, M., Øino, L. E., and Nygård, R. 2000. Stress-Dependent Permeability of a De-Mineralised Fracture in Shale, *Marine and Petroleum Geology* **17**, 895-907.

Kazemi, H., 1969. Pressure Transient Analysis of Naturally Fractured Reservoirs with Uniform Fracture Distribution. *SPEJ* **9** (4) 451-462. SPE 2516-A.

Kazemi, H., Merrill, Jr., L. S., Porterfield, L. L., and Zeman, P. R. 1976., Numerical Simulation of Water-Oil Flow in Naturally Fractured Reservoirs. *SPEJ* **16** (6): 317-326. SPE 5719-PA.

Kreyszig, E. (2010). Advanced Engineering Mathematics. John Wiley & Sons.

Kwon, O., Kronenberg, A. K., Gangi, A.F., Johnson, B., and Herbert, B.E., 2004. Permeability of illite-bearing shale: 1. Anisotropy and effects of clay content and loading. *Journal of Geophysical Research* (**109**): B10205.

Luffel, D.L., Hopkins, C.W., Holditch, S.A., and Schettler, P.D., 1993. Matrix Permeability Measurement of Gas Productive Shales. *SPE ATCE*, 3-6 October, Houston, Texas, SPE 26633.

Makurat, A., and Gutierrez, M., 1996, Fracture Flow and Fracture Cross Flow Experiments, SPE ATCE, 6-9 October, Denver, CO, SPE 36732 .

McGuire, W. J., & Sikora, V. J., 1960. The Effect of Vertical Fractures on Well Productivity. *Journal of Petroleum Technology*, *12*(10), 72–74. doi:10.2118/1618-G

Medeiros, F., Ozkan, E., & Kazemi, H., 2006. A Semianalytical Pressure-Transient Model for Horizontal and Multilateral Wells in Composite Layered and Compartmentalized Reservoirs. SPE ATCE, San Antonio, Texas, 24-27 September, SPE 10384-MS.

Moinfar, A., Sepehrnoori, K., Johns, R. T., and Varavei, A., 2013. Coupled Geomechanics and Flow Simulation for an Embedded Discrete Fracture Model, *SPE Reservoir Simulation Symposium*, 18-20 February, The Woodlands, Texas, SPE 163666.

Mukherjee, H., and Economides, M. J., 1991. A Parametric Comparison of Horizontal and Vertical Well Performance *SPEFE* **6** (2) 209–216, SPE 18303-PA.

Omidvar Eshkalak, M., 2013. Synthetic Geomechanical Logs and Distributions for Marcellus Shale. MSc Thesis. West Virginia University. Morgantown, West Virginia.

Ostensen, R. W.,1986. The effect of stress-dependent permeability on gas production and well testing. *SPE Formation Evaluation*, 1(03), 227-235.

Ozkan, E., Brown, M., Raghavan, R., and Kazemi, H., 2009. Comparison of Fractured-Horizontal-Well Performance in Tight Sand and Shale Reservoirs, *SPE Western Regional Meeting,* 24-26 March, San Jose, California, SPE 121290-MS .

Ozkan, E., Brown, M. L., Raghavan, R., & Kazemi, H. (2011). Comparison of fractured-horizontal-well performance in tight sand and shale reservoirs. *SPE Reservoir Evaluation & Engineering*, **14**(02), 248-259.

Pannell, D. (1997). Sensitivity analysis of normative economic models: theoretical framework and practical strategies. *Agricultural Economics*, *16*(2), 139–152. doi:10.1016/S0169-5150(96)01217-0

Patzek, T. W., Male, F., & Marder, M. (2013). Gas production in the Barnett Shale obeys a simple scaling theory. *Proceedings of the National Academy of Sciences of the United States of America*, *110*(49), 19731–6. doi:10.1073/pnas.1313380110

Pedrosa, Jr. 1986. Pressure Transient Response in Stress-Sensitive Formations, SPE *California Regional Meeting*, 2-4 April, Oakland, California, SPE 15115.

Prats, M., 1961. Effect of Vertical Fractures on Reservoir Behavior-Incompressible Fluid Case. *Society of Petroleum Engineers Journal*, ***1***(02), 105–118. doi:10.2118/1575-G

Raghavan, R., and Chin, L. Y., 2004. Productivity Changes in Reservoirs with Stress-Dependent Permeability, SPE ATCE, 29 September-2 October, San Antonio, Texas, SPE 88870.

Raghavan, R. S., Chen, C., and Agarwal, B., 1997. An Analysis of Horizontal Wells Intercepted by Multiple Fractures, *SPEJ* **2** (3): 235-245. SPE 27652-PA.

Serra, K., Reynolds, A.C., and Raghavan, R., 1983. New Pressure Transient Analysis Methods for Naturally Fractured Reservoirs. *JPT* **35** (12): 2271-2283. SPE 10780-PA.

Soeder, J. D. 1988. Porosity and Permeability of Eastern Devonian Gas Shale. *SPE Formation Evaluation* **3** (1): 116-124. SPE 15213-PA.

Stehfest, H. 1970. Numerical Inversion of Laplace Transforms. Communications. ACM 13 (1). 47-49.

Suarez-Rivera, R., Burghardt, J., Edelman, E., Stanchits, S., & Surdi, A., 2013, January. Geomechanics Considerations for Hydraulic Fracture Productivity. *47th US Rock Mechanics/Geomechanics Symposium*, American Rock Mechanics Association..

Tao, Q., Ghassemi, A., and Ehlig-Economides, C.A., 2010. Pressure Transient Behavior for Stress-Dependent Fracture Permeability in Naturally Fractured Reservoirs. CPS/SPE International Oil and Gas Conference and Exhibition, 8-10 June, Beijing, China, SPE 131666.

Terzaghi, K. Van, Die Berechnung der Durchassigkeitsziffer des Tones ansndem Verlauf der hydrodynamischen Spannungserscheinungen, Sitzungsber.Akad. Wiss. Wien Math Naturwiss. Kl. Abt. 2A, 132, 105, 1923

Tinsley, J. M., Williams Jr, J. R., Tiner, R. L., & Malone, W. T., 1969. Vertical fracture height-its effect on steady-state production increase. *Journal of Petroleum Technology*, **21**(05), 633-638.

Van Everdingen, A. F., and Hurst, W., 1949. The Application of the Laplace Transformation to Flow Problems in Reservoirs. *Journal of Petroleum Technology*, *1*(12). doi:10.2118/949305-G

Warren, J. E., and Root, P. J., 1963. The Behavior of Naturally Fractured Reservoirs. *Society of Petroleum Engineers Journal*, **3** (03), 245–255. doi:10.2118/426-PA

Wilbur, C., and Amadei, B., 1990, Flow pump measurements of fracture transmissivity as a function of normal stress, June 18-20, US Symposium on Rock Mechanics, Golden, Colorado.

Zhao, Y., and Chen, M., 2006. Fully coupled dual-porosity model for anisotropic formations. *International Journal of Rock Mechanics and Mining Sciences*, **43**(7), 1128–1133. doi:10.1016/j.ijrmms.2006.03.001

.

.